Proposed Improvements to Overlay Test for Determining Cracking Resistance of Asphalt Mixtures

by

Wangyu Ma

A thesis submitted to the Graduate Faculty of
Auburn University
in partial fulfillment of the
requirement for the Degree of
Master of Science

Auburn, Alabama
May 3, 2014

Keywords: asphalt, overlay, cracking, test

Approved by

Nam Tran, Chair, Associate Research Professor of Civil Engineering
Randy West, Director of National Center for Asphalt Technology
David Timm, Brasfield & Gorrie Professor of Civil Engineering
Richard Willis, Associate Research Professor of Civil Engineering

ABSTRACT

There is an increasing need in evaluating the cracking resistance of asphalt mixtures as more recycled materials are used in the mixes. A promising method that has been used to evaluate the mixture cracking resistance is the overlay test conducted in accordance with the Texas Department of Transportation procedure (Tex-248-F). This test can be conducted on specimens prepared from gyratory-compacted samples or from field cores. It can be conducted in an Overlay Tester or in the Asphalt Pavement Performance Tester (AMPT) with an Overlay Test Kit.

The overall objective of this thesis is to evaluate and refine the overlay test conducted in the AMPT for determining the cracking resistance of asphalt mixtures. The evaluation was conducted using five plant-produced mixtures that were used in the bottom asphalt layers of five test sections at the NCAT Pavement Test Track.

Key findings of this study include (1) a modified method for better determining the number of cycles to failure (i.e., the failure point) and (2) a higher test frequency (1.0 Hz) for reducing the testing time without significantly affecting the test result and its variability. Furthermore, the overlay test results were compared with those of the bending beam fatigue (BBF) test. Good correlation was found between the overlay test results and the BBF test results determined at 800 and 400 με.

ACKNOWLEDGEMENT

First of all, I would like to acknowledge the guidance and support given to me by my supervisor Dr. Nam H. Tran for his support and encouragement in my professional and personal life throughout the years. Without his guidance, I could not overcome those obstacles. In my study, Dr. Tran encouraged me to investigate many fields of my interest. Every time I had a new idea in conducting the experiments or data analysis, I would like to talk to him at the first time. Even though some ideas were not ready to be implemented, he was always patient and offered invaluable suggestions for me to explore with. I have gained a lot through this process. Dr. Tran taught me the importance of writing skill to a researcher. He provided me a great support in developing the technical writing skill, especially during the writing process of the thesis work. Dr. Tran is not only the teacher but also the mentor in my self-development. The most important thing I learned from him is the way of critical thinking. He taught me how to propose question on phenomenon, make assumptions, and find the truth based on critical analysis for the experimental data. His tutoring made me realize only through hardworking and great efforts can I make any progress in the career.

Next, I would like to thank all my committee members for their agreeing to serve and also for their great help in my past studies. Dr. Randy West offered me the great opportunity to study in Auburn University and work with those excellent engineers in NCAT. In the class of

design and control of asphalt paving mixtures, he taught me the importance of paying attention to details and listening to others. Dr. David Timm made me understand the pavement design systematically. I benefited a lot from his great teaching in pavement design classes. I would like to thank Dr. Richard Willis for his agreeing to serve as my committee. He provided me very good advices for my study plan in the future.

Also, I would like to acknowledge all my colleagues in NCAT during my working. Adam Taylor gave me tremendous support in the experimental work. He helped me to conduct the experiments more efficiently, and to deal with the issues on AMPT facility. Without his help, I cannot go through the hard time with the machine and software problems. I want to thank Tina Ferguson for her assistance in my experiment. She cleaned asphalt residue on the base plates using acetone after every test. For many times, she came back to the laboratory late evening to check the testing machine. I would like to acknowledge Dr. Saeed Maghsoodloo for his advices on my statistical analysis. I also would like to say thanks to Jason Moore, Brian Waller, Grant Julian, Vickie Adams, and Pamela Turner for their unselfish help to my working in the laboratory. Finally, I want to say thanks to all the visiting scholars, classmates, and corporate students in NCAT. Their understandings, encouragements, and cares made my life in Auburn happy and meaningful.

TABLE OF CONTENTS

LIST OF TABLES

LIST OF FIGURES

CHAPTER 1 INTRODUCTION

1.1 Problem Statement

Recycled materials, including reclaimed asphalt pavement (RAP) and recycled asphalt shingles (RAS), are used in asphalt mixtures to reduce material costs. Since the binder in RAP and RAS is often stiffer than the virgin binder used in the mixture, cracking is one of the major concerns in using an asphalt mixture with higher RAP and/or RAS contents. Therefore, there is an increasing need in evaluating the resistance of the mixture to cracking before it is produced and placed in the field.

One of the standardized test methods for determining the resistance of asphalt mixtures to cracking is the four-point flexural bending or bending beam fatigue (BBF) test conducted in accordance with AASHTO T321 and ASTM D7460. This test was developed to simulate the fatigue cracking behavior at the bottom of the asphalt layer in the field. During the test, a cyclic displacement is applied at the central third points to induce tensile strains at the bottom of the beam, which are representative of those that occur in the field, causing cracks to initiate and propagate to the top of the beam. The main result of the BBF test is the number of cycles to failure (or failure point) at which macro-cracks initiate and start to propagate in the beam specimen. Even though significant research efforts have been conducted to develop and evaluate this test, it has not been widely implemented by transportation agencies because of two main issues: specimen preparation and testing time. Compared to a cylindrical specimen, it is more

expensive and difficult to prepare a beam specimen in the laboratory or extract a beam from a pavement section for testing. In addition, a BBF test can take up to more than 50 days depending on the selected strain level (Prowell et al. 2010). Thus, it is not used for routine asphalt mix design or quality assurance/quality control (QA/QC) testing, which often requires a quick turnaround (Saadeh and Eljairi 2011).

A potential solution is to find an alternative test that does not have these issues. The overlay test (OT) was developed in the 1970s to test an asphalt mixture's resistance to reflective cracking, but it has also been evaluated to determine the bottom-up fatigue cracking and the thermal reflective cracking resistance of asphalt mixture (Tex-248-F-09, Zhou and Scullion 2003, Zhou et al. 2007a, Zhou et al. 2007b, Zhou and Scullion 2005b). Compared to the BBF test, the OT has a couple of advantages. First, it is easier to prepare OT specimens from gyratory-compacted specimens or from field cores. Second, this test can be conducted in an Overlay Tester or in the Asphalt Pavement Performance Tester (AMPT) with an Overlay Test Kit. Many transportation departments have purchased the AMPT through pooled-fund study TPF-5(178) (Withee 2013). Thus, if this test is proved to be effective in AMPT, it can be implemented in the future.

However, in the current TxDOT procedure (Tex-248-F), the maximum opening displacement of 0.635 mm (0.025 in.) is deemed too large for testing stiff asphalt mixtures (e.g., with higher RAP and/or RAS contents) and the mixtures of asphalt overlay placed in different climate conditions (i.e., smaller daily temperature variation). The OT is currently conducted at a frequency of 0.1 Hz according to the current procedure, but the OT can be conducted at a higher frequency to reduce testing time. In the current procedure, the failure point is defined as the number of cycles

where 93% reduction of the initial peak load occurs. This method of determining the failure point is not consistent with those used in other cracking tests, such as the BBF test in accordance with ASTM D7460 procedure. Thus, additional work is needed to evaluate the maximum opening displacement, test frequency, and method for determining the failure point specified in the current OT procedure.

1.2 Objective

The objective of this study is to evaluate the use of overlay test in the AMPT and determine if a smaller maximum opening displacement(s), a higher test frequency, and another method for determining the failure point can be successfully used in the procedure for evaluating the resistance of asphalt mixtures to cracking.

1.3 Organization of This Thesis

This thesis consists of six chapters including this chapter (Chapter 1) which offers the background and objective of this study. Chapter 2 is the literature review focused on the past studies on the methods of analyzing the BBF test result and the development of the overlay test (OT) since the late 1970s. For the BBF test, general test procedures and typical testing results are summarized, followed by several methods used to determine the number of cycles to failure. For the OT, the literature review is focused on the testing procedure, typical testing result, repeatability, crack propagation modeling, and relationship between laboratory test result and field performance.

Chapter 3 presents the overlay test in the asphalt mixture performance tester (AMPT), followed by discussions on the properties of applied mixtures, testing plan, and specimen fabricating procedure. A new method for determining the failure point in the AMPT overlay test is proposed.

Chapter 4 summarizes the AMPT overlay test results and provides the associated analysis. Evaluation for the two failure point determining methods is provided based on the cracking images captured from the recorded video and the peak load development during the test. Then, a better method is selected by correlating determined failure point to the defined failure moment at which crack was first observed to pass through the specimen. The effect of higher frequency on the testing result is also discussed.

Chapter 5 investigates the correlation between the BBF test and OT in evaluating the fatigue cracking resistance of asphalt mixture. The investigation is performed by comparing their ranking for the failure points of five asphalt mixtures used in NCAT Test Track, as well as the fitted relationships between failure points and applied maximum tensile strains (or displacements).

Chapter 6 provides the thesis summary with a list of findings and recommendations. Also, the planned works for the future to verify these findings are also proposed. Appendices of some

important information are attached afterwards. The testing data, statistical analysis outputs, and peak load curves (relationship between peak load and number of cycles) are included.

CHAPTER 2 LITERATURE REVIEW

This chapter provides a review of the past studies on the bending beam fatigue (BBF) test and the overlay test (OT). General procedures, typical results and analyzing methods of two tests are summarized. For the OT, repeatability, crack propagation modeling and application of the test results in predicting the fatigue life of asphalt pavements are further discussed.

2.1 Bending Beam Fatigue Test

The BBF test was designed to determine the fatigue cracking resistance of an asphalt mixture (ASTM D7460-10). The determined number of cycles to failure can be multiplied with a shift factor to predict the fatigue life of the asphalt pavement under repeated traffic loading. This section briefly describes the test procedure, followed by methods for determining test results and a summary of findings from previous studies.

2.1.1 Test Procedure

In the BBF test, the beam specimen (380 ± 6 mm long by 63 ± 2 mm wide by 50 ± 2 mm thick) is trimmed from a laboratory or field compacted beam specimen (ASTM D7460-10). Figure 2.1 shows the laboratory-compacted and trimmed beam specimens.

Figure 2.1 Laboratory compacted specimen (left) and trimmed specimen (right)

The BBF test can be conducted in devices that are commercially available through Cox and IPC. The difference between the Cox and IPC devices is that the Cox device applies load from the top while the IPC device applies load from the bottom. Figure 2.2 shows an IPC device. The beam specimen is held by four equal-spaced clamps (ASTM D7460-10). All contact points have free horizontal translation and rotation. A cyclic displacement is applied at the central H-frame third points.

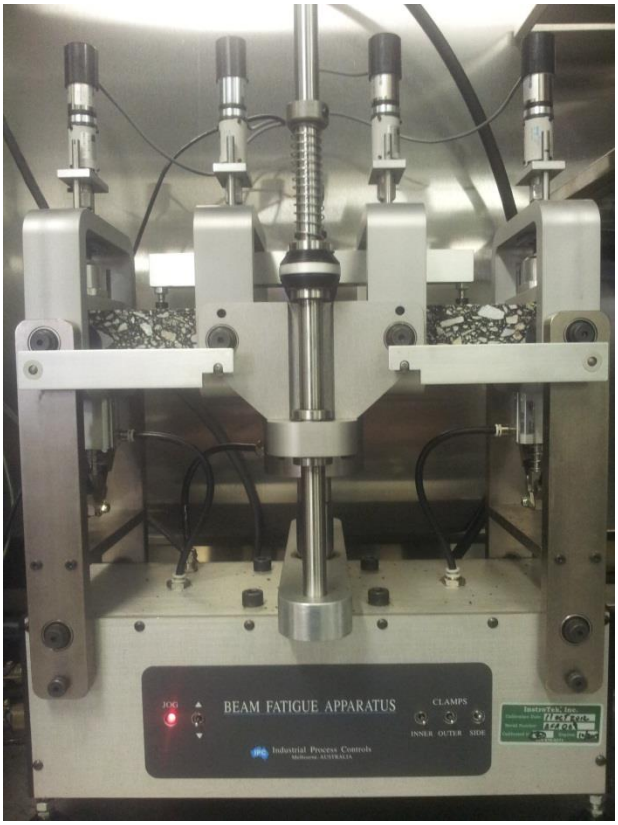

Figure 2.2 BBF test on IPC device

The testing device is kept in an environmental chamber set at a test temperature of 20 ± 0.5°C. The loading frequency ranges from 5 to 10 Hz. Two waveforms can be applied: one is sinusoidal specified in AASHTO T321, and the other is haversine specified in ASTM D7460. The maximum deflection at the center of the specimen is maintained by a closed-loop control system. The resulting maximum strain typically ranges from 200 to 800 microstrains (AASHTO T321-07).

2.1.2 Test Results

Results of the test include the failure point (number of cycles to failure) and the dissipated energy (DE). In AASHTO T321 and ASTM D7460, the failure point is determined differently. A description of each method follows.

In both the methods, the maximum deflection (δ) in each cycle is first used to calculate the resulting maximum tensile strain (ε_t) as shown in Equation 1. The maximum tensile stress (σ_t) is determined using Equation 2. Then, the flexural stiffness (S) is determined using Equation 3 (ASTM D7460-10).

$$\varepsilon_t = \frac{(12\delta h)}{(3L^2 - 4a^2)} \quad (1)$$

Where,

ε_t = maximum tensile strain (m/m);

δ = maximum deflection at center of beam (m);

a = space between inside clamps (m); and

L = length of beam between outside clamps (m).

$$\sigma_t = \frac{3aP}{bh^2} \quad (2)$$

Where,

σ_t = maximum tensile stress (Pa);

a = center to center spacing between clamps (Cox: 0.1190 m; IPC: 0.1185 m);

P = load applied by actuator (N);

b = average specimen width (m); and

h = average specimen height (m).

$$S = \sigma_t / \epsilon_t \quad (3)$$

In AASHTO T321, the relationship between the number of loading cycles (N) and the calculated stiffness is then determined using the exponential model shown in Equation 4. Finally, the failure point can be calculated using Equation 5 corresponding to the 50 percent reduction of the initial stiffness (AASHTO T321-07).

$$S = Ae^{bN} \quad (4)$$

$$N_f = \frac{\ln(0.5 \times S_0) - \ln(A)}{b} \quad (5)$$

Where,

N = number of loading cycles;

A = regression constant;

b = regression constant; and

S_0 = initial beam stiffness (modulus) estimated at 50^{th} cycle.

However, in ASTM D7460, another method is utilized to determine the failure point using "Normalized Stiffness × Cycles" (NSC) as an indicator that is defined in Equation 6. The NSC

value is plotted against the number of loading cycles. Finally, the failure point is the number of loading cycle corresponding to the peak NSC (ASTM D7460-10).

$$NSC = \frac{S_i \times N_i}{S_0 \times N_0} \quad (6)$$

Where,

NSC = normalized stiffness × cycles (Pa/Pa);

S_i = beam stiffness (modulus) at cycle i (Pa);

N_i = cycle number i;

N_0 = cycle number (i.e., 50) at which S_0 is estimated.

Dissipated energy (DE) and phase angle at loading cycle i are determined using Equations 7 and 8. The summation of dissipated energy (DE) per cycle up to the failure point is the cumulative dissipated energy (AASHTO T321-07).

$$DE_i = \pi \sigma_t \epsilon_t \sin \emptyset \quad (7)$$

$$\emptyset = 360fs \quad (8)$$

Where,

DE_i = dissipated energy at loading cycle i (J/m^3);

$\emptyset$ = phase angle at cycle i (degree);

F = load frequency (Hz); and

S = time lag between stress and strain curve at peak value (second).

2.1.3 Results of Past Studies

2.1.3.1 Failure Point

In the AASHTO method, the failure point is determined based on the reduction of initial stiffness. However, use of the 50 percent stiffness reduction as a criterion does not always correspond to the initiation of a macro-crack in the specimen (Rowe and Bouldin 2000). In the ASTM method, the failure point is determined based on another approach proposed by Rowe and Bouldin (Rowe and Bouldin 2000, ASTM D7460-10). They proposed a "reduced energy ratio" concept modified from Hopman's "energy ratio" concept (Rowe and Bouldin 2000). Equations 9 and 10 are from the original concept of energy ratio. In a controlled-stress test, strain could be calculated using Equation 11, so Equation 10 can be written as Equation 12. In Equation 12, $\sin\delta_0/\sin\delta_n$ is close to one. E_0 is a constant that does not affect the trend of W_n. Therefore, Equation 12 is simplified to Equation 13. Equation 13 was originally used in a controlled-stress test to determine the failure point by Rowe and Bouldin. A plot of "reduced energy ratio" versus "number of cycles" is demonstrated in Figure 2.3. Then, they applied Equation 13 in a controlled-strain test and obtained a similar curve (Figure 2.4). The number of cycles at which peak value occurred was defined as the transition point from micro-crack to macro-crack propagation. The ASTM standard applied a normalized "reduced energy ratio" to eliminate the effect of initial stiffness, which is slightly different from the method proposed by Rowe and Bouldin (ASTMD 7460-10).

$$W_n = \frac{nw_0}{w_n} \tag{9}$$

$$W_n = \frac{n(\pi\sigma_0\varepsilon_0\sin\delta_0)}{\pi\sigma_n\varepsilon_n\sin\delta_n} \tag{10}$$

$$\varepsilon = \frac{\sigma}{E} \tag{11}$$

$$W_n = \frac{n(\pi{\sigma_0}^2 E_n\sin\delta_0)}{\pi{\sigma_0}^2 E_0\sin\delta_n} \tag{12}$$

$${R_n}^{\sigma} = nE_n \tag{13}$$

Where,

W_n = energy ratio;

n = cycle number;

w_0 = dissipated energy in first cycle;

w_n = dissipated energy in n^{th} cycle;

σ_0 = stress in the initial cycle;

σ_n = stress in n^{th} cycle;

ε_0 = strain in the initial cycle;

ε_n = strain in n^{th} cycle;

δ_0 = phase angle in the initial cycle;

δ_n = phase angle in n^{th} cycle;

E_0 = modulus in the initial cycle;

E_n = modulus in n^{th} cycle; and

${R_n}^{\sigma}$ = reduced energy ratio for controlled stress test

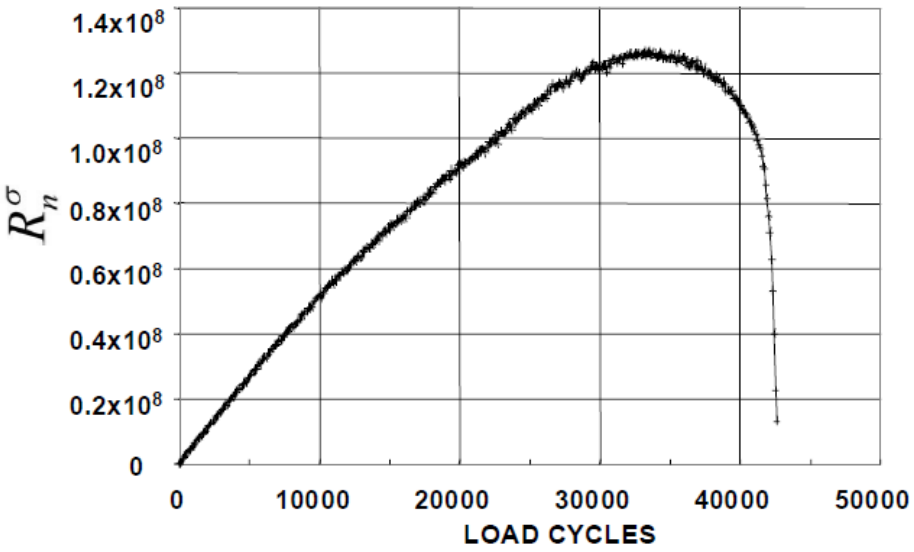

Figure 2.3 Reduced energy ratio versus load cycles in controlled-stress testing model (Rowe and Bouldin 2000)

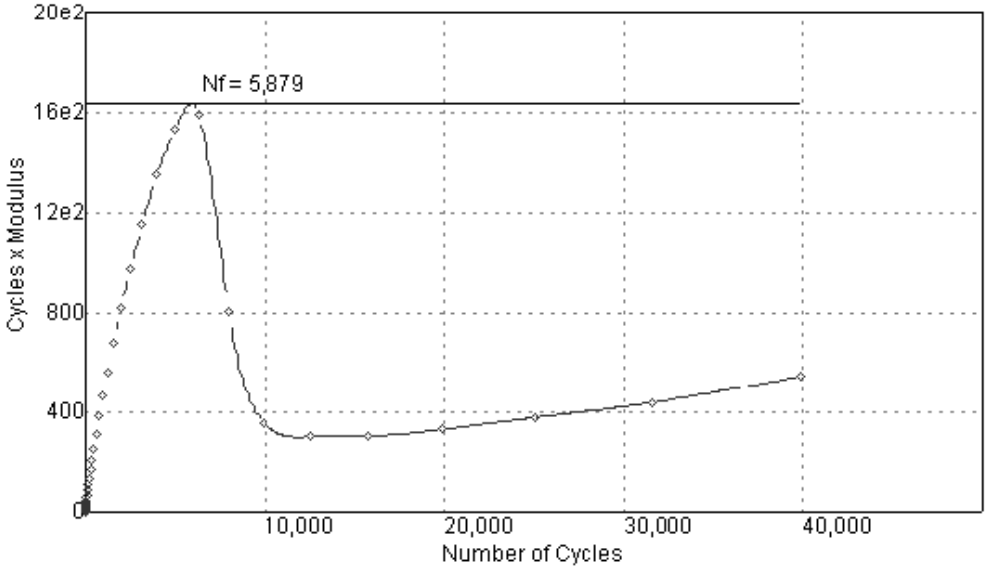

Figure 2.4 Reduced energy ratio versus load cycles in controlled-strain testing model (Rowe and Bouldin 2000)

Another important parameter that can be determined based on the BBF test results is the mix endurance limit, which is the strain level below which cumulative fatigue damage does not occur. In the laboratory, the endurance limit of an asphalt mixture is the strain level corresponding to 50 million cycles to failure (Prowell et al. 2010). Prowell et al. (2010) applied the BBF test to verify the existence of an endurance limit for hot mix asphalt (HMA) and then provided guidance to determine the limit for various types of asphalt mixture. The main challenge in determining the endurance limit of an asphalt mixture is to conduct the BBF test up to 50 million cycles, which would take up to two months for a test. Thus, they studied five models, including the exponential model, logarithmic model, power model, Weibull Survivor function, and rate of dissipated energy change (RDEC) model, to extrapolate the failure point of the asphalt mixture based on the minimum laboratory testing data. They reported that the exponential model specified in the current standard (AASHTO T 321) should not be used to extrapolate the failure point. Also, the logarithmic and power models overestimated the failure point (later than the actual failure point), and the RDEC method was not optimal for endurance limit extrapolation. Instead, they demonstrated that the single-stage Weibull Survivor function was the best among the five models for estimating long-life fatigue tests when the strain level was near or slightly higher than the endurance limit. A discussion of the Weibull Survivor function follows.

The Weibull Survivor function was named after Waloddi Weibull (1951) for his study on the applicability of a statistical distribution function in many areas, including the material strength determination. Then, Garcia-Diaz and Riggins (1984) developed a series of performance models to predict the pavement performance using an “S-shaped” survivor curve instead of a Weibull

Survivor function. Tsai (2002) simplified the general equation of Weibull Survivor function into the form shown in Equation 14. Tsai (2002) also introduced the stiffness ratio (SR) parameter to replace the probability of survival (S) in Equation 14 because the value of SR is equal to the value of S. Accordingly, Equation 14 can be re-written as shown in Equation 15. The scale parameter (λ) and shape parameter (γ) can be determined by a linear regression. The corresponding curve is named the single-stage Weibull Survivor model. However, this single-stage model usually underestimates the failure point (number of cycles to failure) (Prowell et al. 2010).

$$S(t) = \exp(-\lambda \times n^{\gamma}) \tag{14}$$

$$\ln\left(-\ln(SR_n)\right) = \ln(\lambda) + \gamma \times \ln(n) \tag{15}$$

Where,

$S(t)$ = probability of survival until time t;

λ = scale parameter;

γ = shape parameter; and

SR_n = stiffness ratio at cycle n.

Instead of fitting the model with one linear regression, Tsai et al. (2005) modified the model in Equation 15 using three linear regressions. Each linear regression was performed on one of the three sections indicating different damage stage in the beam specimen. The modified Weibull function using three linear regressions was more effective to describe the initiation and

propagation processes of fatigue cracking. Parameters within the modified model were calculated using a genetic algorithm.

2.1.3.2 Dissipated Energy (DE)

The application of the dissipated energy concept on fatigue analysis was started by Van Dijk (1975). Van Dijk found a mathematical relationship between the cumulative dissipated energy and failure point. This relationship has been proven to be unique regardless of loading mode (stress-controlled or strain-controlled), strain level, frequency (20-50 Hz), and rest period. However, the relationship is dependent on mixture type and testing temperature (Chiangmai 2010, Rowe 1993, Shen and Carpenter 2007, Van Dijk 1975, Van Dijk and Visser 1977).

The area under the stress-strain curve indicates the energy used for testing the material. For an elastic material, the stress-strain curves for loading and unloading coincide. No energy is stored in the material due to the complete recovery from deformation. For a viscoelastic material under cyclic loading, the stress-strain curve in each cycle is a hysteresis loop due to the time delay of deformation recovery. The area within the loop represents the dissipated energy for the current loading cycle (Ghuzlan and Carpenter 2000). The dissipated energy could be transferred into various forms, including plastic dissipated energy, heat, and damage (Ghuzlan and Carpenter 2000, Carpenter and Shen 2006).

Rowe (1993) performed a strain-controlled fatigue test on the asphalt mixture trapezoidal beam. He built up a hysteresis loop based on the load-displacement relationship and calculated the

(cumulative) dissipated energy. The current mathematical procedure to calculate dissipated energy is demonstrated in Equation 16 (Yoo and Al-Qadi 2010).

$$\text{Dissipated Energy} = \pi \times \sigma_i \times \varepsilon_i \times \sin\emptyset_i \quad (16)$$

Where,

σ_i = stress amplitude at load cycle i;

ε_i = strain amplitude at load cycle i; and

$\emptyset_i$ = phase angle between stress and strain at load cycle i.

The reason for applying the dissipated energy concept in the fatigue analysis is that the change of dissipated energy can define the failure and indicate specimen behavior independent of the loading mode (Ghuzlan and Carpenter 2000). Ghuzlan and Carpenter (2000) proposed a new criterion based on the change of dissipated energy. They assumed that as material starts to fail at the current cycle, a larger amount of dissipated energy would contribute to damage than the amount of dissipated energy goes into damage in the previous cycle. Based on this assumption, they explained the damage accumulation process in the material during loading. In each cycle, the amount of dissipated energy excluding damage-related portion is relatively constant. If the total dissipated energy changes dramatically, it means the portion goes into damage changes sharply.

The change of dissipated energy is effective in indicating damage accumulation as well as failure. Ghuzlan and Carpenter (2000) defined a ratio between the change of dissipated energy (ΔDE) from cycle "i" to cycle "i+1" and the dissipated energy in the original cycle (DE at cycle

"i"). The value of ΔDE/DE was named as the ratio of dissipated energy change (RDEC). This ratio starts to decrease after a few cycles at the beginning of loading. During this stage, the material undergoes internal microstructure rearrangement. Then, the ratio stays constant at a low level, which indicates the stable damage accumulation rate. Finally, this ratio starts to increase dramatically when failure occurs (Ghuzlan and Carpenter 2000, Carpenter and Shen 2006). Figure 2.5 indicates the ratio's development for a complete test (Shen and Carpenter 2005).

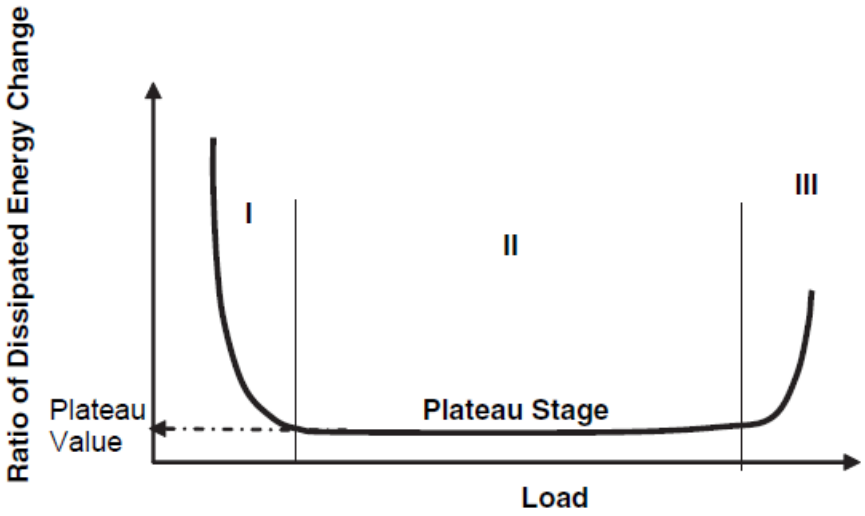

Figure 2.5 Relationship between RDEC and number of load cycle (Shen and Carpenter 2005)

This ratio can be used for both the controlled-strain and controlled-stress loading modes. The constant value of the ratio in the stable damage accumulation stage was named the plateau value. It has been shown that the plateau value (PV) had a unique relationship with the cycles to failure (N_f) regardless of loading mode (Ghuzlan and Carpenter 2000, Carpenter and Janson 1997). Shen and Carpenter (2005) investigated this PV-N_f relationship using 10 sources of mixtures under the controlled-strain loading mode. In each source, there were several types of mixtures. They concluded that PV-N_f relationships had no statistical difference in each source they tested.

Typically, the dissipated energy development in the controlled-stress test increases with loading cycles, whereas in the controlled-strain test it decreases as cyclic loading continues (Ghuzlan and Carpenter 2000). Therefore, the RDEC should be an absolute value in the calculation (Yoo and Al-Qadi 2010). Because of the limitation of equipment readout, the ratio was adjusted to measure the change within 100 cycles (Ghuzlan and Carpenter 2000). Longer intervals, such as 1,000 and 10,000 cycles, were also recommended if the dissipated energy change was too small within 100 cycles (Carpenter and Shen 2006). Carpenter and Shen (2006) suggested a calculation method to determine plateau value in Equation 17.

$$\text{Plateau Value} = [1 - \left(1 + \frac{100}{N_{f_{50}}}\right)^{f}]/100 \quad (17)$$

Where,

Nf_{50} = number of cycles to 50 percent stiffness reduction; and

f = slope of regressed DE and number of cycles relationship up to $N_{f_{50}}$.

In addition, they used the PV-N_f relationship to indicate the existence of the endurance limit and healing (Shen and Carpenter 2005, Carpenter and Shen 2006). The endurance limit calculated by this relationship was compared with that determined using the Weibull function. It was concluded that the PV-N_f relationship was able to extrapolate the long fatigue life but was not necessarily the endurance limit. In other words, the Weibull function was a better tool to estimate the endurance limit based on extrapolation method (Prowell et al. 2010).

2.1.3.3 Relationship between Laboratory and the Field Performance

There is a difference between the fatigue life determined from the BBF test and the fatigue life of pavement in the field. This difference is due to many factors including asphalt binder aging, traffic densification, healing, and rest period happening in the field. To mitigate this difference, the laboratory fatigue test result is multiplied by a shift factor of 10 recommended by SHRP to predict the fatigue life of pavement in the field (Prowell et al. 2010). Certain shift factors for local pavement have been recommended by many researchers (Harvey et al. 1997, Pierce and Mahoney 1996). But these researchers had proposed factors in different range and demonstrated contrary conclusions on the relationship between shift factor and strain level. Recently, Prowell (2010) verified a shift factor of 10 based on the performance of 2003 NCAT Test Track structural sections and bending beam fatigue test result.

2.2 Overlay Test

Asphalt overlay is a common rehabilitation method for old asphalt and concrete pavements. A major distress of HMA overlays is the reflective cracking occurring right above the underlying crack or the concrete slab joint. Reflective cracking is caused by stress concentration in the overlay due to the bending and/or shearing movements at joints and/or cracks, induced by daily temperature and moisture cycles, or traffic loading (Hu et al. 2010).

The overlay tester was first developed by Germann and Lytton (1979) in the 1970s to predict the reflective cracking resistance of asphalt overlay. It has been further refined by the researchers at the Texas Transportation Institute (TTI) (Zhou and Scullion 2003, Zhou and Scullion, 2005a). The overlay test has also been evaluated to determine the asphalt mixture resistance to fatigue

cracking and low temperature cracking (Zhou et al. 2007b, Walubita et al. 2011, Zhou and Scullion 2003). While the test procedure is continuously being improved, the overlay test has been used to evaluate the cracking resistance of asphalt mixtures in the mixture design process and in the proposed asphalt overlay thickness design and analysis tool in Texas (Hu et al. 2011, Hu et al. 2010, Walubita et al. 2012, Hu et al. 2008). Figure 2.6 shows the concept of the overlay tester (Zhou et al. 2007a).

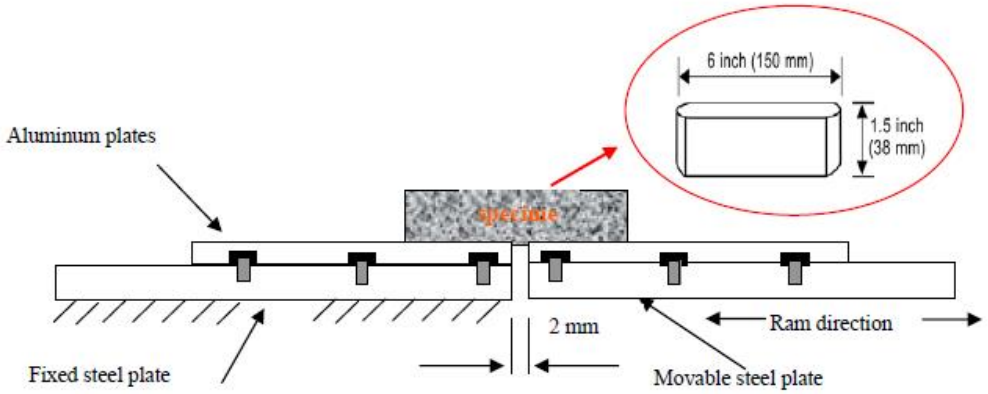

Figure 2.6 Concept of Texas Overlay Tester (Zhou et al. 2007a)

2.2.1 Test Procedure

2.2.1.1 Specimen Preparation

The test specimen (150 mm long by 76 mm wide by 38 mm high) can be trimmed from a laboratory-molded specimen or a field core according to Tex-248-F-09 procedure (Figure 2.7). The laboratory-molded specimen should be compacted to 150 mm (6 in.) in diameter and 115 ± 5 mm (4.5 ± 0.2 in.) in height. The size requirement for a field core is 150 ± 2 mm (6 ± 0.1 in.) in

diameter and at least 38 mm (1.5 in.) in height. The air voids requirement is 7 ± 1 % for the trimmed laboratory-molded specimen. After the specimen is trimmed, it is glued on the plate with 4.5-kg (10-pounds) weight on the top, and the test can start when the glue has been cured.

Figure 2.7 Laboratory molded specimen (left) and trimmed specimen (right)

2.2.1.2 Temperature Control

An environmental chamber is used to keep the specimen at a constant temperature. The specimen is kept at 25 ºC (77 ºF) for at least one hour before testing. During testing, the testing temperature is maintained at 25 ±0.5 ºC (77 ±1 ºF), which allows the test to be conducted at the room temperature (Walubita et al. 2011).

2.2.1.3 Loading Requirement

The test specimen is glued on a set of two steel base plates. During the test, one plate is fixed; the other slides horizontally until the specimen fails. The tensile load and displacement of the moving plate are recorded every 0.1 second (Tex-248-F-09). The Texas Overlay Tester is equipped with an electronic load cell which should have the capability to measure 25 KN (5000 pounds) load. The test is performed in controlled-displacement mode. During the test, a cyclic saw-tooth load is applied to the moving plate to maintain the constant maximum opening displacement (hereafter referred to as the MOD) at 0.635 mm (0.025 in.). Loading is continuously applied with the rate controlled as 10 seconds per cycle until the peak load has been reduced by at least 93 percent relative to the peak load at the first cycle. The test will also be terminated if it has been conducted for 1200 cycles even though it has not reached 93-percent reduction (Zhou and Scullion 2003, Zhou and Scullion 2005a).

Recently, a new overlay test kit for the asphalt mixture performance tester (AMPT) was designed and manufactured by the IPC Global. Using this kit, the cyclic loading is performed vertically different from the Texas Overlay Tester, the top plate remains fixed while a cyclic saw-tooth load is applied to the bottom plate. The testing is also conducted in accordance with Tex-248-F-09. Figure 2.8 illustrates the overlay test kit with specimen glued in the AMPT (IPC Global).

Figure 2.8 AMPT Overlay Test kit (IPC Global)

2.2.1.4 Displacement Measurement

In the Texas Overlay Tester, displacement of the plate movement is measured by a linear variable differential transducer (LVDT) installed underneath the fixed plate. The AMPT overlay test, there are two LVDTs: one for measuring the actuator displacement and the other for measuring the opening displacement between two plates. During the test, a constant maximum opening displacement (MOD) is maintained by adjusting the maximum displacement of actuator (IPC Global).

2.2.2 Test Results

The number of cycle to failure is the result of the overlay test. It is recorded when the peak load is reduced by 93 percent from the initial peak load (Tex-248-F-09).

2.2.3 Results of Past Studies

2.2.3.1 Failure Criterion in Overlay Mixture Design and Termination Point

The failure point (number of cycles to failure) in Tex-248-F-09 is determined based on a 93-percent peak load reduction. It is interpreted as the moment when a crack has passed through the entire thickness of the specimen (Walubita et al. 2012). The failure point determined based on this method can be used as a pass-fail criterion in the asphalt mixture design. That is, if the failure point (number of cycles to failure) is below the criterion, the mixture should be redesigned. Zhou and Scullion (2005a) performed the overlay test on the field cores from selected highway sections with known field performance in Texas. A preliminary criterion to distinguish the reflective crack resistant mixture was suggested: at least 750 cycles for rich bottom layer and 300 cycles for mixtures used for other layers. Zhou et al. (2007a) reported that the preliminary criterion (300 cycles) for distinguishing the reflective cracking resistance was also reasonable for distinguishing the fatigue cracking resistance of asphalt mixtures. In the overlay design for joint concrete pavements, Holdt and Scullion (2006) proposed that the minimum loading cycles to failure for crack resistant mixtures (i.e. crumb rubber mix, Strata interlayer mix comprised of polymer modified binder and dense fine aggregate) in the overlay

test should be 750; for dense graded mixture, the minimum loading cycles to failure should be 300 (Holdt and Scullion 2006, Bischoff 2007).

The Tex-248-F-09 procedure specifies that the test be conducted until the peak load reaches 93-percent reduction from its initial value or concluded at the termination point (the 1200th cycle). Walubita et al. (2012) suggested reducing the current termination point from 1200 cycles to 1000 cycles when the 93-percent load reduction cannot be reached.

2.2.3.2 Maximum opening displacement

The maximum opening displacement (MOD) recommended in the Tex-248-F-09 procedure is 0.635 mm (0.025 in.). It was derived by evaluating asphalt mixtures used in overlays on top of old concrete pavements in Texas and was calculated based on the thermal expansion of a 4.5-m (15-ft) long concrete slab under a 17 °C (30 °F) daily temperature variation (Zhou and Scullion 2003). Two types of concrete slab with gravel and limestone aggregates were considered. The average calculated thermal expansion of these two types of concrete slab was 0.635 mm, which is used in the current procedure. Equation 18 shows the method for calculating the MOD in the overlay test (Zhou and Scullion 2003). Bennert (2009) used this method to calculate the MOD in the overlay test for determining the fatigue cracking resistance of asphalt mixture for the overlay projects in New Jersey and Massachusetts. For the project in New Jersey, the calculated MOD was the same as that in Tex-248-F-09 procedure. But the calculated MODs for the overlay project in Massachusetts (0.74 mm and 0.53 mm) were different from the recommended value in the procedure.

$$\Delta L = \alpha \times L_{eff} \times \Delta T \times \beta \quad (18)$$

Where,

ΔL = horizontal movement of slab due to temperature change (m);

α = coefficient of linear thermal expansion (10^{-6}/m/°C);

L_{eff} = effective PCC joint spacing (m);

ΔT = maximum 24-hour temperature difference (°C); and

β = PCC/ Base friction factor.

Walubita et al. (2010) performed overlay round-robin tests among six laboratories to evaluate the repeatability and variability of testing results using the Tex-248-F procedure. One of these laboratories applied 0.584-mm (0.023-inch) MOD due to the calibration issue of machine before it was adjusted. Comparing the failure point at this lower MOD to the result after calibration (at the recommended 0.635-mm MOD), the 0.051-mm (0.002-inch) difference caused a significant difference in the overlay test result. Walubita et al. (2012) studied the effect of smaller MOD on the testing result. Two levels of MOD were applied: one is 0.508 mm (0.020 inch), the other is 0.381 mm (0.015 inch). They did not find definitive trend of change in the result variability when MOD decreases. However, the variability of result obtained at 0.381-mm (0.015-inch) MOD was smaller than the variability of result at two larger MOD levels.

Zhou et al. (2009) pointed out that applying too large or too small MOD is not desirable for determining crack development. A large displacement causes the specimen to fail much more

quickly. Small displacement lasts too long to perform the test. Zhou and Scullion (2005a) provided a recommended range of the MOD based on past studies. For 77 °F (25 °C) testing temperature, the MOD should be smaller than 2.0 mm (0.08 inch). For 32 °F (0 °C) testing temperature, the MOD should not exceed 0.125 mm (about 0.005 inch).

2.2.3.3 Testing Temperature

Zhou and Scullion (2005a) studied the effect of temperature on the overlay test result by performing the test at two temperatures: 25 °C as specified in current procedure and 10°C. Three replicates with 4.0 percent air void were used for both conditions. Maximum opening displacement (MOD) was controlled as 0.635 mm (0.025 inch). The average failure points obtained at two temperatures were compared, and the results at 10 °C were much smaller. Zhou et al. (2009) suggested that chamber of the overlay tester should have the capacity to provide the testing temperature between -5 °C and 35 °C. They also proposed two desired testing temperatures: 25 °C and 15 °C. At 25 °C, they recommended using 0.635-mm (0.025-inch) MOD in the first run. If the failure point was less than 20 cycles, the 0.381-mm (0.015-inch) MOD should be used. At 15 °C, a 0.381-mm (0.015-inch) MOD should be tried first. Similarly, if fatigue life was less than 20 cycles, the MOD should be reduced based on past experiences. Walubita et al. (2012) investigated the effect of temperature on the overlay test result and its variability. Two types of mixtures were tried at five temperature levels between 22.8 °C (73 °F) and 27.2 °C (81 °F). The failure point was found to increase with temperature, but the peak load was found to decrease with temperature. However, no definitive trend was observed on the variability of failure point or peak load due to variation of temperature.

2.2.3.4 Dissipated Energy

Zhou and Scullion (2005a) discussed the possibility of using dissipated energy-related failure point determining method for the overlay test. However, they did not recommend that method to be used in the overlay test due to two reasons. First, the energy calculation was complicated due to non-uniform distribution of load and displacement on the cross-section of the specimen. Second, size of specimens cannot be exactly the same, making energy calculated not comparable.

2.2.3.5 Specimen Preparation

(1) Cutting

To address the problem with wasting material in the overlay test specimen preparation, three alternative molding methods were studied and compared to the method in Tex-248-F procedure (Walubita et al. 2012). It was found that the current molding method which involves cutting one specimen from a 115-mm (4.5-inch) tall molded sample yielded the most material waste. The first alternative to prevent this waste was cutting two specimens from the 115-mm (4.5-inch) tall molded sample; however, it had workability issues. The second alternative was cutting two specimens from a taller sample with 127 mm (5.0 inch) in height. The third alternative was obtaining only one specimen from a 63.5-mm (2.5-inch) tall molded sample. Comparing the latter two alternatives, cutting two specimens from a taller sample with 127 mm (5.0 inch) in height saved much time and enhanced the workability. However, there was no considerable

variation between the overlay test results obtained from the current procedure and alternative fabricating methods. Since cutting accuracy is very important to the test result, Hu et al. (2008) performed the other investigation of the fabrication process to examine the use of a double-blade saw. Using the double-blade saw, the cutting procedure was automated once the thickness of specimen was entered into the system. They cut more than 50 specimens and found that most specimens met the size limit of ± 0.254 mm (± 0.01 inch). However, hard aggregates may push the two blades apart leading to the problem of cutting accuracy. They recommended reducing the blade traveling speed to minimize the accuracy issue with the hard aggregate and calibrating the machine every time the aggregate type was changed.

(2) Drying

After the specimen is cut, the Tex-248-F procedure requires the specimen be oven-dried under 60 ±3°C (140 ±5°F) until the specimen reaches constant weight (within 0.05% change in 2 hours). Instead of the oven drying method, the TTI laboratory applied air drying overnight which involved drying the specimen in front of a fan at room temperature. TxDOT CST laboratory dried the specimen in an oven at 40 °C (104 °F) (Walubita et al. 2012). Walubita et al. (2012) compared these two methods (air drying and oven drying at 40 °C) and obtained similar failure points. However, the variability of result from oven drying specimen was lower than that of the air drying. It indicated that the oven can provide more uniform heat and constant temperature environment than the air drying method. In addition, the use of core dryer machine was evaluated. The evaluation showed that the core dryer method was faster but has larger variability.

They concluded that the best method was oven drying at 40 ±3 °C (104 ±5 °F) for 12 hours at minimum.

(3) Glue

The use of two-part epoxy with required tensile strength and shear strength after 24-hour curing time is specified in the current procedure. However, the current procedure does not suggest the amount and the specific type of glue should be used. Walubita et al. (2012) tried three types of two-part epoxies: Devcon plastic steel 5-min epoxy, Devcon high strength epoxy, and Devcon two-part, two-ton epoxy S-31. The first one had workability issues (hard to spread and clean), higher cost, and longer curing time. The second and third types both had COV values of failure point less than 30 percent, but the second type cost much more than the third one. Therefore, the third type (Devcon two-part, two-ton epoxy S-31) was recommended. In addition, three quantities of epoxy (14, 16, and 18 g) were examined to find the best bond between the specimen and plate without excess. Based on the analysis, they suggested using 16-g (±0.5-g) Devcon two-part, two-ton epoxy to glue the specimen on the base plates.

(4) Sitting Time

The aging of HMA can be induced by several effects such as volatilization, oxidation or steric hardening of the asphalt binder. The procedures for the overlay test from molding to testing (molding, first bulking, cutting, second bulking, drying, gluing, curing, conditioning) take at least three days. Thus, some specimens may take long time prior to testing. To determine the

aging effect on the testing result, Walubita et al. (2012) performed several overlay tests in which the sitting time varied from 3 to 60 days. The average failure point and associated coefficient of variation (COV) were analyzed. The failure point was found to decrease rapidly after a 7-day sitting time and then stayed relatively steady. The COV were at the peak after a 7-day sitting period. Walubita et al. (2012) concluded that the effect of initial oxidative aging may cause this trend. Thus, a 3- to 5-day sitting time was recommended to minimize the effect of oxidative aging.

(5) Air Void Content

The Tex-248-F procedure requires that the target air void content for testing specimen should be 7 ±1.0 percent. However, it is difficult to control air void contents uniformly during fabrication. Walubita et al. (2012) investigated the effect of air void content on the variability of the overlay test results by dividing the 5.0 to 8.5 percent air void content range into seven groups. Results showed that two groups in which the air void contents ranged from 6.5 to 7.5 percent had COV values in the 30 percent tolerance. However, they still recommended the 7 ±1.0 percent air void content, since the ± 0.5 percent tolerance is difficult to obtain.

(6) Base Plate Setting

According to Tex-248-F procedure, the width of the gap between the plates is 2 mm. Also, there is a 6.35-mm wide (0.25-inch) tape over the gap. Walubita et al. (2012) tried a new plate set with a metal bar in the gap instead of the covered tape. This new plate set has a 6.35 mm (0.25 inch)

wide gap with a metal bar between the gap to avoid removing the epoxy after curing. The notch design on the new plate set was modified to make specimen easier to glue on. Failure points and peak loads using the new plates were compared to the old plates after testing. Even though the test results obtained using two sets of base plates were not statistically different, they still recommended using the new plate set without metal bar for its better workability.

2.2.3.6 Variability in Test Result

The Tex-248-F procedure does not suggest a limit for acceptable variability of the test result. The decision to discard or redesign the mixture in the overlay test is based on the pre-determined pass-fail criterion (certain number of loading cycles before failure). The test result below that criterion is deemed unacceptable (Zhou and Scullion 2005a). Walubita et al. (2012) performed a ruggedness study on several factors that may contribute to the variability of the test result and recommended an acceptable COV limit. These factors included the number of replicates, drying method, sitting time, air void content, gluing method, loading parameters, specimen dimension, base plates setting, and testing temperature. Walubita et al. (2011) compared the overlay test with other three tests including the Indirect Tensile Test (IDT), the Semi-Circular Bending Test (SCB) and the Direct Tension (DT) test to find the best applicable method for crack resistance characterization. The result from overlay test showed highest variability. To reduce the variability in the overlay test, three replicates are recommended in the Tex-248-F procedure. However, it was reported that one of three replicates had a result significantly different from other two. Walubita et al. (2012) explored this issue and suggested selecting the best three replicates out of five tested specimens. They tested five types of mixtures with five specimens

for each mixture. The groups of two, three, and four specimens with the lowest variability were chosen as the best based on the minimum COV and then compared with the variability of all five specimens' results. The result showed that only best of the two- and three-specimen groups had COV in the acceptable limit (30%). However, it is possible for the two-specimen group to have misleading result due to its small sample size. Therefore, it was not recommended, even though the variability was the smallest.

2.2.3.7 Alternate Method to Determine the Failure Point

The current method to determine the test result (failure point) is based on the reduction of peak tensile load during the test (Tex-248-F-09, Bennert 2009, Walubita et al. 2012, Hu et al. 2008). Some alternative failure point determining methods including those based on 50-, 75-, and 85-percent reduction of peak load should be well explained and validated (Walubita et al. 2012). Walubita et al. (2012) evaluated the rate of load decrease (slope) on the plot of peak load versus number of cycles for determining the failure point. However, they concluded that it was difficult to find an exact point on the peak load curve where a sharp change in the slope occurs after the peak load drops more than 50 percent from the first cycle.

2.2.3.8 Development of Testing Method

The overlay test method has been evaluated and modified since it was first developed in the 1970s. Two specimen sizes had been used: a larger one was 500 mm long by 150 mm wide; a smaller one was 375 mm long by 75 mm wide. These two sizes were successfully used to

fabricate the specimen and perform reflection crack resistance study on geosynthetic materials (Zhou and Scullion 2003). Later, an upgraded overlay tester was developed and the size requirement was modified: (1) the length of specimen was reduced to 150 mm; (2) the width was reduced to 75 mm; and (3) the thickness varied from 38 mm to 50 mm (Zhou and Scullion 2003, Zhou et al. 2009). The new size requirement made the overlay test possible to be performed routinely using laboratory-compacted specimen and field cores. The proposed length of specimen (150 mm) was validated by finite element analysis because the tensile stress distributed only in the mid-length of specimen. Currently, the Tex-248-F procedure specifies specimen thickness as 38 mm and the specimen width as 76 mm. In regard to the control software, the upgraded overlay tester was able to perform both one-phase triangle repeated loading and two-phase mixed loading. Two-phase loading was applied by a static constant tension followed by controlled-displacement repeated loading (Zhou and Scullion 2003). Cleveland et al. (2003) suggested using this two-phase loading method to perform advanced mechanical analysis.

2.2.3.9 Determination of Crack Length

The completion of overlay test was considered as moment when crack has propagated through the thickness of specimen (Walubita et al. 2012). Therefore, it is important to know the development of crack during the test. Typically, the approaches used to obtain the crack length during the fatigue cracking test for asphalt mixture can be categorized into two types: direct measurement and backcalculation.

(1) Direct Measurement

Two common direct measurements are crack foil and digital image correlation (DIC) (21). Jacob (1995) used crack foil measurement to determine the crack length in asphalt mixtures. However, he did not recommend using this measurement in the calculation of the Paris' law parameters (A and n) because the small cracks in the micro-crack zone in front of macro-crack were not measured by the foil approach, leading to a large difference between measurement and actual length. Instead, he suggested using crack opening displacement (COD) gauge measurements combined with finite element analysis to determine the Paris' law coefficients.

The other direct measurement approach is DIC, which was applied by Seo et al. (2004). They used the DIC in studying the deformation in the fracture process zone, which is a nonlinear zone around the crack tip. They used a digital camera to capture images of a surface-painted specimen under uniaxial tensile loading. After test, post-processing methods were applied to measure the grayscale and compare the deformed images with the undeformed images. Displacements and strain within the captured area were calculated. However, the measurement was still limited to the surface image, not inside condition, of the specimen. Zhou et al. (2007a, 2009) used the DIC approach to measure the crack growth on the overlay test specimen to verify the backcalculated crack length. The backcalculation method is discussed in the next section. They used two digital cameras and found that the crack growth on the two sides of specimen was different due to the heterogeneity of specimen.

(2) Backcalculation

Zhou et al. (2007a, 2009) backcalculated the crack length during overlay test using maximum tensile load at each cycle. Three assumptions were made to simplify the backcalculation procedure. First, the macro-crack initiates at the bottom of the specimen and propagate vertically to the top surface. Secondly, crack length development was highly correlated to the reduction of the maximum tensile load. Third, the asphalt mixture was regarded as a quasi-elastic material with specific modulus and Poisson's ratio corresponding to the testing conditions (maximum opening displacement, temperature, frequency, etc.). Jacob (1995) also applied the crack length backcalculation approach using a relative crack opening displacement (COD) to obtain the equivalent crack length in a 2-D finite element program. The use of relative COD instead of absolute COD normalized the effect of gauge location in the notch on the measurement. Equivalent crack is simulated single crack with the same COD measurement as that of the combined existing macro-crack and micro-crack zone.

2.2.3.10 Crack Propagation Model for Asphalt Mixture

Paris and Erdogan (1963) first proposed an empirical crack propagation law named Paris' law (also known as the Paris-Erdogan law). Germann and Lytton (1979) first applied this law in the overlay test to determine the reflective cracking resistance of the asphalt overlay. Recently, Zhou et al. (2007a) validated the upgraded overlay test in predicting fatigue cracking resistance of asphalt mixture and verified the predicted result by the performance data from the FHWA-Accelerated Loading Facility. In the prediction method, they obtained the coefficients of Paris' law (A and n) and predicted the number of cycles to initiate and propagate macro cracks through the asphalt layer in the field. After the J-integral was introduced in Paris' law for replacing the

stress intensity factor (K), viscoelastic behavior of asphalt mixture could be investigated (Zhou and Scullion 2003). Cleveland et al. (2003) developed a modified Paris' law based on the J-integral and the linear viscoelastic continuum damage theory to study the cracking resistance of asphalt mixtures modified by different geosynthetic materials. Schapery (1973, 1975, 1978) proposed a well-derived theory to determine the Paris' law parameters for viscoelastic material using a series of simple performance tests. However, this method for general viscoelastic material study was not directly applicable for asphalt mixture. Jacob (1995) summarized Schapery's method (Equation 19, 20, 21) and suggested a simplified way to estimate the parameters for asphalt mixture. Jacob (1995) suggested that two parameters (A and n) could be estimated using the master curve from dynamic stiffness (modulus) test and the results from uniaxial monotonic tensile test at constant displacement rate. Equation 22, 23, 24, 25 and 26 show the recommended calculation approach. Equations 22, 23 and 24 estimate the value of "n". Then, Equations 25 and 26 can be applied to estimate "A". The estimation using Equation 26 is more accurate than that of Equation 25. However, his suggestion was based on many regression coefficients for certain types of mixtures applied in the study. These coefficients may not be valid in determining Paris' law for other mixtures.

$$A = \frac{\pi}{6{\sigma_m}^2 {l_1}^2}\left[\frac{(1-v^2)D_2}{2\Gamma}\right]^{\frac{1}{m}}\left(\int_0^{\Delta t} w(t)^n dt\right) \tag{19}$$

$$n = \begin{cases} 2\left(1+\frac{1}{m}\right) & \text{For load} - \text{controlled test} \quad (20) \\ \frac{2}{m} & \text{For displacement} - \text{controlled test} \quad (21) \end{cases}$$

Where,

σ_m = material tensile strength;

l_1 = integration of stress near crack tip over the failure zone using Barenblatt (1962) approach;

v = Poisson's ratio;

D_2, m = regression coefficient from creep compliance master curve;

Γ = work done to produce a unit crack surface, determined by dissipated energy and crack length;

Δt = time required to complete one cycle in the controlled-displacement crack growth test; and

$w(t)$ = Integral of sinusoidal "K versus time" relationship in the period of one cycle.

$$D_{mix} = a_3 + a_4 \log t + a_5 (\log t)^2 \tag{22}$$

$$n_{est} = \frac{2}{(a_4 + 2a_5 \log t)CF} \tag{23}$$

$$\ln(CF) = b_0 + b_1 S_{mas} + b_2 S_{bit} + b_3 S_{mas} \ln(S_{bit}) \tag{24}$$

$$\log A_{est} = a_A + b_A n_{est} \tag{25}$$

$$\log A_{est} = d - 2a \log(\sigma_m) - b \frac{n_{est}}{2} \log(2\Gamma_{stat}) - c \frac{n_{est}}{2} \log(S_{mas}) \tag{26}$$

Where,

D_{mix} = creep compliance determined from the master curve in dynamic stiffness test (10^{-4}/MPa);

n_{est} = estimated n-value;

a_3, a_4, a_5 = regression coefficients from "creep compliance versus log (t)" relationship;

t = loading time, determined by 1/(10f) (second);

CF = correction factor;

b_0, b_1, b_2, b_3 = regression coefficients from "CF versus S_{mas}" relationship, S_{bit} can be calculated from S_{mas};

S_{mas} = mixture stiffness determined from temperature and frequency sweep tests (MPa);

S_{bit} = bitumen stiffness, backcalculated from S_{mas} by Bonnaure's method (MPa);

A_{est} = estimated A-value;

Γ_{stat} = fracture energy (N·mm/mm^2), determined from "log $(\frac{\Gamma_{stat}}{\Gamma_{stat,max}})$ versus log S_{bit}" relationship, $\Gamma_{stat,max}$ is the maximum fracture energy from static loading test; and

a, b, c, d = regression coefficients determined from the relationship between A_{est} and other factors in Equation 26.

Jacob (1995) also performed a more straightforward way to determine the Paris' law parameters for asphalt mixtures. This method started with crack length backcalculation as discussed in section 2.2.3.9. Combining COD measurement and finite element modeling, five mathematical relationships were obtained based on the specific material, temperature, frequency and maximum opening displacement (Jacob 1995). This measurement-based method determining the Paris' law parameters was also applied by Zhou et al. (2007a) in the overlay test and by Roque et al. (1999) in the indirect tension test (IDT).

It should be noted that Jacob (1995), Zhou et al. (2007a), and Roque et al. (1999) used the same crack growth calculation method except for the choices of factors they applied to backcalculate the crack length. The factors they applied were all from direct measurements. Jacob (1995) used the relative COD (or normalized COD) in an uniaxial tensile test performed on a beam-shaped specimen (50mm×50mm×150mm). Zhou et al. (2007a) selected the normalized load in the OT. Roque et al. (1999) reported that normalized horizontal displacement on the specimen of the indirect tensile test (IDT) was good to use. These direct measurements (peak values within each loading cycle) were all normalized to represent the damage process of specimen relative to its intact state. Table 2.1 summarizes the similarities among these three studies in determining the Paris' law parameters for asphalt mixture. "NF" represents the normalized factors: crack opening displacement, applied load, or horizontal displacement.

Table 2.1 Similarities between Three Studies

No. of Step and Correlations	Procedures
1	NF vs. Number of loading cycles (NF vs. N)
2	NF vs. Crack length (NF vs. C) (Jacob performed this procedure by combining two correlations: NF vs. K and K vs. C)
1+2→3	Crack length vs. Number of loading cycles (C vs. N)
4	Stress intensity factor vs. Crack length (K vs. C)
3+4→5	dC/dN vs. ΔK (or in log-log scale)

2.2.3.11 Application of crack propagation law in predicting fatigue life of asphalt layer

Zhou et al. (2007a) validated the application of OT in predicting traditional fatigue cracking of asphalt mixtures. In the development of fatigue cracking, the number of loading cycles to failure (N_f) includes the cycles required for crack initiation and propagation (N_i and N_P), respectively. The initiation stage (N_i) is the number of cycles needed for micro-cracks to coalesce to form a macro-crack. The propagation stage (N_p) is the number of cycles for a macro-crack to propagate through the thickness of asphalt layer. Equation 27 demonstrates the correlation between the number of cycles to failure (failure point) and the number of cycles in the two stages.

$$N_f = N_i + N_p \quad (27)$$

Where,

N_f = number of cycles to failure (failure point);

N_i = number of cycles initiate a macro-crack; and

N_p = number of cycles for macro-crack to propagate through asphalt layer.

Crack propagation dominates crack development in the overlay test and it has strong correlation with crack initiation. Zhou et al. (2007a) suggested that the overlay test was able to demonstrate cracking behavior before macrocrack initiates. Typically, number of cycles for crack initiation (N_i) was calculated by the traditional method using Equation 28. Asphalt mixture in OT was assumed to behave like elastic material with modulus and Poisson's ratio. This assumption made Paris' law in linear elastic fracture mechanics applicable for analyzing OT results (Zhou et al. 2009). Thus, the number of cycles for crack propagation (N_p) was calculated by Paris' law using Equation 29. Lytton et al. (1993) suggested that the stress intensity factor (K) in Equation 29 can be calculated by using Equation 30. Therefore, by integrating and rearranging Equation 29, the value of N_p can be determined from a function of strain as showed in Equation 31 based on known material properties and testing conditions. Lytton et al. (1993) also pointed out that Paris' Law was also valid to calculate the growth of microcrack in the crack initiation stage for viscoelastic material. Therefore, Equation 28 used for calculating traditional crack initiation can be equated to Equation 31 (Zhou et al. 2007b). After equating these two functions, the coefficient k_2 was found to equal to "n" (Equation 33). Coefficient k_1 can be determined as a function of "A" and "n" (Equation 32). After the Paris' law parameters were determined from the overlay test, Equation 32 and 33 were used to calculate the parameters k_1 and k_2 in Equation 28 (Zhou et al. 2007b). Entering the maximum tensile strain at the bottom of asphalt layer (ε) into Equation 28, crack initiation cycles (N_i) can be obtained (Zhou et al. 2007a, Zhou et al. 2007b).

$$N_i = k_1 \times (1/\varepsilon)^{k_2} \tag{28}$$

$$dc/dN = A \times (\Delta K)^n \tag{29}$$

$$K = r\left(\frac{c}{d}\right)^q \sigma\sqrt{d} \tag{30}$$

$$N_p = \frac{{d_1}^{(1-n/2)}}{Ar^n(1-nq)E^n}\left[1-\left(\frac{c_0}{d_1}\right)^{(1-nq)}\right]\left(\frac{1}{\varepsilon}\right)^n \tag{31}$$

$$k_1 = \frac{{d_1}^{(1-n/2)}}{Ar^n(1-nq)E^n}\left[1-\left(\frac{c_0}{d_1}\right)^{(1-nq)}\right] \tag{32}$$

$$k_2 = n \tag{33}$$

Where,

k_1, k_2, q, r = regression coefficients;

ε = maximum tensile strain at the bottom of asphalt layer;

c = crack length;

c_0 = initial macrocrack length;

N = number of loading cycles;

A, n = Paris' law parameters;

ΔK = change of stress intensity factor;

d = thickness of test specimen;

d_1 = thickness of asphalt layer (the total length of crack to grow);

σ = maximum stress in the specimen; and

E = asphalt layer modulus at specific frequency and temperature.

However, the method for calculating the coefficient k_1 (Equation 32) seems complicated. Therefore, Zhou et al. (2007a) simplified this method based on the relationship between

parameter A, n, and log E. Equation 34 shows the simplified way to obtain coefficient k_1. The coefficients (a_1, a_2, a_3) were obtained through a regression analysis of the data from 1348 bending beam fatigue tests in other studies. With the values of log k_1, k_2, and log E known, the optimized form of Equation 34 can be determined using least squares estimation.

$$\log k_1 = a_1 + a_2 k_2 + a_3 \log E \tag{34}$$

Where,

a_1, a_2, a_3 = regression coefficients; and

E = dynamic modulus of asphalt mixture at specific temperature and frequency.

After the number of cycles for crack initiation (N_i) is determined, the second stage for crack propagation needs to be considered in order to predict the fatigue life of asphalt layers using Equation 27. In the overlay test, small crack growth could be predicted by small change of stress intensity factor and the number of loading repetitions causing these changes (Equation 35) (Zhou et al. 2007a). However, to predict the crack propagation in the pavement layer, the effect of actual load on the crack propagation needs to be considered. Zhou et al. (2007a) proposed that one axle passing the top of crack-initiated overlay had three effects on the crack propagation. When the load was right on the top of crack tip, bending of the overlay may take place and drive the Mode-I cracking. As the load was approaching and leaving the crack, the major driving force for the crack propagation was shearing leading to the Mode-II cracking. Therefore, two times of $K_{shearing}$ changes along with one-time $K_{bending}$ change were the result of one axle load pass. These three changes of stress intensity factor (ΔK_i) should be directly reflected by the change of crack

length according to Paris' law. Zhou et al. (2007a) calculated these stress intensity factors using the finite element method. It should be noted that they assumed the parameters ("A" and "n") for bending and shearing to be the same based on their past studies. Equation 36 calculated the change of crack length until the accumulated crack growth was equal to asphalt layer thickness. Summation of the required loading passes during every small crack growth was the number of loading cycles for crack propagation (N_p) (Equation 37). According to Equation 27, N_f can be calculated by the summation of N_i (Equation 28) and N_p (Equation 37).

$$\frac{dc}{dN} = \frac{\Delta c}{\Delta N} = A(\Delta K)^n \tag{35}$$

$$\begin{aligned} \Delta c &= 2A\left(\Delta K_{shearing}\right)^n \Delta N + A\left(\Delta K_{bending}\right)^n \Delta N \\ &= A\left[2\left(\Delta K_{shearing}\right)^n + \left(\Delta K_{bending}\right)^n\right] \Delta N \end{aligned} \tag{36}$$

$$N_p = \sum \Delta N \tag{37}$$

Where,

Δc = change of crack length;

$\Delta K_{shearing}$ = change of stress intensity factor induced by shearing;

$\Delta K_{bending}$ = change of stress intensity factor induced by bending; and

ΔN = number of load pass.

Zhou et al. (2007a) verified this prediction approach based on the Paris' law parameters from overlay test on six FHWA-ALF test lanes. The measured fatigue life was the number of ALF

loading repetitions when cracking occurred on 50 percent lane area. The average ratio of the measured fatigue life to the predicted fatigue life was equal to 1.3. In addition, Zhou et al. (2007a) applied Miner's law (Equation 38) to calculate the accumulated damage under certain amount of loading repetitions. The amount of damage was entered into the crack model (Equation 39) in the Mechanistic-Empirical Pavement Design Guide (MEPDG). They commented that the current cracking model (Equation 39) in the MEPDG did not predict the fatigue crack area in the field very well. Therefore, a calibration with the predicted and the observed crack area data to determine a_1, a_2 in Equation 39 was recommended.

$$\text{Damage} = \sum_{i=1}^{T} \frac{n_i}{N_f} \times 100\% \tag{38}$$

$$\text{Crack area (\%)} = \frac{100}{1 + e^{(a_1 + a_2 \times \log \text{damage})}} \tag{39}$$

Where,

T = total number of periods;

n_i = actual load repetitions in i^{th} period; and

a_1, a_2 = calibration coefficients (a_1 and a_2 are functions of asphalt layer thickness).

2.2.3.12 Correlation between overlay test and BBF test

Zhou et al. (2007b) compared BBF test results with overlay test results for three types of HMA. In the BBF test, specimens were tested using 374 microstrain at 20 °C. In the overlay test,

specimens were tested using 0.63 mm (0.025 inch) maximum opening displacement at 25 °C. After comparing the number of cycles to failure from two tests, they found that the ranking of three types of HMA were the same. Therefore, Zhou et al. (2007b) proposed that the overlay test could be an alternative for BBF test in determining the fatigue cracking resistance.

2.2.3.13 Correlation between overlay test result and field performance

Zhou and Scullion (2005a) performed a validation study on the application of the overlay tester in differentiating asphalt overlay mixtures in terms of cracking resistance performance. Field cores from several pavement sections on US175, US84, SH3, SH6 and IH10 in Texas were taken and trimmed according to the size requirement of overlay test. For SPS5 sections on US175, only the bottom asphalt layer on the core was used to fabricate the specimen. Before taking these cores, the cracking performance of each pavement was already known. One section (SPS5) on US175 had no reflective crack after 10-year service. Other sections demonstrated different levels of reflective cracking distress shortly after laydown and opening to traffic. After overlay testing was performed, results showed that virgin mixture from the section (SPS5) with no-reflective crack on US175 had the longest reflective cracking life (number of cycles to failure): about 300 cycles. Most mixtures from other sections were tested to failure within 50 cycles. Zhou and Scullion (2005a) also took cores from three cells (15, 18, and 20) on the MnROAD to study the low temperature cracking resistance using the overlay tester. Two cores were taken from the mid-lane within each cell and tested after trimming off the micro-surfacing layer. After trimming, only the top asphalt layer was used for testing. Good correlation was found between the observed cracking performance and the overlay test results. Accordingly, they proposed that

the overlay test was also good to predict low temperature cracking resistance. Zhou et al. (2007b) also validated the overlay test result with the FHWA-ALF fatigue test results on 6 lanes where loading was applied by a super single tire on the experimental pavement lanes. The ranking of fatigue cracking performance for asphalt mixtures by the FHWA-ALF test was similar to the ranking by the overlay test. The OT was adopted to conduct a reflective crack resistance control for the very thin overlay mixes in Texas (Scullion et al. 2009). The compacted specimen should withstand more than 750 loading cycles before failure. A half year after laydown, the overlay performance was inspected. Some reflective transverse cracks, humps, and a longitudinal crack due to foundation problem were found. But overall performance was good without load-related reflective cracking issue.

2.2.3.14 Effect of mixture properties on overlay test result

Texas Transportation Institute (TTI) conducted the overlay test to study the cracking resistance of Evotherm warm mix and compared with that of hot mix. During the tests, specimens of warm mix lasted longer than those of hot mix before failure occurred. It was concluded that Evotherm warm mix had better cracking resistance than hot mix (Crews 2009).

Zhou and Scullion (2005a) found that mixture properties (i.e. binder content, binder grade, aggregate type, and aggregate gradation) significantly affect the result of the overlay test. Mixtures with higher binder content, lower binder high-temperature performance grades, less absorptive rock, and finer gradations tend to have more reflective crack resistance. When they investigated the effect of aggregate absorption, they compared the crushed gravel aggregate with

limestone. Immediately after test, they examined the failure plane and found that gravel aggregates with little absorption demonstrated a shining failure plane; absorptive limestone showed a dry failure plane. Analysis of the testing data showed that the crushed gravel mixture required more cycles to failure than that of the limestone mixture. To verify this finding, they compared the overlay test result using three additional limestone aggregates with various absorption levels. Controlling the asphalt type and aggregation gradation, they found that the number of cycles to failure decreased when aggregate absorption increased.

Recently, Hu et al. (2011) investigated the effects of material properties on the overlay test result. Seven factors (or properties) were studied, including binder grade, effective binder content, air void content, VMA, asphalt absorption, surface area of aggregates (SA), and film thickness of binder (FT). Two statistical methods were used to analyze the testing results. The first one was Pearson's correlation which was commonly used to determine the level of linear correlation between two variables. In their analysis among the six factors (except for the binder grade), three pairs of factors with high correlations include (1) V_{be} and FT, (2) FT and VMA, and (3) asphalt absorption and FT. After applying Pearson's correlation method, the other statistical method named analysis of covariance (ANCOVA) was performed to determine the regression model between N_{OT} and those uncorrelated factor(s). Typically, ANCOVA was an adjusted ANOVA that can consider both quantitative and qualitative factors (Scheffe 1959). The analysis results showed that effects of air void content and asphalt absorption were not statistically significant on the overlay test result (i.e., failure point). Finally, three factors (binder type, film thickness (FT), and surface area (SA)) were determined to be included in the model as shown in Equation 40. FT and binder content (P_b) calculation methods were also proposed as shown in

Equation 41 and 42. The minimum asphalt content for cracking resistance can be calculated using Equation 42 by entering the minimum FT. The recommended limit for binder content was verified by performance examination on nine overlay sections placed on I-20 interstate highway near Atlanta, Texas.

$$N_{OT} = a_1 \times e^{(a_2 \times FT)} \times SA^{a_3} \tag{40}$$

$$FT = \frac{(P_{be}/G_b)}{(SA \times P_s)} \times 1000 \tag{41}$$

$$P_b = \frac{100 \times FT \times SA \times G_b + 1000 \times P_{ba}}{1000 + FT \times SA \times G_b + 10 \times P_{ba}} \tag{42}$$

Where,

a_i = regression coefficient determined by binder type and FT value (i=1,2,3);

FT = film thickness (μm);

SA = surface area of binder coating on aggregates (m^2/kg);

P_{be} = effective binder content by mass of mixture;

G_b = specific gravity of binder;

P_{be}/G_b = effective binder volume;

P_s = aggregate content by mass of mixture;

P_b = binder content by mass of mixture; and

P_{ba} = binder absorption by mass of mixture.

2.3 Summary of Literature Review

Generally, the bending beam fatigue (BBF) test and the overlay test (OT) are similar. Both tests are cyclic fatigue tests and the obtained results indicate asphalt mixture's resistance to cracking at ambient temperature. Consistent tensile strain is applied at the bottom of specimen by controlling the maximum displacement in each loading cycle during the test. However, some differences need to be considered when comparing the results of two tests are as follows.

- Fabrication. Two specimens are different in size and compacted by different methods.
- Loading mode. BBF test specimen endures bending deformation while OT specimen cannot bend due to the fixed plates on which the specimen is glued. Frequency is much higher and tensile strain is much lower in BBF test compared to those of OT.
- Cracking behavior. Microcrack is the major damage type in the bending beam specimen while macrocrack dominates in OT specimen.
- Failure point determining method. Failure point in BBF test is determined based on stiffness development while peak load development is used for determining that in OT.
- Other useful test results. Dissipated energy can be obtained in BBF test and crack propagation model coefficients (Paris' Law coefficients) can be calculated from OT result.

CHAPTER 3 LABORATORY TESTING

This chapter describes the overlay test in the asphalt mixture performance tester (AMPT), followed by discussions on asphalt mixtures selected for this testing, experimental plan, and specimen fabrication procedure. A discussion of the current method and a new method for determining the failure point of the overlay test are also provided.

3.1 Overview of Overlay Test in the AMPT

The overlay test procedure described in the TxDOT test method (Tex-248-F-09) can be conducted in both the Texas Overlay Tester and the AMPT using an Overlay Test Kit (IPC Global). Figure 3.1 shows an overlay test being conducted in an AMPT. A test specimen (150 mm long, 76 mm wide and 38 mm thick) can be cut from a gyratory compacted specimen or a field core. The test specimen is epoxied to a set of two steel plates and then loaded vertically into the AMPT. During the test, the top plate remains fixed while a cyclic triangle-wave load is applied to the bottom plate to maintain a constant maximum opening displacement between the two base plates.

Figure 3.1 AMPT with overlay test kit

3.1.1 Displacement Measurement Method

The AMPT overlay test uses two LVDTs for measuring the actuator displacement and the opening displacement between the two base plates. The second LVDT in the AMPT overlay test is located on the back of the base plates, as shown in Figure 3.2. The actuator LVDT measures the displacement of actuator in a range of ± 15 mm, and the external LVDT has a lower measurement range of ± 0.5 mm.

Figure 3.2 External LVDT on the back of steel plates

In the AMPT overlay test, the MOD is measured directly by the external LVDT (Figure 3.2). This MOD measurement is kept constant during the test by adjusting the actuator displacement and is referred to as the target displacement. The overlay test software in the AMPT has an Adaptive Level Control (ALC) option. With this option enabled, the external LVDT reading is monitored during the test. If the target displacement is not achieved, the actuator displacement will be adjusted to maintain the specified target displacement.

3.1.2 Machine Compliance in the AMPT Overlay Test

For the AMPT overlay test, the two LVDTs are expected to produce different readings because the actuator LVDT measures the actuator displacement that consists of the specimen deformation

and the loading frame deformation. Equation 43 shows the relationship between two LVDT-measured displacements. The machine compliance can be calculated using Equation 43 and 44 (Kalidindi et al. 1997).

$$\delta_2 = \delta_1 - \delta_3 \tag{43}$$

$$C_m = \delta_2 / F \tag{44}$$

Where,

δ_1 = displacement measured by actuator LVDT;

δ_2 = deformation of loading system;

δ_3 = deformation of specimen measured by external LVDT;

C_m = machine compliance; and

F = measured load.

Figure 3.3 shows the difference between the maximum actuator displacements measured using the actuator LVDT and the maximum opening displacements measured by the external LVDT in the AMPT. Results plotted in Figure 3.3 were obtained from a test conducted on a specimen at a frequency of 0.1 Hz and using an MOD of 0.381-mm. The displacement measured by the external LVDT is constant throughout the test except for several cycles in the beginning. The actuator LVDT is adjusted in every loading cycle to maintain the target external displacement. The actuator displacement increases gradually before 125th cycle, followed by a rapid increase. Then, the actuator displacement becomes close to the external displacement to the end of the test.

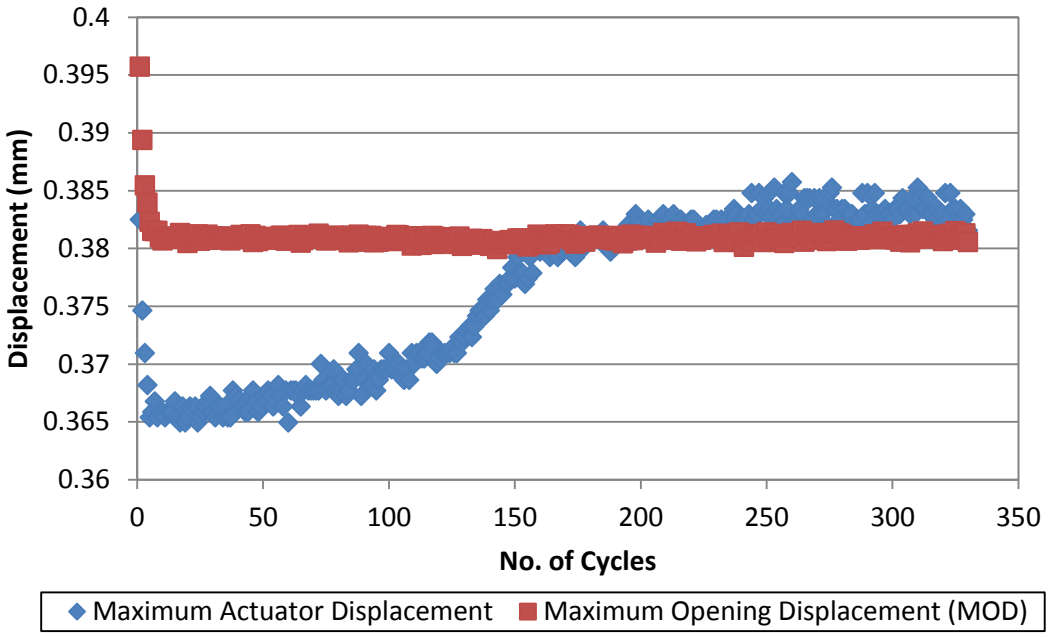

Figure 3.3 Maximum actuator displacements versus maximum opening displacements in AMPT Overlay Test

The difference between the two measurements is due to the machine compliance, and this difference is varied during the test depending on stiffness of the specimen being tested and the level of damage occurring in the specimen. Therefore, controlling the maximum opening displacement is better than controlling the maximum actuator displacement in the AMPT overlay test, eliminating a need for correcting the machine compliance after the test is completed.

3.2 Properties of Asphalt Mixtures

Five mixtures used in the bottom asphalt layers of the five test sections (S8-3, S10-3, S11-3, N10-3, and N11-3) of the Group Experiment in the 2009 research cycle of the NCAT Test Track

were selected for this study. These mixes were chosen so that results of the laboratory evaluation can be compared with field performance of these mixes at the Test Track in the future. The evaluation of these mixes is still underway at the Test Track (West et al. 2012).

Table 3.1 shows the volumetric properties of all the mixtures used for preparing overlay test specimens in this study. They were plant-produced and sampled during the construction of these test sections. The S8-3 mixture served as the control mixture in this study was produced hot without reclaimed asphalt pavement (RAP). The S10-3 and S11-3 mixtures, which used the same mix design without RAP as the S8-3 mixture, were produced warm using foaming and additive WMA, respectively. The N10-3 and N11-3 mixtures were based on a mix design with 50 percent RAP. The N10-3 mixture was produced hot, and the N11-3 mixture was produced warm using foaming WMA. The 50 percent RAP in the mixtures included 20 percent fine fraction RAP and 30 percent coarse fraction RAP. More information about the mixtures used in this study is available elsewhere (Powell 2013).

Table 3.1 Mixture Properties

Properties	Mixtures				
	S8-3	S10-3	S11-3	N10-3	N11-3
NMAS (mm)	19	19	19	19	19
Virgin Asphalt PG Grade	67-22	67-22	67-22	67-22	67-22
% RAP	0	0	0	50	50
WMA	No	Foam	Additive	No	Foam
Design Air Voids (VTM), %	3.6	4.1	3.0	4.2	4.1
Total Combined Binder (P_b), % wt	4.9	4.7	5.0	4.7	4.6
Effective Binder (P_{be}), %	4.4	4.2	4.5	4.1	4.0
Dust Proportion (DP)	1.2	1.2	1.2	1.4	1.3
Maximum Specific Gravity (G_{mm})	2.532	2.533	2.522	2.537	2.544
Voids in Mineral Aggregate (VMA), %	14	14.0	13.7	13.8	13.7
Voids Filled with Asphalt (VFA), %	75	71	78	72	70

3.3 Testing Plan

As specified in the TxDOT procedure, the overlay test should be conducted using a maximum opening displacement (MOD) of 0.635 mm (0.025 in.) and at a test frequency of 0.1 Hz. This recommended MOD was originally applied for evaluating asphalt mixtures used in overlays on top of old concrete pavements in Texas. The MOD was calculated based on the thermal expansion of a 4.5-m (15-ft) long concrete slab under a 17°C (30°F) daily temperature variation. Two types of concrete slab with gravel and limestone aggregates were considered, and the average thermal expansion (0.635-mm) was recommended in the current TxDOT procedure (Zhou and Scullion 2003).

However, if this test is used to evaluate the cracking resistance of stiff asphalt mixtures (e.g., mix with higher RAP and/or RAS contents) and those mixes for overlays placed in other states that have different climatic conditions (i.e., smaller daily temperature variation), the maximum opening displacement may need to be lower (Tran et al. 2012). For this study, three MOD levels (i.e., 0.381, 0.318, and 0.254 mm) were selected to evaluate the relationships between the MOD, number of cycles to failure and field performance (it should be noted that the field evaluation of these test sections is underway and thus not presented in this thesis). At the lower MOD levels, the overlay test takes much longer, especially at the MOD of 0.254 mm. Thus, it is desirable to evaluate the overlay test for conducting at a higher frequency (i.e., 1 Hz) to reduce the testing time. Results of this evaluation are presented in the next chapter.

Table 3.2 shows a laboratory testing plan designed to investigate the alternative method for determining the failure point and the use of a higher frequency (i.e., 1 Hz). Due to the availability of plant-produced mix, the overlay test was conducted at two test frequencies (0.1 and 1 Hz) for the N11-3 mix and only at the higher frequency (1 Hz) for other mixtures. For each mix, overlay testing was conducted at three MOD levels (i.e., 0.254, 0.318, and 0.381 mm) and using three replicates for each testing combination. This experimental plan was designed in the interest of time and availability of plant-produced mixes for this study.

Table 3.2 Laboratory Testing Plan

Section	Mixture (19 mm NMAS)	Frequency (Hz)	Maximum Opening Displacement	No. of Replicates
S8-3	Control	1	0.254	3
		1	0.318	3
		1	0.381	3
S10-3	WMA Foam	1	0.254	3
		1	0.318	3*
		1	0.381	3
S11-3	WMA Additive	1	0.254	3
		1	0.318	3
		1	0.381	3
N10-3	50% RAP	1	0.254	3
		1	0.318	3
		1	0.381	3
N11-3	50% RAP + Foam	1	0.254	3
		1	0.318	3
		1	0.381	3
		0.1	0.254	3*
		0.1	0.318	3
		0.1	0.381	3*
Total Number of Specimens Tested				54

Notes: Due to issues with some recorded videos, a total of 48 (instead of 54) videos were analyzed for this study. The number in the last column labeled with "*" indicates those tests have incomplete video records. S10-3 mix tested at 0.318-mm MOD and 1Hz has one specimen without video record; N11-3 mix tested at 0.254-mm MOD and 0.1Hz has three; N11-3 mix tested at 0.381-mm MOD and 0.1Hz has two. The specific number of specimen analyzed and its result are listed in the Appendix B.

3.4 Specimen Fabrication Procedure

1) Heated a bucket of a plant-produced mixture in an oven at compaction temperature for 4 hours.
2) Splitted the heated mixture into the appropriate sample size for compaction.
3) Reheated the samples until the mixture temperature reached the compaction temperature.
4) Compacted each sample using the gyratory compactor to the height of 115 mm.
5) Cooled down the molded samples and determined the bulk specific gravity.
6) Cut each compacted sample to prepare one overlay test specimen.
7) Dried each test specimen in front of a fan overnight and determined the bulk specific gravity and the specimen air void content.
8) If the air void content is within 7.0 ± 1.0 percent, dry the specimen in front of a fan overnight and measured the size (length, width, and thickness).
9) Sealed each test specimen with a wrap if it is to be tested more than two weeks later.

3.5 Test Setup

To monitor the development of cracks on each specimen during overlay testing, a rectangular area was painted white on one side of each specimen, and a 2 mm × 2 mm black grid was then drawn on the painted surface before the specimen was glued on the base plates. The development of cracks on the painted side was monitored using a high definition camcorder for analysis later in the study. The following steps were taken to prepare specimens for testing.

In the first step, the two base plates were aligned and bolted on a mounting jig. A small gap was left between two plates, and a tape (6.09 mm wide) is placed over the gap. Figure 3.4 (a) shows the setup of the two base plates for the AMPT overlay test. Figure 3.4 (b) shows a smaller set of base plates used in the AMPT overlay test and a larger set of base plates used in the Texas Overlay Tester. The steel base plates are grooved to increase the bond between the test specimen and the base plate after they were glued together. Table 3.3 shows the dimensions of the base plates.

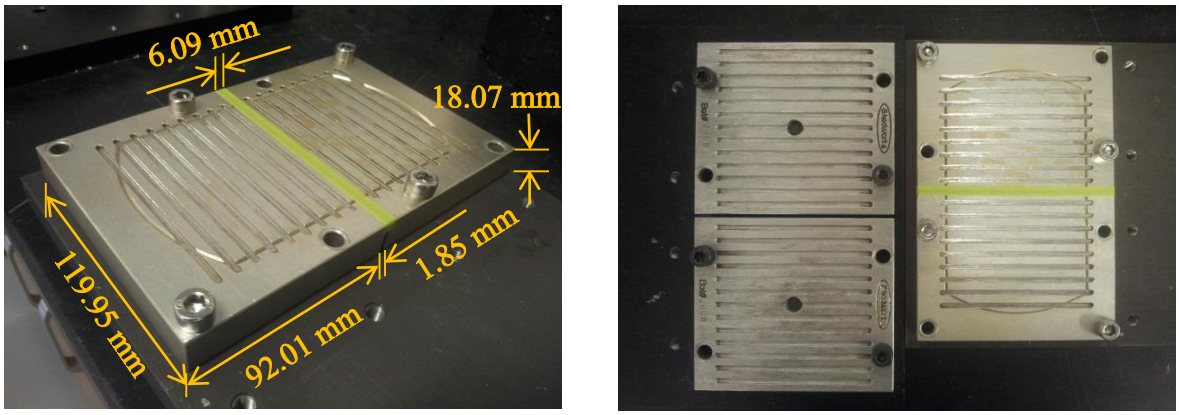

(a) AMPT base plates (b) Overlay tester and AMPT base plates

Figure 3.4 Base plates

Table 3.3 Base Plate Dimensions

Dimension	AMPT Overlay Test (mm)	Texas Overlay Tester (mm)
Plate Dimension		
Length	92.01	108.09
Width	119.95	120.74
Height	18.07	17.90
Gap width	1.85	2.10
Gap tape width	6.09	6.09
Groove Dimension		
Groove width	3.10	3.16
Groove depth	1.73	1.68
Groove interval	4.90	4.75

In the second step, glue (DEVCON 2-ton Epoxy in Figure 3.5(a)) was applied on the bottom side of the specimen. Glue amount measurements on 45 specimens showed that the average amount for each specimen in this study was 8.3 g, and the standard deviation was 1.1 g. Figure 3.5(b) shows the glue was uniformly applied on the specimen, and Figure 3.5(c) shows the residual glue after the specimen was removed at the end of testing. In this study, a glue amount of 9.0 g was enough to provide good bonding between a specimen and base plates. It was observed that it may be excessive if a glue amount of 10 g is used.

(a) Glue type

(b) Glue uniformly applied on specimen

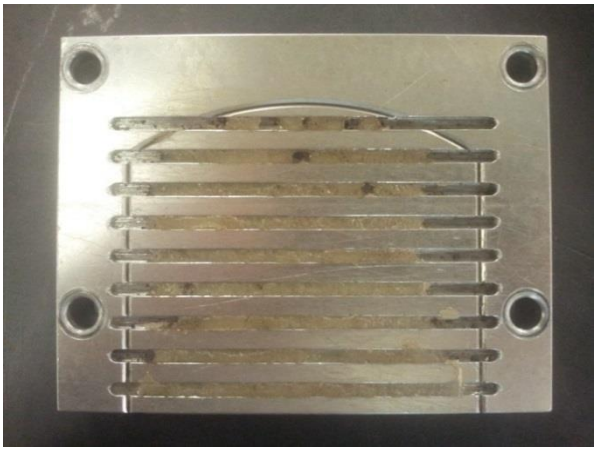

(c) Residual glue after specimen removed (9.0-g glue applied)

Figure 3.5 Glue type and amount

In the final step, the specimen with uniformly applied glue was placed on the top of the base plates. Then, the glue was cured overnight as shown in Figure 3.6. The specimen was then conditioned in an environmental chamber at 25 °C for at least 1 hour before testing. After conditioning, the test specimen with the base plates was set up in the AMPT (Figure 3.7).

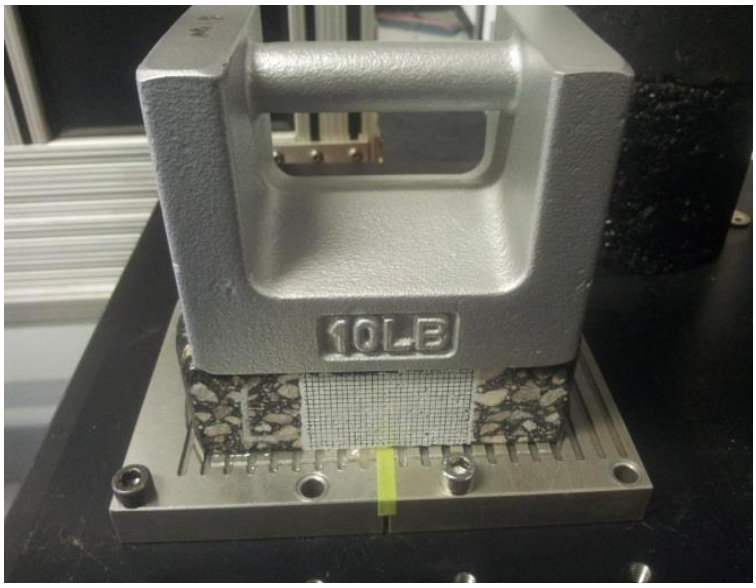

Figure 3.6 Glue curing setup

Figure 3.7 Setup of specimen glued on base plates in AMPT

3.6 Method for Determining the Failure Point

The TxDOT procedure defines the failure point (i.e., the number of cycles to failure) as the number of cycles at which the applied peak load is reduced by 93 percent compared to the applied peak load measured at the beginning of the test (hereafter referred to as the 93% reduction method). Based on this method, cracks are often seen propagated through the entire thickness of the specimen long before the applied load is reduced by 93 percent of the initial load.

An alternative method, referred to as the "normalized load × cycle" or NLC, was evaluated in this study for use in the overlay test. The NLC method is developed based on the "normalized stiffness × cycle" method described in the ASTM D7460 standard (a description of this method

was presented in the previous chapter). The "normalized stiffness × cycle" method was modified from the "reduced energy ratio" method/theory (Rowe 1993, Rowe and Bouldin 2000) to determine the failure point for the BBF test. In the BBF test, failure point is defined as the transition point from micro-crack to macro-crack propagation, and as described in ASTM D7460, it is the number of cycles at which the curve of "normalized stiffness × cycle" versus number of cycles reaches the maximum value.

For the alternative method, the "normalized stiffness" term is replaced with the "normalized load" term. The failure point or the number of cycles to failure for the overlay test can be determined in three steps. First, the "normalized load × cycle" is determined using Equation 45 for each load cycle. Then, the NLC is plotted against the number of cycles. Finally, the failure point is determined corresponding to the peak of the NLC curve. Figure 3.8 illustrates how the failure point can be determined for an overlay test. In this study, the alternative method for determining the failure point was evaluated. Results of this evaluation are presented in the next chapter.

$$\mathrm{NLC} = \frac{\mathrm{P_i} \times \mathrm{N_i}}{\mathrm{P_1} \times \mathrm{N_1}} \tag{45}$$

Where,

NLC = normalized load × cycles (kN/kN);

P_i = peak load at cycle number i (kN);

P_1 = peak load at 1st cycle (kN);

N_i = cycle number i; and

N_1 = cycle number at which P_1 is estimated.

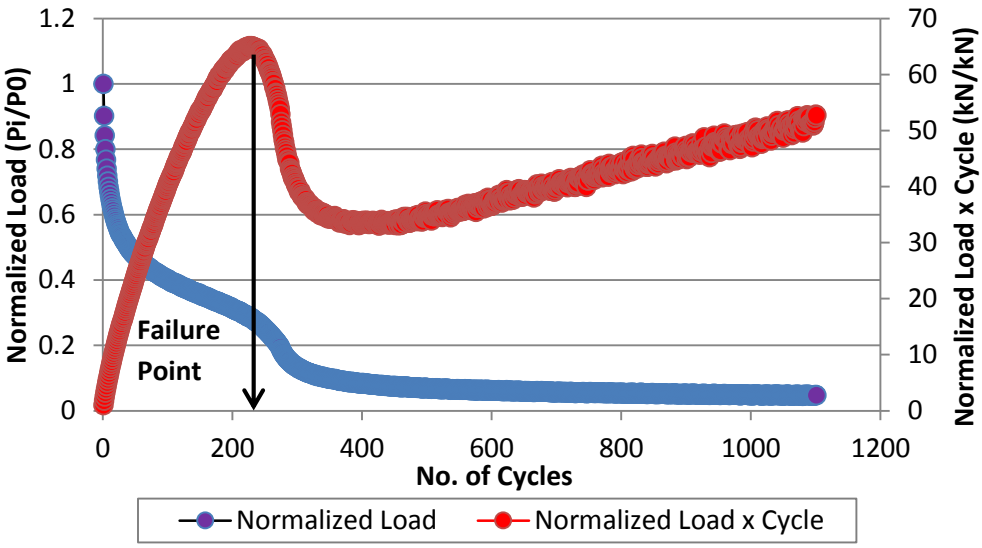

Figure 3.8 Determination of failure point

CHAPTER 4 RESULTS AND ANALYSIS

This chapter summarizes the results of overlay testing in the AMPT and analysis. First, the proposed "normalized load × cycle" (NLC) method and the 93-percent load reduction method for determining the failure point in the overlay test are evaluated using the video recorded during testing and the relationship of peak load versus the number of cycles. Second, the failure points determined by both methods are obtained and compared to the moment of failure when crack was first visually observed to propagate through the specimen. After that, the effect of higher frequency on the testing result is discussed.

4.1 Evaluation of Methods for Determining the Failure Point

For each specimen, still images capturing the specimen cracking conditions corresponding to the failure points determined according to NLC and 93-percent reduction methods were extracted from the video being recorded during the test. Figure 4.1 include three images showing cracking conditions at the two failure points and at the moment when the crack was first observed to propagate through the specimen. A brief discussion of these images follows.

- Figure 4.1(a) shows the cracking condition at the number of cycles determined as the failure point based on the NLC method (N_f(NLC)). At this failure point, the crack typically has not visually propagated through the specimen thickness.

- Figure 4.1(c) shows the specimen condition at the number of cycles determined as the failure point determined based on the 93% reduction method (N_f(93%)). At this failure point, the crack typically has propagated through the specimen long before the test ends at the 93% reduction of the peak load.
- Figure 4.1(b) shows the specimen condition when the crack was first visually observed to propagate through the specimen (N_f(Thru Crack)). The number of cycles corresponding to this moment was determined for each specimen for analysis. Of 48 specimens with good recoded videos, four specimens (# 86, 88, 89 and 121) had multiple cracks captured in the video, and the number of cycles when the first continuous crack propagates through the thickness was determined as N_f(Thru Crack). Other seven specimens (# 26, 40, 74, 75, 110, 111, and 123) had multiple short cracks throughout the thickness of the specimen, but those cracks were not connected even after the peak load had reached the 93% reduction of the initial value. For these seven specimens, the N_f(Thru Crack) was determined as the first number of cycles at which the shapes of the cracks remained unchanged through the end of the test. Further investigation of the test data and recorded videos of these 11 specimens did not find any unusual behaviors, so they were included in the analysis.

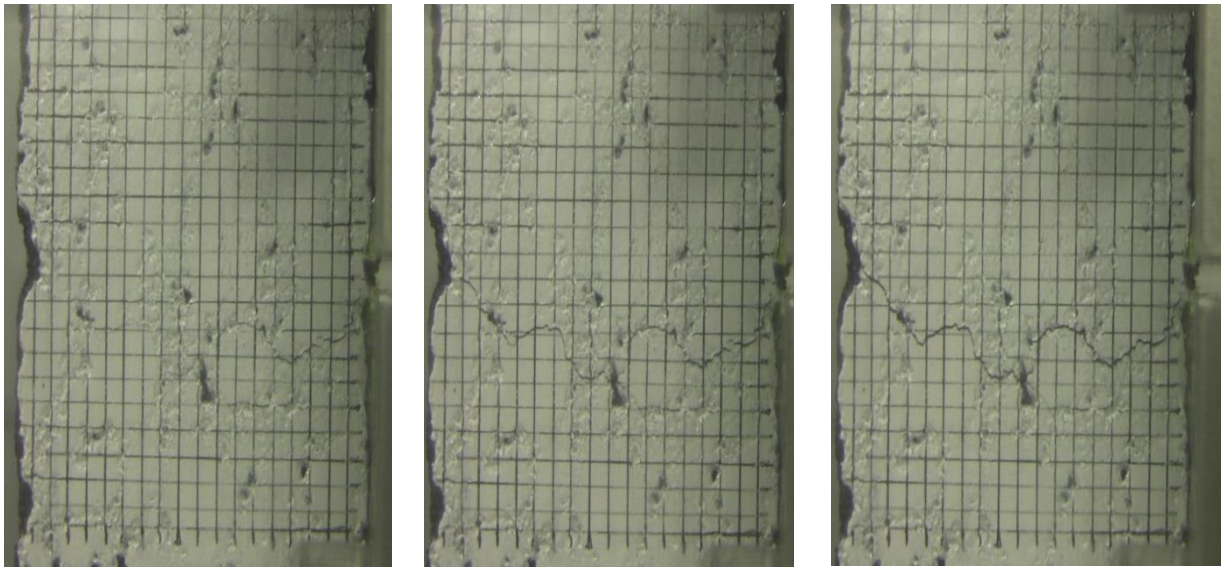

(a) N_f(NLC) (b) N_f(Thru Crack) (c) N_f(93%)

Figure 4.1 Specimen cracking condition at three moments (0.318-mm MOD and 0.1-Hz frequency)

The numbers of cycles corresponding to the three specimen conditions shown in Figure 4.1 are plotted on the curve of peak load versus number of cycles in Figure 4.2. As shown in Figure 4.2, the peak load versus number of cycles curve typically has four different stages as follows:

1. In Stage I, the peak load decreased sharply.
2. In Stage II, the peak load decreased at an approximately constant rate. The failure point determined based on the NLC method was approximately at the end of Stage II. Even though the crack was not visually observed to propagate though the thickness of the specimen at the N_f(NLC), micro-cracking may have occurred in the portion of the specimen that did not have visible cracks. Thus, the crack was able to propagate through this portion of the specimen quicker.

3. In Stage III, the load started to decrease at a higher rate after the N_f(NLC) failure point. For most specimens tested, the failure point corresponding to the moment the crack was first observed to propagate through the specimen in the video was near the end of this stage (Of 48 specimens with good recorded videos, 32 specimens exhibit this trend).
4. In Stage IV, the peak load started to decrease at a much lower rate. It took a lot more cycles before the peak load reached the 93-percent reduction of the initial peak load. The N_f(93%) failure point was also set as the end of the overlay test.

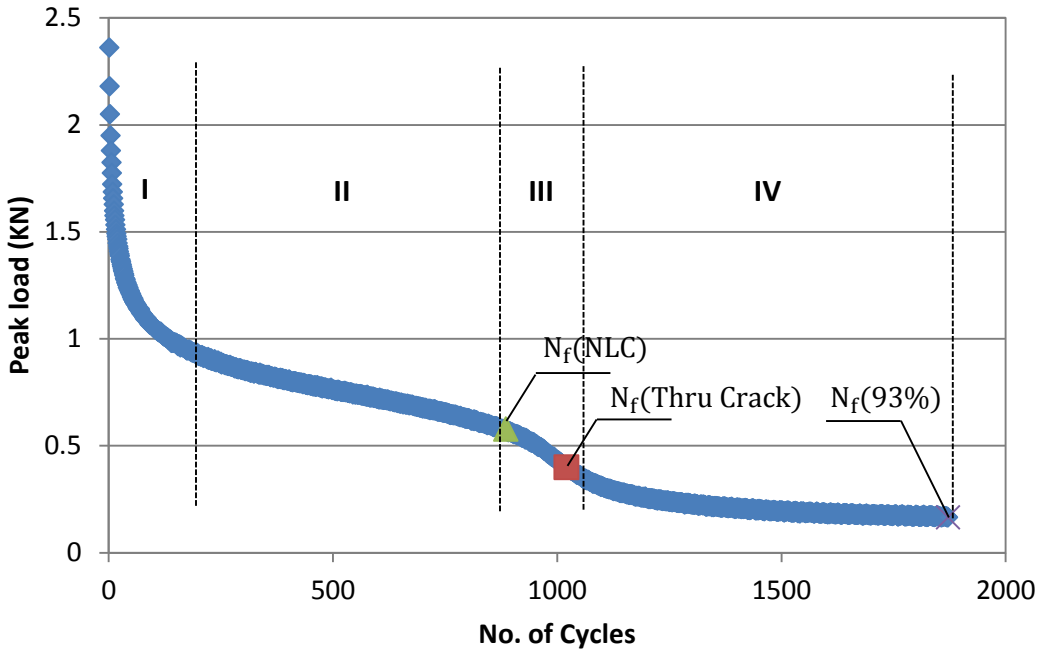

Figure 4.2 Three failure points and four stages on the peak load curve (0.318-mm MOD and 0.1-Hz frequency)

In the field, cracks are reported once they are observed on the pavement surface or when they propagate through the asphalt layer. Therefore, the number of cycles corresponding to the moment when the crack is first observed to propagate through the specimen in the video is

considered to best represent the way cracks are reported in the field. However, the determination of this failure point cannot be done quickly or accurately based on the recorded video. Thus, further analysis is conducted to determine if another method (either the NLC method or the 93% reduction method) that can be easily determined based on measured testing data instead of a recorded video may be used. The method recommended for future use should yield the failure point closer to the N_f(Thru Crack).

4.2 Overlay Test Results

For each mix, the numbers of cycles to failure were determined based on both the failure point determination methods (the NLC and the 93% reduction methods). The number of cycles when crack was first observed to propagate through the specimen (N_f(Thru Crack)) was also determined by analyzing the recorded video of crack propagation during testing. The average (Avg.), standard deviation (Std. Dev.), and coefficient of variation (COV) of results from three replicates are summarized in Table 4.1.

Table 4.1 Summary of OT Results at Three MODs for Five Mixtures

Mix	Freq. (Hz)	MOD (mm)	N_f(NLC)			N_f(93%)			N_f(Thru Crack)		
			Avg.	Std. Dev.	COV	Avg.	Std. Dev.	COV	Avg.	Std. Dev.	COV
S8-3	1	0.381	762	119	16%	1363	418	31%	937	223	24%
	1	0.318	1718	371	22%	2986	762	26%	1947	467	24%
	1	0.254	7346	1665	23%	9967	2344	24%	8334	2018	24%
S10-3	1	0.381	885	196	22%	1400	83	6%	1211	193	16%
	1	0.318	2029	329	16%	2946	817	28%	2048	154	7%
	1	0.254	4416	1051	24%	5916	1117	19%	5303	979	18%
S11-3	1	0.381	1037	297	29%	1619	665	41%	1237	450	36%
	1	0.318	2794	828	30%	4291	1516	35%	3215	885	28%
	1	0.254	4770	629	13%	7287	1354	19%	5800	571	10%
N10-3	1	0.381	140	99	71%	380	259	68%	210	108	51%
	1	0.318	348	104	30%	1130	83	7%	497	130	26%
	1	0.254	1611	598	37%	5107	2343	46%	1888	707	37%
N11-3	1	0.381	520	26	5%	1143	258	23%	622	60	10%
	1	0.318	674	139	21%	2390	702	29%	851	166	19%
	1	0.254	4262	1225	29%	8756	3726	43%	4769	1182	25%
	0.1	0.381	156	64	41%	355	123	35%	221	N/A	N/A
	0.1	0.318	1463	521	36%	2821	837	30%	1969	839	43%
	0.1	0.254	4264	1741	41%	8848	97	1%	N/A	N/A	N/A

Note: 1. The average and standard deviation with the unit of cycle are rounded up to the nearest integer.
2. "N/A" means only one or none of N_f(Thru Crack) was recorded due to issue of video.

Further analysis was performed to evaluate the two methods – NLC and 93-percent determination methods. The failure points determined by the NLC method and the 93%

reduction method were plotted against the N_f(Thru Crack) failure points in Figure 4.3 and Figure 4.4, respectively, to evaluate the correlation. The results from the 48 specimens with good recorded videos were used. A trendline and a line of equality were added in each plot for comparison. The difference between two correlating parameters in each plot can be graphically represented by the difference between the corresponding trendline and the line of equality.

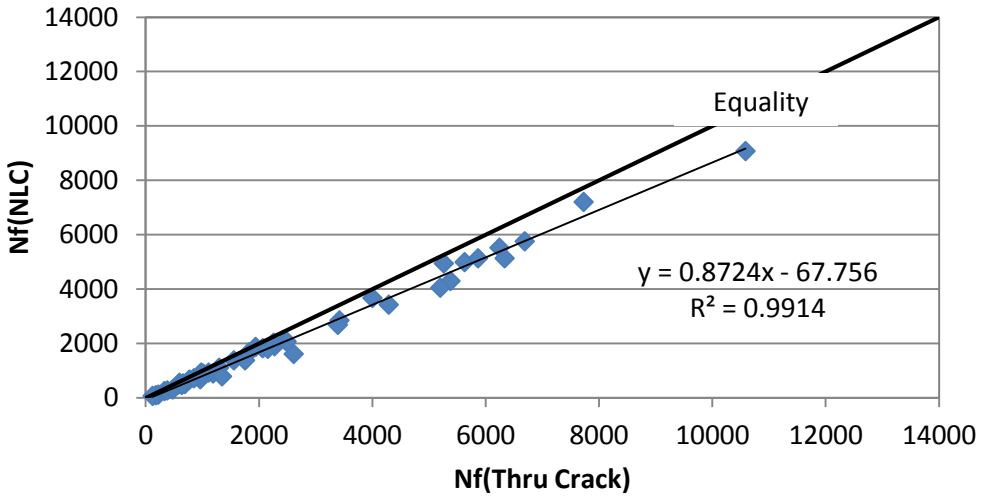

Figure 4.3 N_f(NLC) versus N_f(Thru Crack)

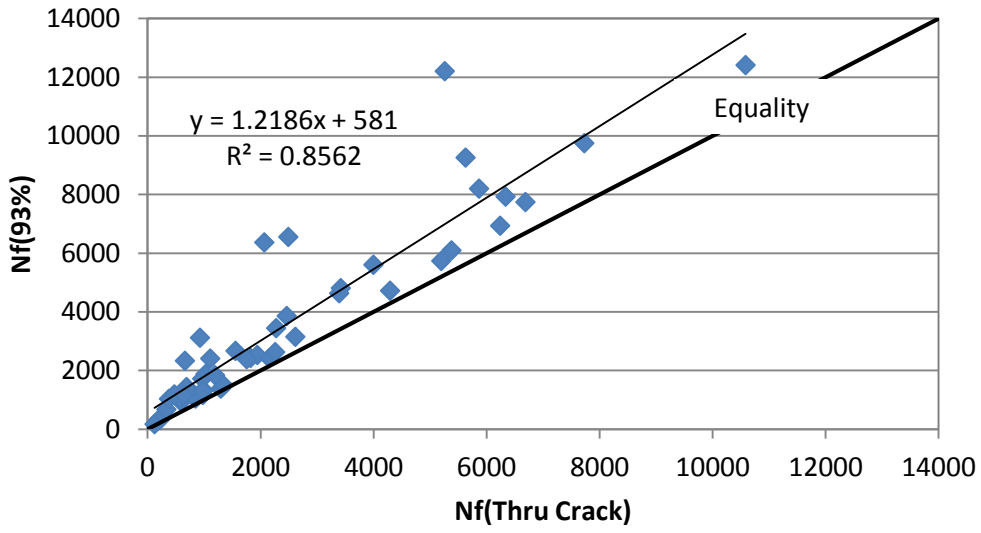

Figure 4.4 N_f(93%) versus N_f(Thru Crack)

As shown in Figure 4.3, the slope and intercept of the trendline are 0.8724 and -67.756, respectively. This means the overall difference between the N_f(NLC) and N_f(Thru Crack) is approximately 13%. Also, the R^2 value is 99.1%, which means the N_f(Thru Crack) varies closely with the N_f(NLC).

In Figure 4.4, the slope, intercept and R^2 value of the trendline are 1.2186, 581 and 85.6%, respectively. This indicates the overall difference between N_f(93%) and N_f(Thru Crack) is approximately larger than 21%. In this case, correlation coefficient (r) is equal to the square root of R^2 value. Their correlation coefficient (r = 0.925) is smaller than that between the N_f(NLC) and N_f(Thru Crack) (r = 0.995). However, better correlation (indicated by larger coefficient coefficient) is not sufficient to determine if the NLC method yields the failure point closer to the observed moment of failure than the 93% load reduction method.

Figure 4.5 compares the failure points determined by two methods (N_f(NLC) and N_f(93%)) to the visually observed moment of failure (N_f(Thru Crack)) which is ranked from the smallest to the largest following a non-decreasing curve. The horizontal axis is the number of specimens (or number of observations). The N_f(NLC) curve is much closer to the N_f(Thru Crack) curve with less variations. The N_f(93%) curve has more variations or departures from the N_f(Thru Crack) curve. Mathematically, the variation from the N_f(Thru Crack) can be regarded as the error. The sum of squared error (SSE) of N_f(NLC) versus N_f(93%) indicates their overall departure from the "observed" failure point (N_f(Thru Crack)). Table 4.2 summarizes the calculated SSE for the two failure point determination methods. The SSE in N_f(93%) is more than 10 times of that in N_f(NLC).

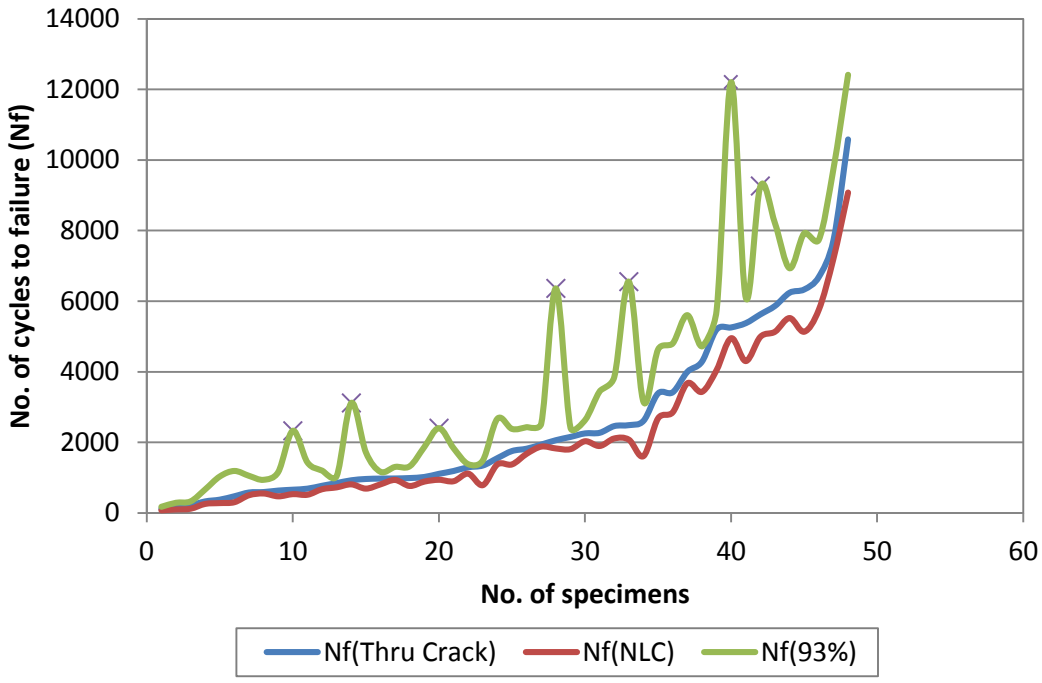

Figure 4.5 Comparing N_f(NLC) and N_f(93%) to N_f(Thru Crack)

Table 4.2 Sum of Squared Error in the Two Failure Points

Failure Point	SSE
N_f(NLC) by NLC method	1.33E+07
N_f(93%) by 93% load reduction method	1.40E+08

In Figure 4.5, the N_f(93%) curve has several local peaks (indicated by "×") where the variation from N_f(NLC) is quite large. The contribution of error from these peak points to the total error should be considered. Table 4.3 provides the information of test specimens and associated conditions corresponding to these peak points (from the left to the right in Figure 4.5). In the last column, the contribution of individual error to the total error is indicated by the ratio of SE to

SSE. The largest contribution can be 34% from a single test. More importantly, the specimens in Table 4.3 are all fabricated using the mixes with 50% RAP. It indicates that the 93% load reduction method may not be able to determine the failure point of high RAP mix in the overlay test very well.

Table 4.3 Information Test Specimens with Large Squared Error (SE) in N_f(93%)

Section No.	Mix Type	MOD (mm)	Freq. (Hz)	SE	SE/SSE
N11-3	50%RAP+WMA Foam	0.318	1	2.79E+06	2%
N11-3	50%RAP+WMA Foam	0.318	1	4.80E+06	3%
N10-3	50%RAP+HMA	0.254	1	1.67E+06	1%
N10-3	50%RAP+HMA	0.254	1	1.85E+07	13%
N10-3	50%RAP+HMA	0.254	1	1.65E+07	12%
N11-3	50%RAP+WMA Foam	0.254	1	4.82E+07	34%
N11-3	50%RAP+WMA Foam	0.254	1	1.32E+07	9%

As mentioned before, the N_f(Thru Crack) is the moment of failure when the crack was first observed to propagate through the specimen. The above analysis shows the NLC method would be a better alternative for defining the moment of failure. Therefore, it determines the number of cycles to failure in the overlay test more accurately.

4.3 Evaluation of Higher Frequency in the AMPT Overlay Test

Another improvement for the overlay test is to increase the test frequency. Since the overlay test may be conducted at lower MOD levels for other material and climate conditions in the future, it is desirable in these cases to conduct the overlay test at a higher frequency to shorten testing

time. Practically, for a specimen that requires 10,000 cycles of testing prior to failure, the difference in testing time is approximately 25 hours (approximately 3 hours for a 1-Hz test versus approximately 28 hours for a 0.1-Hz test). Due to the availability of the plant-produced mix, overlay testing was conducted at both 0.1- and 1-Hz frequencies for the N11-3 mixture only to evaluate the overlay test at 1 Hz (instead of 0.1 Hz as specified in the TxDOT procedure). The failure point for each N11-3 test specimen was determined based on two failure point determination methods—the NLC and 93% reduction methods.

Figure 4.6 compares the average and associated standard deviation of the test results determined at 0.1- and 1-Hz frequencies for the three MOD levels based on the NLC and 93% reduction methods. The results are very similar, especially at the lowest MOD level.

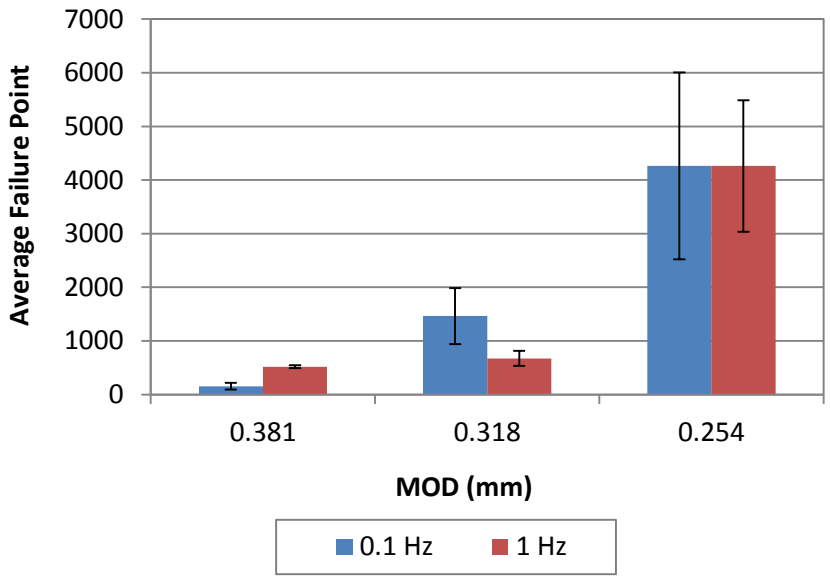

(a) NLC method

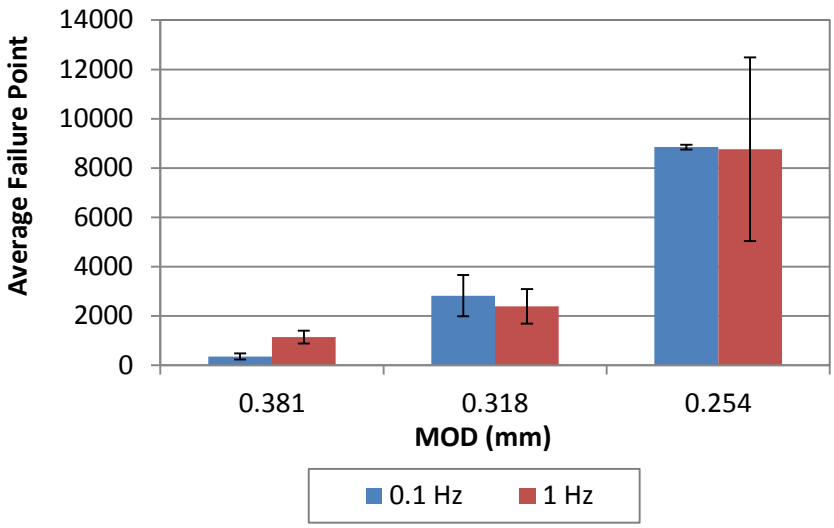

(b) 93% reduction method

Figure 4.6 Comparing overlay test results at 0.1- and 1-Hz frequencies

The test results determined at the two frequencies are also compared statistically using a two-factor Analysis of Variance (ANOVA) (significance level $\alpha = 0.05$). The two factors analyzed are frequency and MOD. First, three assumptions of ANOVA (normality, homogeneity of variance, and independency) were checked to make sure the analysis result was valid (PROPHET StatGuide 1997). The variance was found not homogenous. Therefore, the logarithmic transformation (to base 10) was performed to stabilize the variance (Nettleton 2004). The ANOVA based on the transformed data shows that (1) the interaction effect of two factors and the MOD effect are statistically significant (p-value < 0.05); (2) the frequency effect is not statistically significant (p-value > 0.05) (Montgomery 2009).

Further analysis using Tukey's test was conducted to make pairwise comparison for each MOD. Since Tukey's test has the same assumptions as the ANOVA, the analysis here still uses the

transformed data in ANOVA (Coble 2014). Table 4.4 summarizes Tukey's test results for the NLC and 93% reduction methods. Based on the grouping information shown in the last column of Table 4.4, two testing conditions that share the same letter are considered statistically the same. Thus, at lower MOD level (0.254 and 0.318 mm), the overlay test conducted at 0.1 and 1 Hz would not yield statistically different results. However, at the highest MOD level (0.381 mm), test results at 0.1 and 1 Hz are statistically different (Montgomery 2009).

Table 4.4 Tukey's Test Results

Frequency (Hz)	Maximum Opening Displacement (mm)	No. of Replicates	Mean Failure Point (Cycle)	Grouping
Tukey's Test Results for the NLC Method				
0.1	0.254	3	4264	A
1.0	0.254	3	4262	A
0.1	0.318	3	1463	B
1.0	0.318	3	674	B C
0.1	0.381	3	156	D
1.0	0.381	3	520	C
Tukey's Test Results for the 93% Reduction Method				
0.1	0.254	2	8848	A
1.0	0.254	3	8756	A
0.1	0.318	3	2821	B
1.0	0.318	3	2390	B
0.1	0.381	3	355	C
1.0	0.381	3	1143	B

The next step of the evaluation process was determining the test variability at the two frequencies. The coefficient of variation (COV) and F-test were used for comparing the

variability. Figure 4.7 shows the coefficients of variation of the overlay testing results determined at the two frequencies. As shown, the overlay test results determined at 0.1 Hz have higher COVs (or larger variation) than the test results determined at 1 Hz, except for the 93% reduction method at the 0.254-mm MOD level.

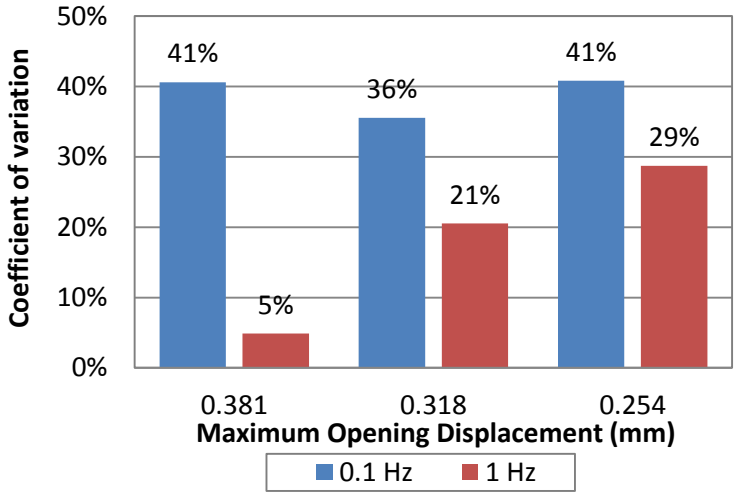

(a) NLC method

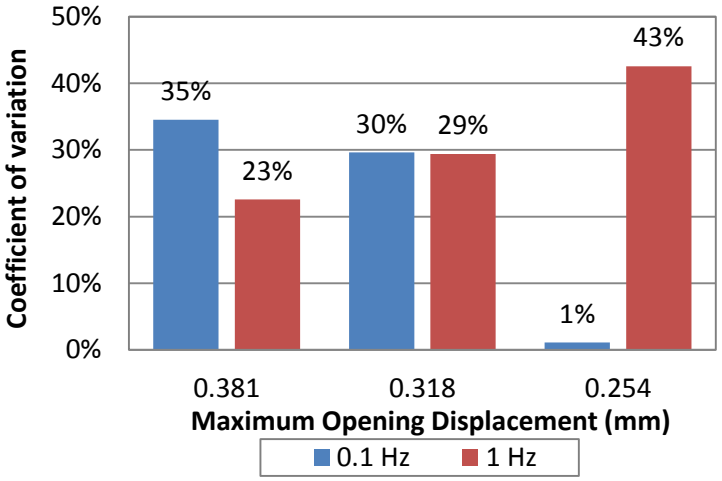

(b) 93% reduction method

Figure 4.7 Comparing coefficients of variation at 0.1- and 1-Hz frequencies

Then, F-test was performed to compare the variance of the overlay test results at the two frequencies. First, the test results are grouped only by frequency (0.1 and 1 Hz), regardless of the MOD level. F-test shows the variances from two groups (each has 9 data points) are not statistically different a significance level of 0.05. Second, the test results are grouped by both frequency and MOD level into six groups (each has 3 data points) in order to test the equality of variances at different MOD levels (0.254, 0.318, and 0.381 mm). The F-test results show that the variances at two frequencies are not statistically different at higher MOD levels (0.381 and 0.318 mm) for either N_f (NLC) or N_f (93%) results. At the lowest MOD level (0.254 mm), the variances at two frequencies are not statistically different for the N_f (NLC) results but are statistically different for the N_f (93%) results. The detailed F-test results are included in Appendix D. The small samples sizes (especially for groups of 3 data points) make it difficult to check the normality assumption of F-test, and also diminish its power (PROPHET StatGuide 1997). More overlay test results are required to validate these F-test results in the future.

In addition, Figure 4.8 compares the average testing time (in minutes) required for conducting the overlay test at the two frequencies for the NLC and 93% reduction methods. The 1-Hz test requires much shorter testing time, especially at lower MOD levels (0.318 and 0.254 mm). At the 0.254-mm MOD level, the overlay test can take more than 24 hours at 0.1 Hz but approximately 2.5 hours at 1 Hz (Figure 4.8(b)).

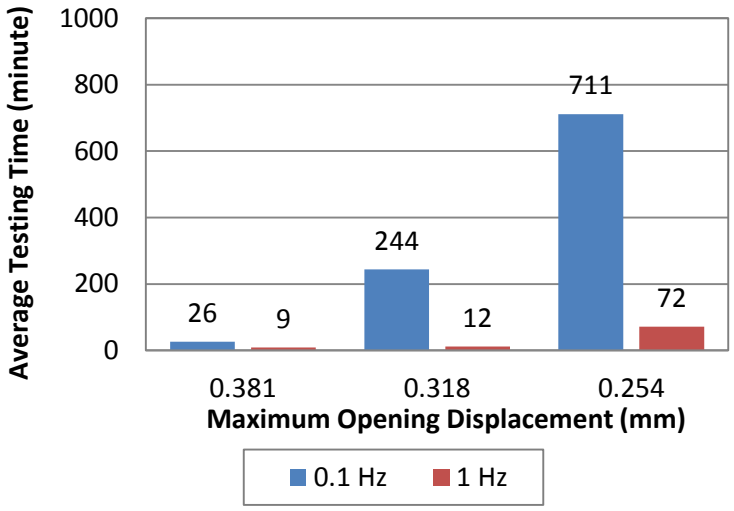

(a) NLC method

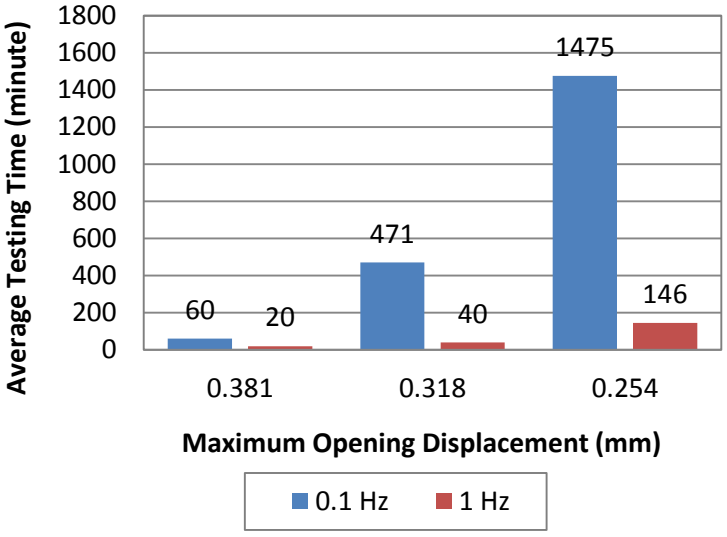

(b) 93% reduction method

Figure 4.8 Comparing testing time at two frequencies

Based on the above analysis, the overlay test may be conducted at 1 Hz to reduce the testing time without significantly affecting the test variability. While the ANOVA showed that the two frequencies could be used interchangeably without statistically affecting the test results at smaller MOD levels (0.254 and 0.318 mm), only one frequency should be used to evaluate different mixes in a project.

CHAPTER 5 COMPARING AMPT OVERLAY TEST AND BENDING BEAM FATIGUE TEST RESULTS

In this study, the proposed "normalized load × cycle" (NLC) failure point determining method in the AMPT overlay test was derived from the "normalized stiffness × cycle" method in bending beam fatigue test (ASTM D7460). The two tests were designed to determine the cracking resistance of asphalt mixture. Therefore, it is desirable to determine the correlation between the results of the two tests because the BBF test results have been determined for these mixes in another study. This chapter compares results of the two tests using the ranking of mixtures and the relationship between failure point and applied maximum strain (or displacement).

5.1 Comparing Ranking of Mixtures

In this section, the five asphalt mixtures were ranked based on the average bending beam fatigue (BBF) test and the AMPT overlay test (OT) results. Then, correlation of rankings between two tests was analyzed.

5.1.1 Ranking Mixtures Based on BBF Test Results

This section summarized the testing results and ranking of the average BBF test failure points for the five mixtures. These results were obtained from another project and summarized in Table

5.1. The number of cycles to failure or failure point (N_f) was determined according to ASTM D7460 based on the peak "normalized stiffness × cycle" value.

Table 5.1 Summary of BBF Test Results at Three Strains for Five Mixtures

Mixture	Strain (με)	Number of Cycles to Failure/Failure Point		
		Average (Cycle)	Std. Dev. (Cycle)	COV
N11-3	800	2,587	501	19%
	400	124,094	22,542	18%
	200	37,367,084	28,471,254	76%
S8-3	800	9,887	6,874	70%
	400	186,194	39,659	21%
	200	5,038,040	2,533,496	50%
N10-3	800	2,317	1,430	62%
	400	52,524	52,825	101%
	200	9,441,897	5,943,834	63%
S10-3	800	9,147	6,881	75%
	400	184,737	66,911	36%
	200	5,333,954	1,660,846	31%
S11-3	800	10,494	3,682	35%
	400	199,847	93,486	47%
	200	3,710,114	1,703,150	46%

Note: the average and standard deviation with the unit of cycle are rounded up to the nearest integer.

As shown in Table 5.2, the average number of cycles to failure (failure point) at each strain level is ranked from the largest to the smallest. The ranking at 800 and 400 με are the same. But the

ranking at 200 με is much different from those of the other two strain levels, since the mixtures with 50 percent RAP (N11-3 and N10-3) rank higher than the WMA and control mixes. Based on the properties of five mixtures, the mixes with 50 percent RAP should be stiffer than hot and warm mixes without RAP due to higher content of aged binder. Therefore, the failure point of N10-3 and N11-3 mixes should be lower regardless of strain level. The reason for the ranking difference at different strain levels will be discussed later in Section 5.2.1.

Table 5.2 Ranking of Average Failure Point by BBF Test for Five Mixtures

Mixture	Processing Information	Maximum Tensile Strain (με)		
		800	400	200
N10-3	50%RAP+HMA	5th	5th	2th
N11-3	50%RAP+WMA Foam	4th	4th	1th
S8-3	0%RAP+HMA (Control)	2th	2th	4th
S10-3	WMA Foam	3th	3th	3th
S11-3	WMA Additive	1th	1th	5th

5.1.2 Ranking Mixtures Based on AMPT Overlay Test Results

The overlay test has been verified as an alternative to determine the fatigue cracking resistance of asphalt mixture (Zhou et al. 2007a). Since the BBF test is currently used as a typical test characterizing the fatigue cracking resistance, the ranking of five plant-mixes from the NCAT test track regarding the average failure point by OT should be similar to the ranking by BBF test. Since the proposed NLC method can better define the moment of failure, only the results based on NLC method were discussed in the analysis.

Table 5.3 ranks the average failure points of five mixtures in descending order for each MOD based on the NLC determination method. The rankings at 0.381- and 0.318-mm MOD are the same, but the rankings for the S8-3, S10-3, and S11-3 mixtures are different for the 0.254-mm MOD. In addition, at each MOD, the asphalt mixtures with 50 percent RAP (N11-3 and N10-3 mixes) ranks lower than the two warm mixes and HMA without RAP. It is reasonable because the aged binder in the RAP makes the N11-3 and N10-3 mixes much stiffer.

Table 5.3 Ranking of Average Failure Point by OT for Five Mixtures Based on NLC Method

Mixture	Processing Information	Maximum Opening Displacement (mm)		
		0.381	0.318	0.254
N10-3	50%RAP+HMA	5th	5th	5th
N11-3	50%RAP+WMA Foam	4th	4th	4th
S8-3	0%RAP+HMA	3th	3th	1th
S10-3	WMA Foam	2th	2th	3th
S11-3	WMA Additive	1th	1th	2th

5.1.3 Comparing AMPT OT Ranking to BBF Test Ranking for Five Mixtures

Spearman's Rank-Order Correlation Coefficient (r_s) was calculated to determine the strength and direction of correlation (or similarity) among six rankings from Table 5.2 and 5.3. The closer r_s to zero, the weaker the correlation is. The positive or negative sign of r_s shows whether or not the two rankings are in the same direction (Royal Geographical Society). Table 5.4 shows the

correlation coefficient matrix among these six rankings. This matrix compares the ranking at each overlay test MOD to the ranking at each BBF maximum tensile strain. Also, it gives the correlations among three rankings within each test.

Table 5.4 Spearman's Rank-Order Correlation Coefficients

	OT @0.381 mm	OT @0.318 mm	OT @0.254 mm	BBFT @800 με	BBFT @400 με	BBFT @200 με
OT @0.381 mm	1	1	0.7	0.9	0.9	-0.8
OT @0.318 mm		1	0.7	0.9	0.9	-0.8
OT @0.254 mm			1	0.9	0.9	-0.8
BBFT @800με				1	1	-0.9
BBFT @400με					1	-0.9
BBFT @200με						1

A hypothesis test was performed to determine if the ranking correlation truly existed (in this case, the average failure points of five mixes were ranked). For a significance level of 0.05, the critical value for r_s is 0.9. That is, the correlation would occur at 95 percent chance if the coefficient is equal or above 0.9 (Gauthier 2001). As shown in Table 5.4, the rankings of the mixes tested at three overlay test MOD levels correlated well ($r_s = 0.9$) with the rankings of the mixes tested at 800 με and 400 με in the BBF test. However, the rankings of the mixes based on the OT results were almost apposite ($r_s = -0.8$) compared to those based on the BBF test results at 200 με.

The rankings of the mixes for the three OT MOD levels are very similar ($r_s \geq 0.7$). Even though 0.7 is smaller than the critical value of 0.9, it still indicates a positive correlation. However, the

BBF test rankings at 200 με are in a reversed order compared to those at the other strain levels. Overall, the OT rankings at each MOD based on the NLC method is similar to the BBF test rankings at 800 με and 400 με but different from those at 200 με. The good correlations between the two tests indicate the potential use of overlay test to characterize fatigue cracking resistance of asphalt mixtures.

5.2 Failure Point Prediction

5.2.1 BBF Test

Figure 5.1 illustrates the relationship between maximum tensile strain and BBF test number of cycles to failure for five asphalt mixtures. Trendlines are fitted to the testing data for each mixture. In the log-log scale, each trendline is linear. The slopes of trendlines for S8-3, S10-3, and S11-3 mixtures are different from those of N11-3 and N10-3 mixtures. The failure point of high RAP mixes is higher at the smallest strain level (200 με) but lower at the largest strain level (800 με) compared to other three mixes. Therefore, Table 5.2 shows the different failure point rankings of the mixes at 200 με and at 800 με in BBF test. A possible explanation of this difference is that high RAP mixes tend to be more elastic at lower strain, but more brittle at higher strain than other mixes. Field cracking performance should be investigated in the future study to verify this explanation.

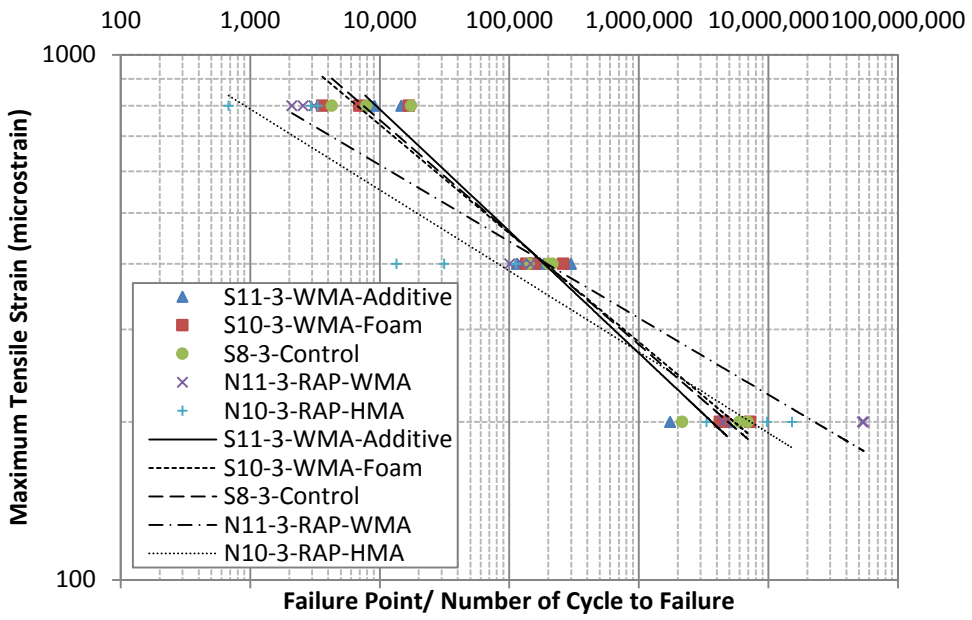

Figure 5.1 Maximum tensile strains versus failure points for five mixtures from BBF test

The failure point (or the number of cycles to failure) at certain maximum tensile strain in the BBF test can be determined by a fatigue transfer function shown in Equation 46 (Huang, 1993). Table 5.5 includes the power model coefficients determined by fitting Equation 46 to the BBF test data for the five mixtures.

$$N_f = \alpha_1 \left(\frac{1}{\varepsilon}\right)^{\alpha_2} \tag{46}$$

Table 5.5 Fitting Power Model Coefficients for the BBF Test

Mixture Type	Processing Information	Power Law Regression Coefficients		
		α_1	α_2	R^2
S11-3	WMA Additive	1×10^{16}	4.1923	0.9743
S10-3	WMA Foam	4×10^{17}	4.7140	0.9753
S8-3	0%RAP+HMA (Control)	1×10^{17}	4.5321	0.9686
N11-3	50%RAP+WMA Foam	3×10^{22}	6.5846	0.9600
N10-3	50%RAP+HMA	4×10^{20}	6.0192	0.9288

5.2.2 AMPT Overlay Test

Figure 5.2 shows the maximum opening displacement (MOD) versus the OT number of cycles to failure determined based on the NLC method for the five mixtures. All the failure points were determined at 1-Hz. The power model (Equation 47) was used to fit the data. As shown in Figure 5.2, the slopes of S10-3, and S11-3 trendlines are different from the slopes of the S8-3, N10-3, and N11-3 mixes. As MOD level changes, the rate of change of failure point for high RAP mixes and control mix is higher than that of warm mixes. This is similar to the result of BBF test showed in Figure 5.1. Probably, high RAP mixes and control mix tend to be more sensitive than warm mixes to the change of MOD level.

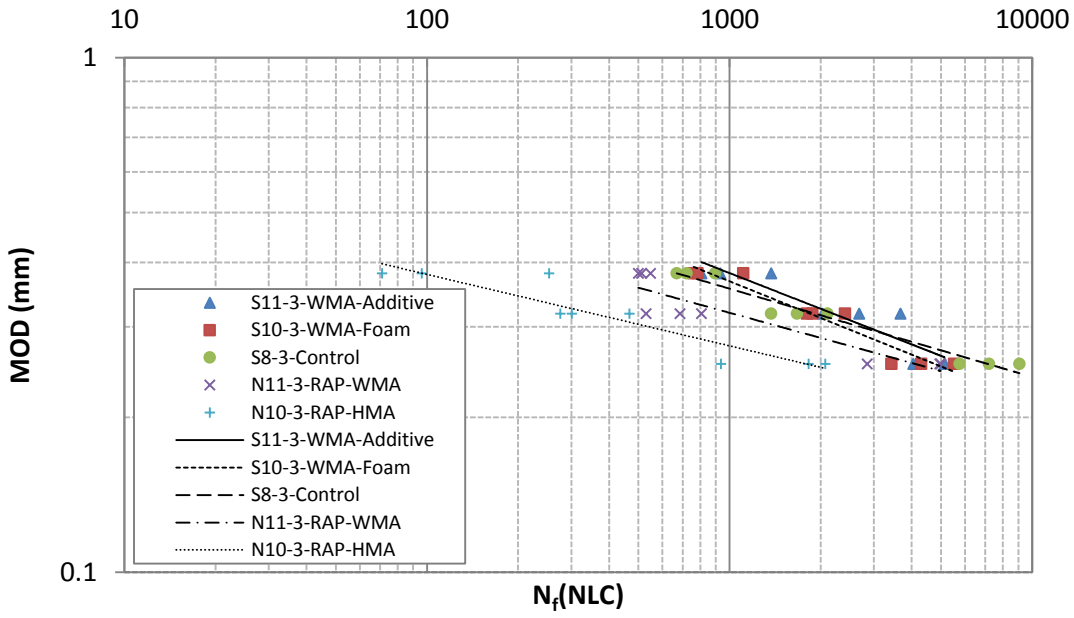

Figure 5.2 Maximum opening displacements versus failure points for five mixtures by OT

Equation 47 shows the fitted power-model relationship between failure point and the reciprocal of MOD (1/MOD). The fitted model can be used to predict the failure point at the desired maximum opening displacement. Table 5.6 summarizes the model coefficients "β_1" and "β_2" for five mixtures. All the R^2 values are larger than 0.80 which indicates good fitting.

$$N_f(NLC) = \beta_1 \left(\frac{1}{MOD}\right)^{\beta_2} \quad (47)$$

Coefficient "β_1" is a scaling factor moving the trendline up or down (i.e. larger "β_1" moves the trendline up). Coefficient "β_2" governs the rate of growth or decline of the trendline (i.e. smaller

absolute value of "β_2" corresponds to lower changing rate). The mixture with smaller absolute value of "β_2" in the fitted model is less sensitive to MOD change.

Table 5.6 Fitting Power Model Coefficients for the AMPT OT

Mixture Type	Processing Information	Power Law Regression Coefficients		
		β_1	β_2	R^2
S11-3	WMA Additive	29.956	3.760	0.87
S10-3	WMA Foam	20.478	3.934	0.93
S8-3	0%RAP+HMA (Control)	3.158	5.601	0.96
N11-3	50%RAP+WMA Foam	2.595	5.233	0.85
N10-3	50%RAP+HMA	0.269	6.286	0.87

5.2.3 Comparing Failure Point Prediction in Two Tests

Comparing the overlay test and BBF test by plotting the maximum tensile strain (or maximum opening displacement) versus the failure point, the power model can be used to fit both relationships (as shown in Equations 46 and 47). Using these relationships, the failure point at any maximum tensile strain (or maximum opening displacement) of interest within the tested range can be interpolated.

Also, both of the "α_2" column in Table 5.5 and the "β_2" column in Table 5.6 indicate the rate of change of mix's failure point to the change of tensile strain. The coefficients of warm mixes (S10-3 and S11-3) are smaller than those of high RAP mixes (N10-3 and N11-3). Obviously, the

coefficients "α_2" and "β_2" have similar range ($4.192 < \alpha_2 < 6.585$, $3.760 < \beta_2 < 6.286$). Therefore, independent-t test was performed to test the equality of the means of two coefficients for five mixes (the Minitab output is summarized in Appendix E). It shows that the mean of "α_2" and the mean of "β_2" are statistically no different at significance level of 0.05 (p-value = 0.724). Even though the assumption of equal variances is met (as shown in Appendix E), the power of t test is weakened due to small sample size (n=5). In order to draw a reliable conclusion from t-test, more mixture types need to be tested in the future (Montgomery 2009).

CHAPTER 6 CONCLUSION AND RECOMMENDATIONS

Based on the results of this study, the following conclusions and recommendations can be offered:

- The current TxDOT procedure determines the failure point once the applied load is reduced by 93 percent of the initial applied load. However, cracks are often seen to propagate through the test specimen long before the applied load reaches this criterion, especially at lower MOD levels. The NLC method presented in this study may be used to better determine the failure point (shortly before the visible crack propagates through the test specimen). The regression analysis shows that the failure point determined based on the NLC method (N_f(NLC)) is approximately 13% lower than the failure moment determined when the crack was first observed to propagate through the specimen (N_f(Thru Crack)).
- The N_f(Thru Crack) values vary closely with those of the N_f(NLC) (R^2 = 99.1%). Also, the overall difference (the sum of squared error (SSE)) between the N_f(Thru Crack) values and the N_f(NLC) value is 10 times less than the overall difference between the N_f(Thru Crack) values and the N_f(93%) values. Hence, the NLC method is recommended for determining the failure point for overlay test.
- The TxDOT procedure specifies that the overlay test be conducted using an MOD of 0.635 mm (0.025 in.) and at a test frequency of 0.1 Hz for evaluating asphalt mixtures used in overlays on top of old concrete pavements in Texas. However, this test may be

conducted at lower MOD levels for other stiff materials (e.g., mix with high RAP and/or RAS contents) and climate conditions (i.e., small daily temperature variation) in the future. At the lower MOD levels, the overlay test takes much longer. As shown in the analysis, the overlay test may be conducted at 1 Hz to reduce testing time without significantly affecting the test variability. Also, the test results conducted at 0.1 and 1 Hz were not statistically different.

- The BBF and AMPT overlay tests have similar rankings of the five asphalt mixtures based on the number of cycles to failure. The power model used in the BBF test can also be used to determine the relationship between the number of cycles to failure and maximum opening displacement (MOD) for overlay test. Based on the relationships for both the BBF and overlay tests, the warm mixes were less sensitive to the change of maximum tensile strain or MOD than the high RAP mixes.
- To further evaluate the AMPT overlay test in determining the cracking resistance of asphalt mixture, correlation between laboratory test results and field cracking performance at the test track should be investigated in the future. Also, further testing conducted at the 0.635-mm MOD specified in the TxDOT procedure should be performed and compared with the results conducted at the smaller MOD used in this study. More mixes with various binders and aggregates should also be tested to verify the application of overlay test at higher frequency (1Hz).

REFERENCES

American Association of State Highway Transportation Officials (AASHTO) (2007) AASHTO T 321-07: Standard Method of Test for Determining the Fatigue Life of Compacted Hot Mix Asphalt (HMA) Subjected to Repeated Flexural Bending. *AASHTO,* Washington, D.C.

American Society for Testing and Materials (ASTM) (2010). ASTM D7460-10: Standard Test Method for Determining Fatigue Failure of Compacted Asphalt Concrete Subjected to Repeated Flexural Bending, *ASTM International*, West Conshohocken, PA.

Barenblatt, G. I. (1962). The mathematical theory of equilibrium cracks in brittle fracture. *Advances in applied mechanics, 7*(1), 55-129.

Bennert, T. A. (2009). *A rational approach to the prediction of reflective cracking in bituminous overlays for concrete pavements.* Doctoral dissertation, The State University of New Jersey, Rutgers, NJ.

Bischoff, D. (2007). *Evaluation of Strata® Reflective Crack Relief System*, Report FEP-01-07, Wisconsin Department of Transportation.

Carpenter, S. H., & Jansen, M. (1997). Fatigue behavior under new aircraft loading conditions. In *Aircraft/Pavement Technology In the Midst of Change*, 259-271.

Carpenter, S. H., & Shen, S. (2006). Dissipated energy approach to study hot-mix asphalt healing in fatigue. *Transportation Research Record: Journal of the Transportation Research Board, 1970*(1), 178-185.

Chiangmai, C. N. (2010). *Fatigue-fracture Relation on Asphalt Concrete Mixtures*. Master's Thesis, University of Illinois at Urbana-Champaign, IL.

Cleveland, G. S., Lytton, R. L., & Button, J. W. (2003). Reinforcing benefits of geosynthetic materials in asphalt concrete overlays using pseudo strain damage theory. *In Pre-Print CD-ROM, 82nd Annual Meeting of the Transportation Research Board, National Research Council, National Academies,* Washington, D.C.

Crews, E. (2009). *MWV Evotherm™ pavement durability: result of laboratory and field testing*. MWV Specialty Chemical Report. Retrieved from http://www.meadwestvaco.com/mwv/groups/content/documents/document/mwv024063.pdf.

Coble, D. W. (2014) *Week 6 Lecture: Multiple Comparison Tests (Chapter 11)* Retrieved from http://www.faculty.sfasu.edu/cobledean/Biostatistics/Lecture6/MultipleComparisonTests.PDF

Garcia-Diaz, A., & Riggins, M. (1984). Serviceability and distress methodology for predicting pavement performance. *Transportation Research Record: Journal of the Transportation Research Board,* 997, 56-61.

Gauthier, T. D. (2001). Detecting trends using Spearman's rank correlation coefficient. *Environmental Forensics, 2*(4), 359-362.

Germann, F. P., & Lytton, R. L. (1979). Methodology for predicting the reflection cracking life of asphalt concrete overlays. *Interim Report, Sep. 1974-Mar. 1979* Texas A&M University, College Station.

Ghuzlan, K. A., & Carpenter, S. H. (2000). Energy-derived, damage-based failure criterion for fatigue testing. *Transportation Research Record: Journal of the Transportation Research Board, 1723*(1), 141-149.

Harvey, J. T., Deacon, J. A., Taybali, A. A., Leahy, R. B., & Monismith, C. L. (1997). A reliability-based mix design and analysis system for mitigating fatigue distress. In *Eighth international conference on asphalt pavements* (Vol. I), 301-323.

Hu, S., Zhou, F., & Scullion, T. (2010). Reflection cracking-based asphalt overlay thickness design and analysis tool. *Transportation Research Record: Journal of the Transportation Research Board, 2155*(1), 12-23.

Hu, S., Zhou, F., & Scullion, T. (2011). Factors that affect cracking performance in hot-mix asphalt mix design. *Transportation Research Record: Journal of the Transportation Research Board, 2210*(1), 37-46.

Hu, X., Zhou, F., & Scullion T. (2008) *Pilot implementation of the overlay tester and double-blade saw* (FHWA/TX-08/5-4467-01-1) Texas Transportation Institute, Texas A&M University System.

Huang, Y. H. (1993). *Pavement Analysis and Design*, Prentice Hall, Inc., New Jersey.

IPC Global® (2012), *AMPT Overlay Test Kit.* Retrieved from http://instrotek.com/wordpress/wp-content/uploads/AMPT-Overlay-Test-Kit.pdf.

Jacob, M. M. J. (1995). *Crack Growth in Asphalt Mixes.* Doctoral dissertation, Delft University of Technology, Delft, Netherlands.

Kalidindi, S. R., Abusafieh, A., & El-Danaf, E. (1997). Accurate characterization of machine compliance for simple compression testing. *Experimental mechanics, 37*(2), 210-215.

Lytton, R. L., Uzan, J., Fernando, E. G., Roque, R., Hiltunen, D., & Stoffels, S. M. (1993). *Development and validation of performance prediction models and specifications for asphalt binders and paving mixes* (Vol. 357). Strategic Highway Research Program.

Montgomery, D. C. (2009) *Design and Analysis of Experiments: 7th Edition*, John Wiley & Sons, Inc., New York.

Nettleton, D. (2004) *Checking Model Assumptions*
Retrieved from http://www.public.iastate.edu/~dnett/S402/wassumptions.pdf

Paris, P. C., & Erdogan, F. (1963). A critical analysis of crack propagation laws. *Journal of Basic Engineering*, 85, 528.

Pierce, L. M., & Mahoney, J. P. (1996). Asphalt concrete overlay design case studies. *Transportation Research Record: Journal of the Transportation Research Board, 1543*(1), 3-9.

Powell, R. B. (2013) *NCAT Pavement Test Track: Construction.*
Retrieved from http://www.pavetrack.com/construction.htm.

Prowell, B. D. (2010). Estimate of fatigue shift factors between laboratory tests and field performance. *Transportation Research Record: Journal of the Transportation Research Board, 2181*(1), 117-124.

Prowell, B. D., Brown, E. R., Anderson, R. M., Daniel J. S., Swamy A. K., Quintus, H. V., … Maghsoodloo, S. (2010). *Validating the fatigue endurance limit for hot mix asphalt* (Vol. 646). National Academies Press.

PROPHET StatGuide (1997) *Do your Data Violate F-test Assumptions?*
Retrieved from http://www.basic.northwestern.edu/statguidefiles/ftest_ass_viol.html

Roque, R., Zhang, Z., & Sankar, B. (1999). Determination of crack growth rate parameter of asphalt mixtures using the Superpave IDT. *Journal of the Association of Asphalt Paving Technologists, 68,* 404-433.

Rowe, G. M. (1993) Performance of asphalt mixtures in the trapezoidal fatigue test. *Association of Asphalt Paving Technologist*, 62, 344.

Rowe, G. M., & Bouldin, M. G. (2000). Improved techniques to evaluate the fatigue resistance of asphaltic mixtures. In *2nd Eurasphalt & Eurobitume Congress Barcelona (Vol. 2000)*.

Royal Geographical Society. *Spearman's Rank Correlation Coefficient - Excel Guide.*
Retrieved from http://www.rgs.org/NR/rdonlyres/4844E3AB-B36D-4B14-8A20-3A3C28FAC087/0/OASpearmansRankExcelGuidePDF.pdf.

Saadeh, S. & Eljairi, O. (2011). *Development of a quality control test procedure for characterizing fracture properties of asphalt mixtures*, Final Report of Project No. 10-24, California State University, Long Beach.

Schapery, R. A. (1973). *A theory of crack growth in visco-elastic media*, Report No. MM 2764-73-1, Mechanics and Materials Research Center, Texas A&M University.

Schapery, R. A. (1975). A theory of crack initiation and growth in viscoelastic media. *International Journal of Fracture, 11*(1), 141-159.

Schapery, R. A. (1978). A method for predicting crack growth in nonhomogeneous viscoelastic media. *International Journal of Fracture, 14*(3), 293-309.

Scheffe, H. (1959). *The analysis of variance*, John Wiley & Sons, Inc., New York.

Scullion, T., Zhou, F., Walubita, L., & Sebesta, S. (2009). *Design and performance evaluation of very thin overlays in Texas* (FHWA/TX-09/0-5598-2). Texas Transportation Institute, Texas A&M University System.

Seo, Y., Kim, Y. R., Schapery, R. A., Witczak, M. W., & Bonaquist, R. (2004). A study of crack-tip deformation and crack growth in asphalt concrete using fracture mechanics. *Journal of the Association of Asphalt Paving Technologists, 73*, 200-228.

Shen, S., & Carpenter, S. H. (2005). Application of the dissipated energy concept in fatigue endurance limit testing. *Transportation Research Record: Journal of the Transportation Research Board, 1929*(1), 165-173.

Shen, S., & Carpenter, S. H. (2007). *Dissipated energy concepts for HMA performance: fatigue and healing*. COE Report No.29. Department of Civil and Environmental Engineering, University of Illinois at Urbana-Champaign, Advanced Transportation Research and Engineering Laboratory.

Texas Department of Transportation (TxDOT) (2009) Tex-248-F: Test Procedure for Overlay Test.

Tran, N. H., Taylor, A. J., & Willis, J. R. (2012) *Effect of rejuvenator on performance properties of HMA mixtures with high RAP and RAS contents*, Report 12-05, National Center for Asphalt Technology, Auburn University, AL.

Tsai, B. W. (2001). *High temperature fatigue and fatigue damage process of aggregate-asphalt mixes*. Doctoral dissertation. University of California, Berkeley.

Tsai, B. W., Harvey, J. T., & Monismith, C. L. (2005). Using the three-stage Weibull equation and tree-based model to characterize the mix fatigue damage process. *Transportation Research Record: Journal of the Transportation Research Board, 1929*(1), 227-237.

Van Dijk, W. & Visser, W. (1977) Energy approach to fatigue for pavement design, In *Proceeding of Annual Meeting of the Association of Asphalt Paving Technologist, 46*, 1-40.

Van Dijk, W. (1975). Practical fatigue characterization of bituminous mixes. *Journal of the Association of Asphalt Paving Technologists, 44*, 38-72.

Von Holdt, C., & Scullion, T. (2006). *Methods of reducing joint reflection cracking: field performance studies* (FHWA/TX-06/0-4517-3). Texas Transportation Institute, Texas A&M University System.

Walubita, L. F., Faruk, A. N., Das, G., Tanvir, H. A., Zhang, J., & Scullion, T. (2012). *The overlay tester: a sensitivity study to improve repeatability and minimize variability in the test results* (FHWA/TX-12/0-6607-1). Texas Transportation Institute, Texas A&M University System.

Walubita, L. F., Jamison, B. P., Das, G., Scullion, T., Martin, A. E., Rand, D., & Mikhail, M. (2011). Search for a laboratory test to evaluate crack resistance of hot-mix asphalt. *Transportation Research Record: Journal of the Transportation Research Board*, *2210*(1), 73-80.

Walubita, L. F., Umashankar, V., Hu, X., Jamison, B., Zhou, F., Scullion, T., ... Dessouky, S. H. (2010). *New generation mix-designs: laboratory testing and construction of the APT test sections* (FHWA/TX-10/0-6132-1). Texas Transportation Institute, Texas A&M University System.

Weibull, W. (1951). A statistical distribution function of wide applicability. *Journal of applied mechanics*, *18*(3), 293-297.

West, R. C., Timm, D. H., Willis, J. R., Powell, R. B., Tran, N. H., Watson, D. E., … Nelson, J. (2012) *Phase IV NCAT pavement test track findings*. Report 12-10, National Center for Asphalt Technology, Auburn University, AL.

Withee, J. (2013). *Implementation of the asphalt mixture performance tester (AMPT) for Superpave validation*, TPF-5(178) Project Quarterly Report (1st Quarter), Federal Highway Administration.

Yoo, P. J., & Al-Qadi, I. L. (2010). A strain-controlled hot-mix asphalt fatigue model considering low and high cycles. *International Journal of Pavement Engineering*, *11*(6), 565-574.

Zhou, F., & Scullion, T. (2003). *Upgraded overlay tester and its application to characterize reflection cracking resistance of asphalt mixtures* (FHWA/TX-04/0-4467-1). Texas Transportation Institute, Texas A&M University System.

Zhou, F., & Scullion, T. (2005a). *Overlay tester: a rapid performance related crack resistance test* (FHWA/TX-05/0-4467-2). Texas Transportation Institute, Texas A&M University System.

Zhou, F., & Scullion, T. (2005b). Overlay tester: a simple performance test for thermal reflective cracking (with discussion and closure). *Journal of the Association of Asphalt Paving Technologists, 74*.

Zhou, F., Hu, S., & Scullion, T. (2007a). *Development and verification of the overlay tester based fatigue cracking prediction approach* (FHWA/TX-07/9-1502-01-8). Texas Transportation Institute, Texas A&M University System.

Zhou, F., Hu, S., & Scullion, T. (2009). Overlay tester: a simple and rapid test for HMA fracture property. *Road Pavement Material Characterization and Rehabilitation selected papers from the 2009 GeoHunan International Conference*. 65-73.

Zhou, F., Hu, S., Chen, D. H., & Scullion, T. (2007b). Overlay tester: simple performance test for fatigue cracking. *Transportation Research Record: Journal of the Transportation Research Board*, *2001*(1), 1-8.

APPENDICES

Appendix A

AMPT Overlay Test Results of All Specimens

Table A.1 N11-3 Mixture (50%RAP+WMA Foam)

Mix	No. of specimen	Frequency (Hz)	Maximum Opening Displacement (MOD) (mm)	N_f (NLC)	N_f (93%)	N_f (Thru Crack)
N11-3	6	0.1	0.381	116	330	221
	3	0.1	0.381	123	246	N/A
	2	0.1	0.381	229	487	N/A
	117	0.1	0.318	885	1871	1021
	40	0.1	0.318	1894	3446	2273
	41	0.1	0.318	1608	3146	2612
	8	0.1	0.254	2280	N/A	N/A
	33	0.1	0.254	4980	8916	N/A
	34	0.1	0.254	5532	8780	N/A
	26	1	0.381	512	1433	690
	24	1	0.381	548	941	594
	23	1	0.381	499	1054	581
	45	1	0.318	530	2332	661
	49	1	0.318	686	1718	964
	116	1	0.318	806	3118	927
	112	1	0.254	4948	12204	5258
	114	1	0.254	4988	9260	5628
	124	1	0.254	2848	4804	3421

Table A.2 S8-3 Mixture (0%RAP+HMA)

Mix	No. of specimen	Frequency (Hz)	Maximum Opening Displacement (MOD) (mm)	N_f (NLC)	N_f (93%)	N_f (Thru Crack)
S8-3	69	1	0.381	895	1837	1190
	53	1	0.381	669	1202	772
	54	1	0.381	722	1049	849
	55	1	0.318	1672	2432	1822
	61	1	0.318	2108	3854	2463
	62	1	0.318	1372	2672	1555
	64	1	0.254	5756	7740	6689
	67	1	0.254	7204	9748	7727
	68	1	0.254	9076	12412	10584

Table A.3 N10-3 Mixture (50%RAP+HMA)

Mix	No. of specimen	Frequency (Hz)	Maximum Opening Displacement (MOD) (mm)	N_f (NLC)	N_f (93%)	N_f (Thru Crack)
N10-3	73	1	0.381	96	291	178
	74	1	0.381	71	177	122
	75	1	0.381	253	670	329
	76	1	0.318	276	1036	379
	79	1	0.318	301	1192	475
	80	1	0.318	467	1161	636
	81	1	0.254	936	2404	1110
	70	1	0.254	1824	6364	2063
	72	1	0.254	2072	6552	2490

Table A.4 S10-3 Mixture (WMA Foam)

Mix	No. of specimen	Frequency (Hz)	Maximum Opening Displacement (MOD) (mm)	N_f (NLC)	N_f (93%)	N_f (Thru Crack)
S10-3	85	1	0.381	1110	1385	1296
	86	1	0.381	761	1326	991
	88	1	0.381	784	1489	1346
	90	1	0.318	1876	2532	1939
	91	1	0.318	2406	3886	N/A
	92	1	0.318	1804	2418	2156
	93	1	0.254	5520	6932	6241
	89	1	0.254	3428	4720	4289
	95	1	0.254	4300	6096	5379

Table A.5 S11-3 Mixture (WMA Additive)

Mix	No. of specimen	Frequency (Hz)	Maximum Opening Displacement (MOD) (mm)	N_f (NLC)	N_f (93%)	N_f (Thru Crack)
S11-3	101	1	0.381	1372	2382	1756
	105	1	0.381	807	1168	975
	107	1	0.381	931	1307	979
	108	1	0.318	2028	2632	2256
	110	1	0.318	2680	4636	3390
	111	1	0.318	3672	5604	3999
	121	1	0.254	4044	5732	5198
	122	1	0.254	5132	8204	5867
	123	1	0.254	5132	7924	6334

Appendix B

Peak Load Curve Labeled with N_f(NLC), N_f(Thru Crack), and N_f(93%)

(48 figures in total for the specimens with good video recorded)

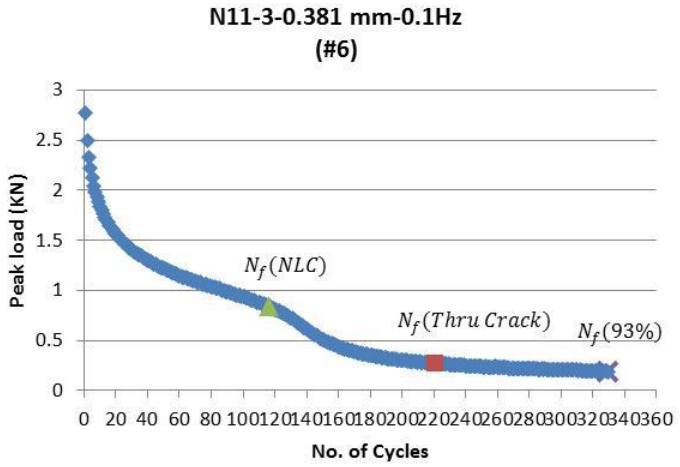

Figure B.1

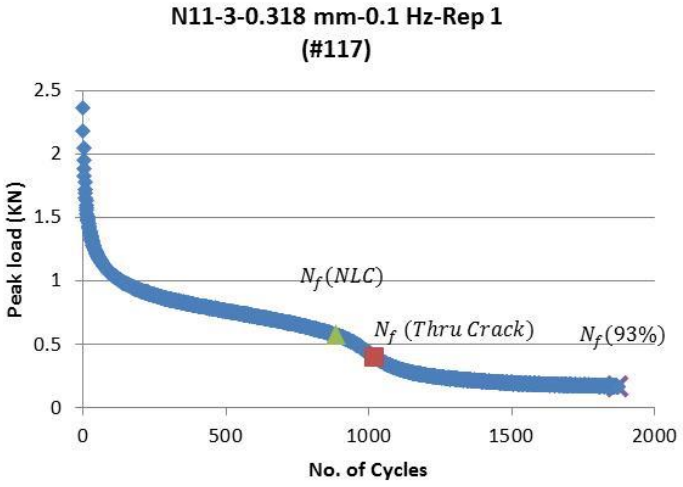

Figure B.2

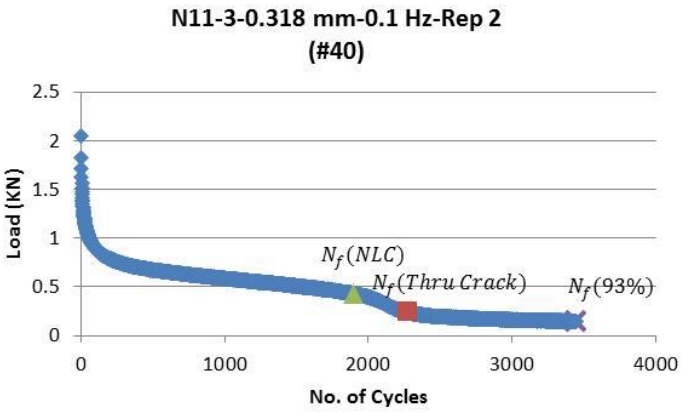

Figure B.3

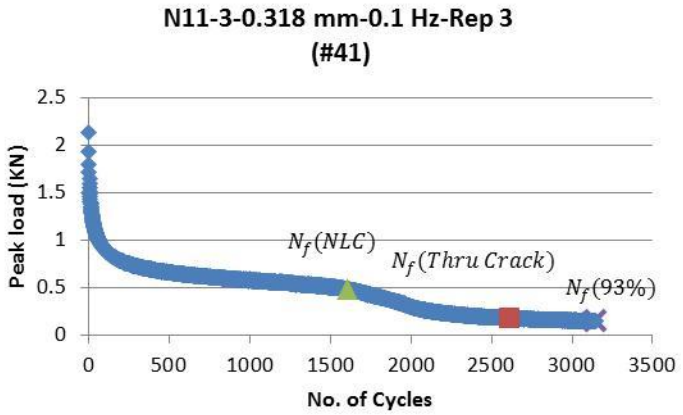

Figure B.4

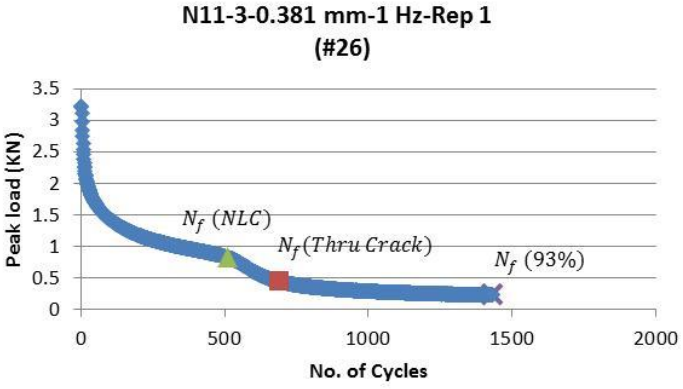

Figure B.5

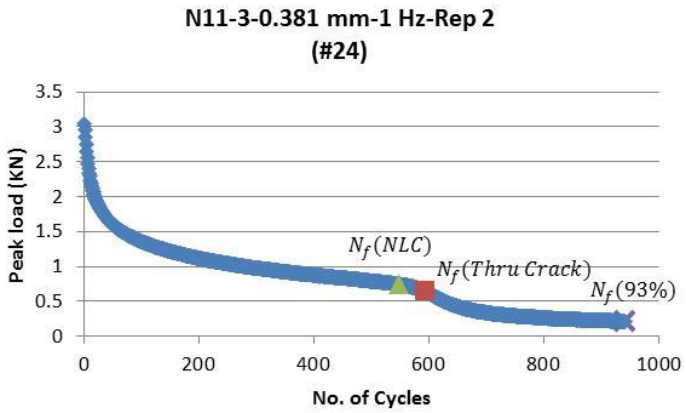

Figure B.6

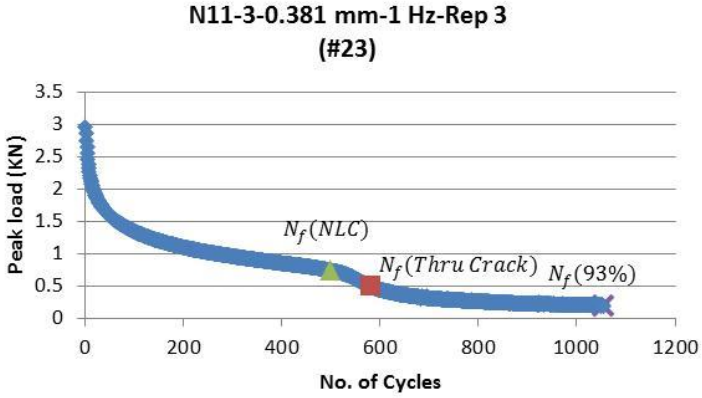

Figure B.7

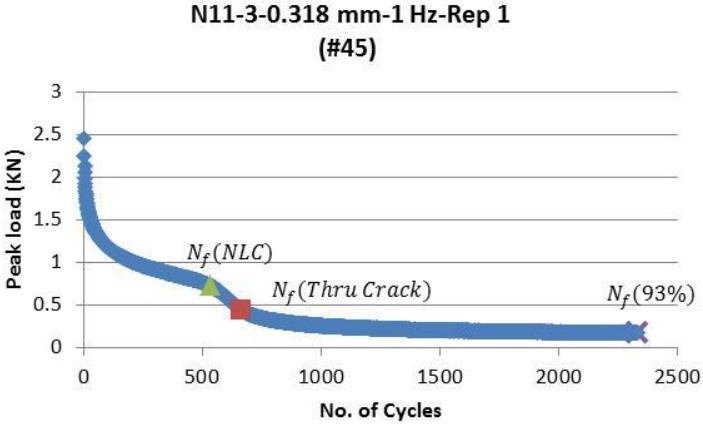

Figure B.8

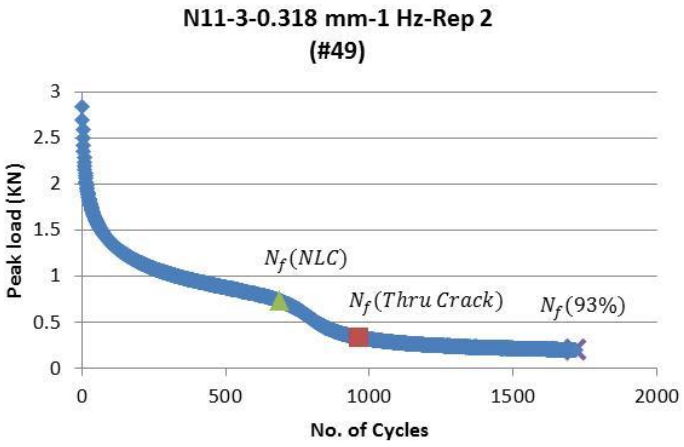

Figure B.9

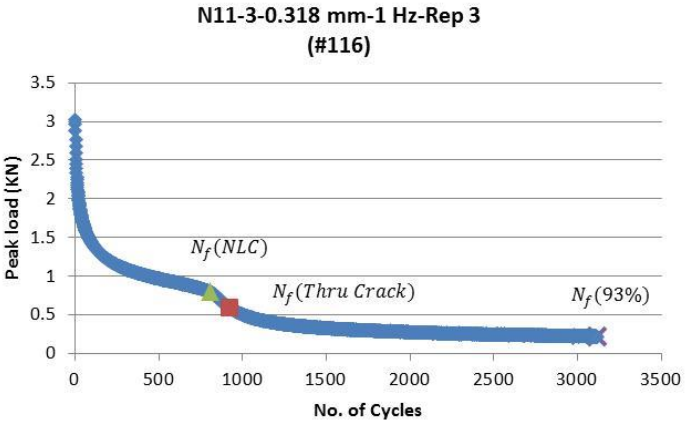

Figure B.10

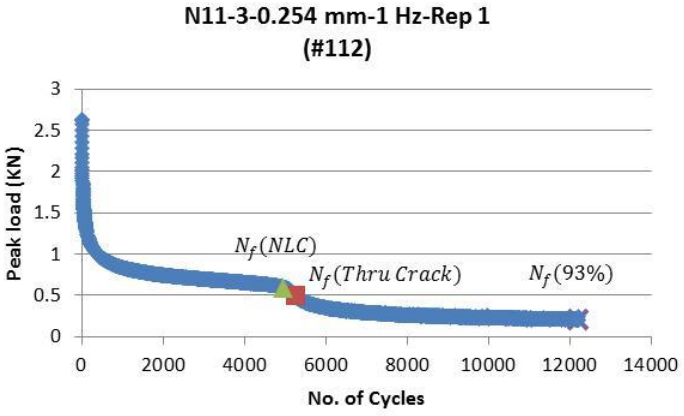

Figure B.11

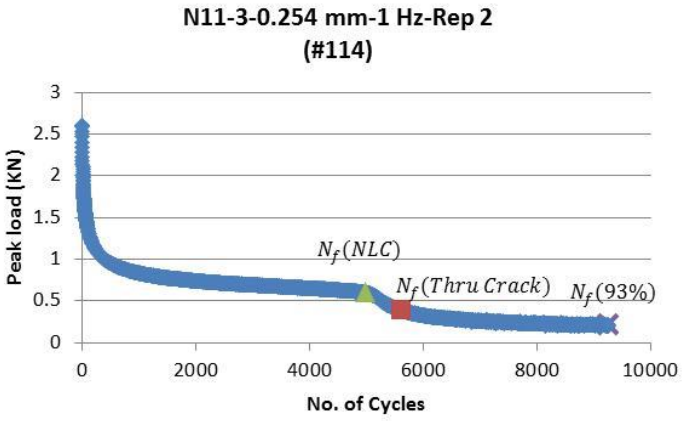

Figure B.12

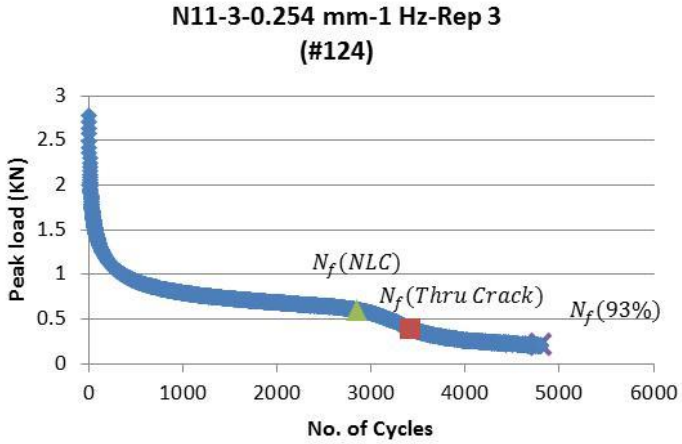

Figure B.13

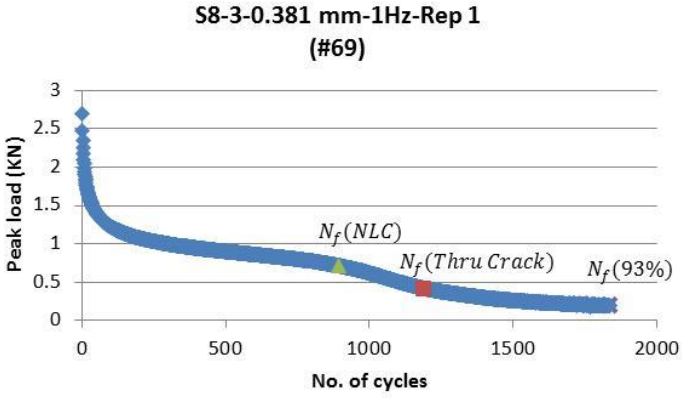

Figure B.14

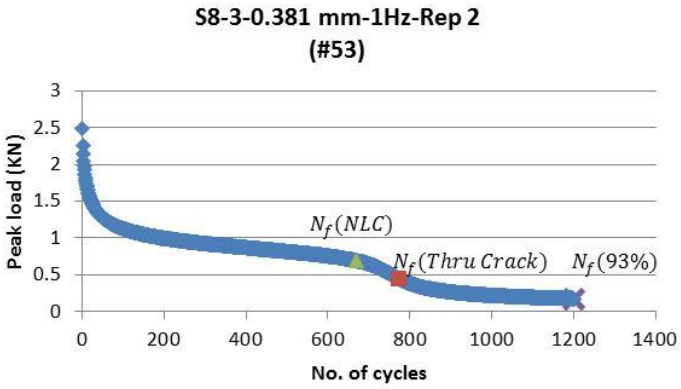

Figure B.15

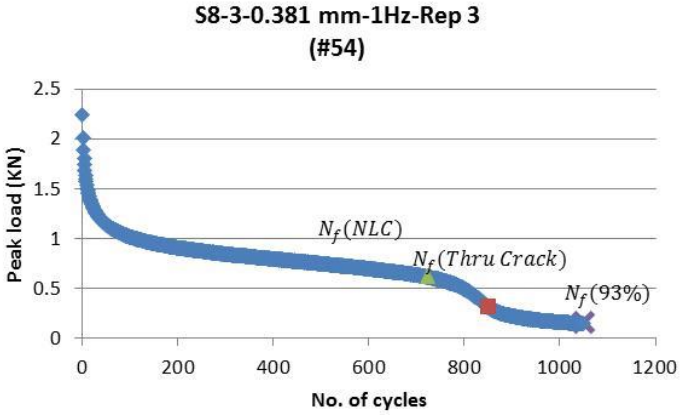

Figure B.16

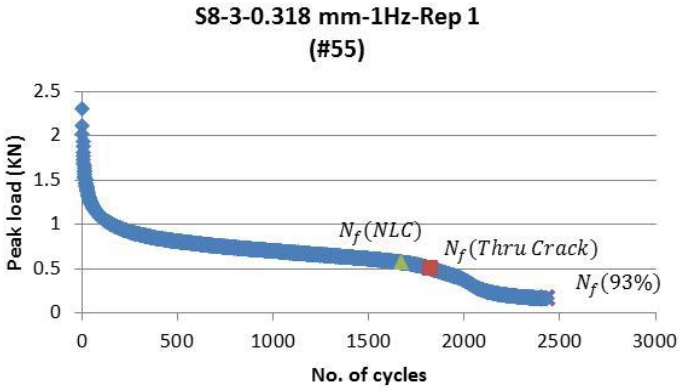

Figure B.17

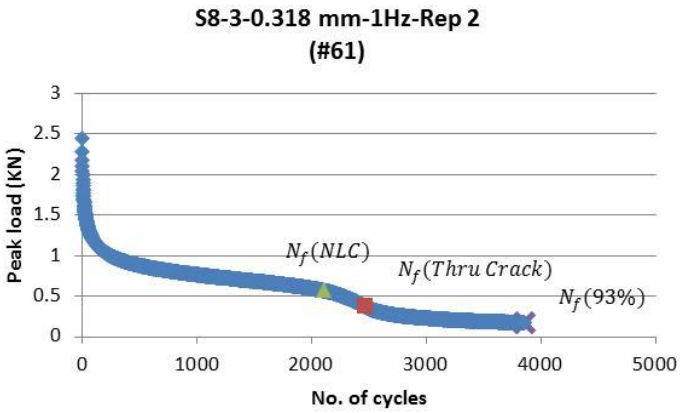

Figure B.18

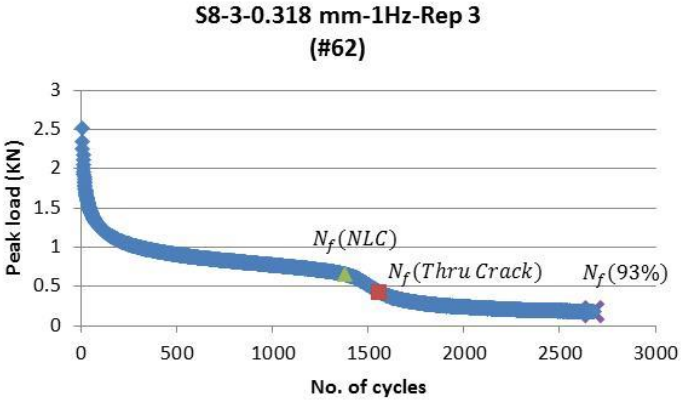

Figure B.19

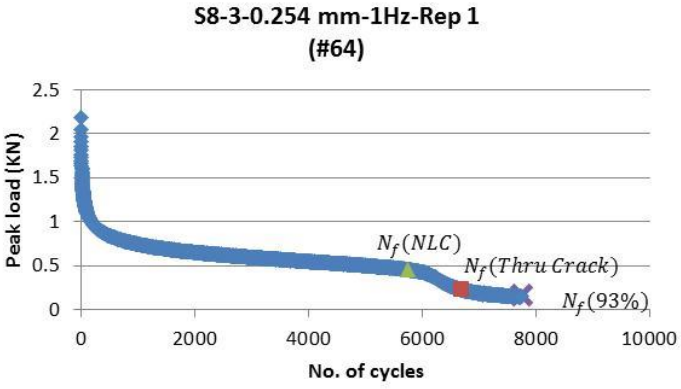

Figure B.20

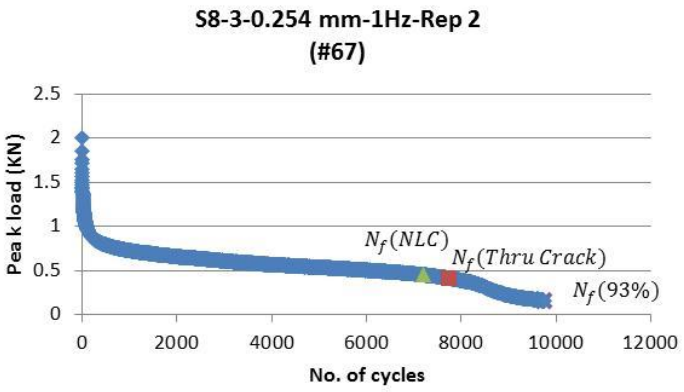

Figure B.21

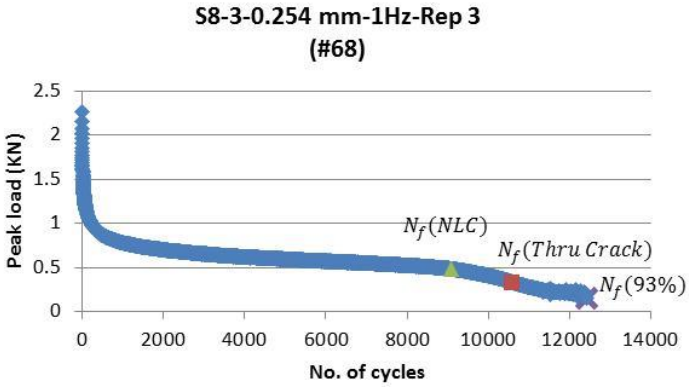

Figure B.22

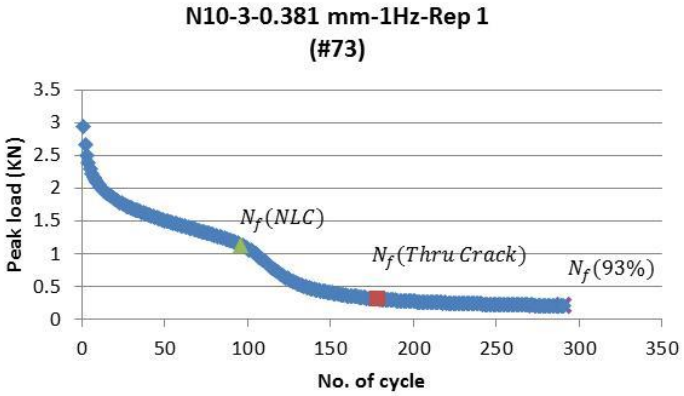

Figure B.23

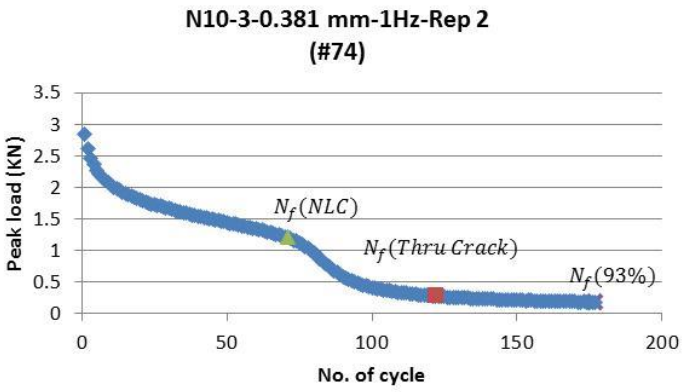

Figure B.24

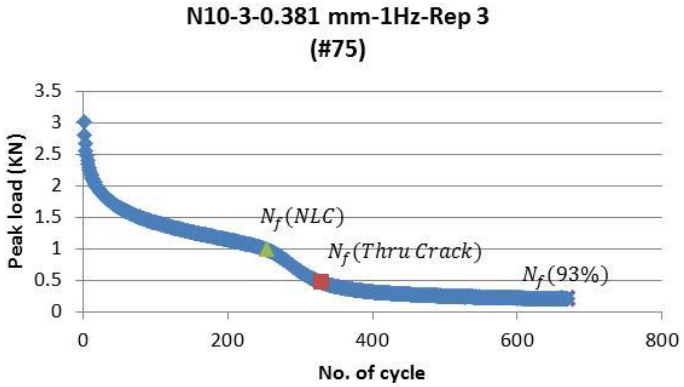

Figure B.25

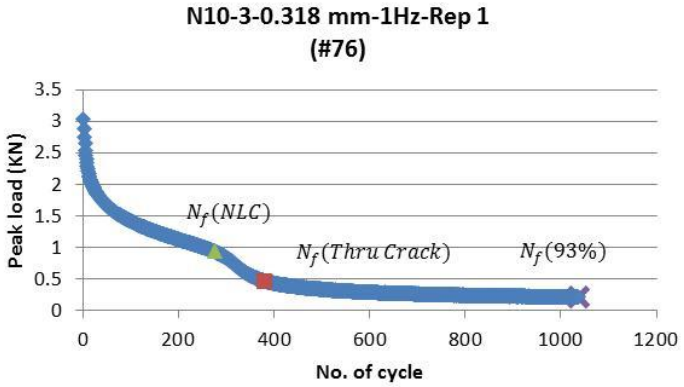

Figure B.26

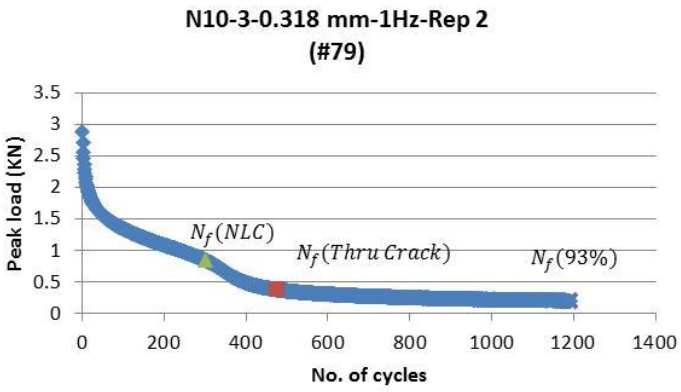

Figure B.27

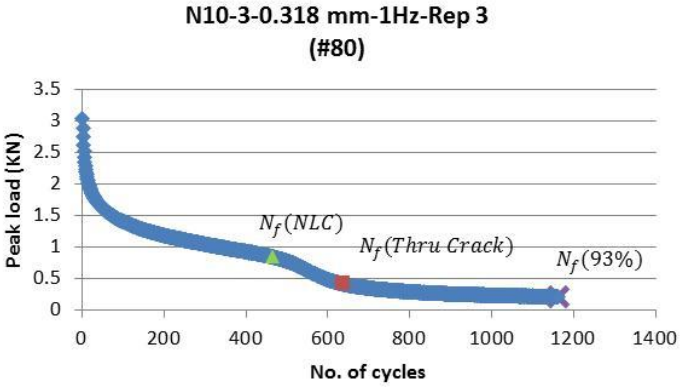

Figure B.28

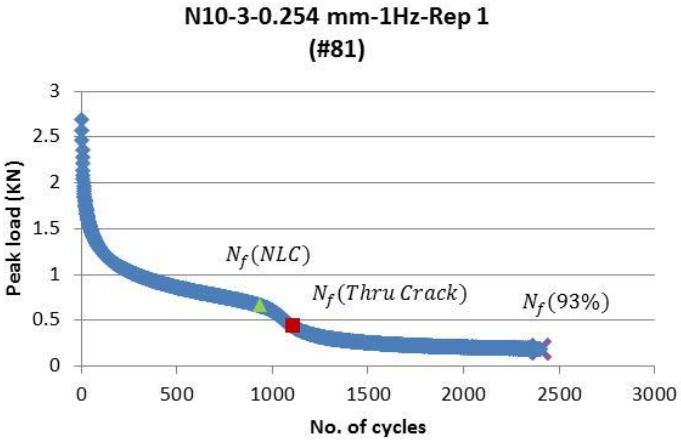

Figure B.29

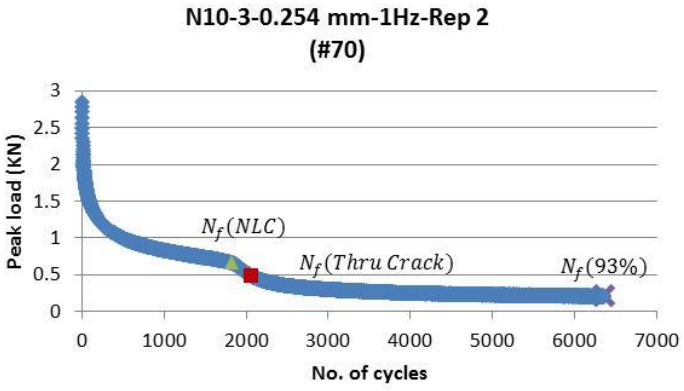

Figure B.30

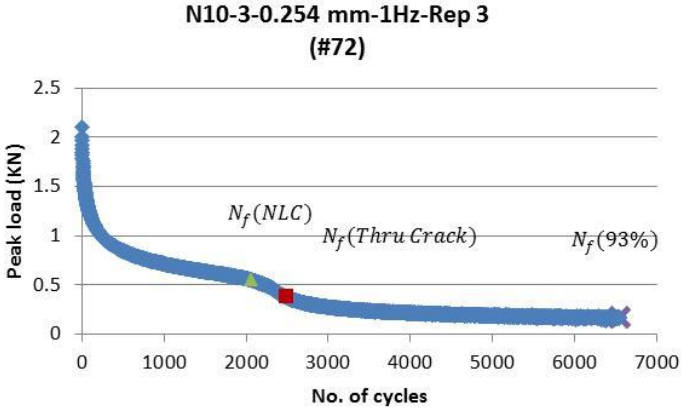

Figure B.31

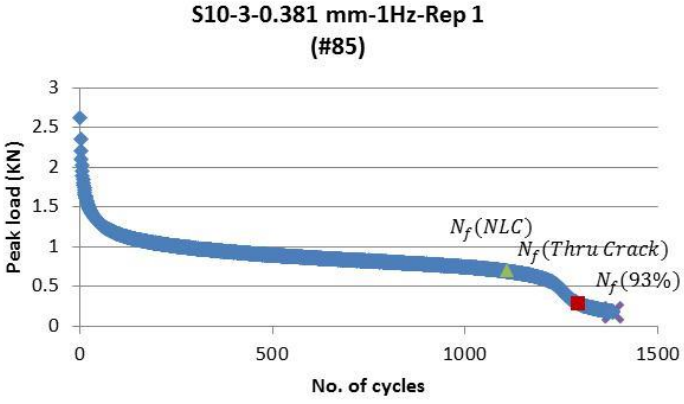

Figure B.32

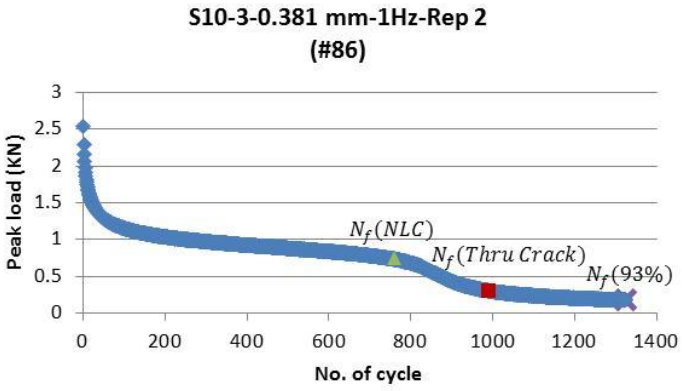

Figure B.33

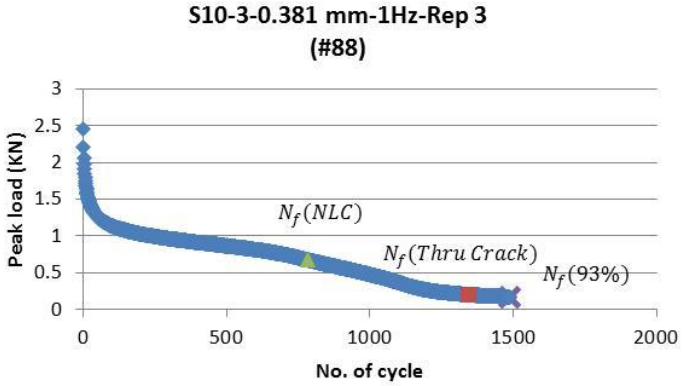

Figure B.34

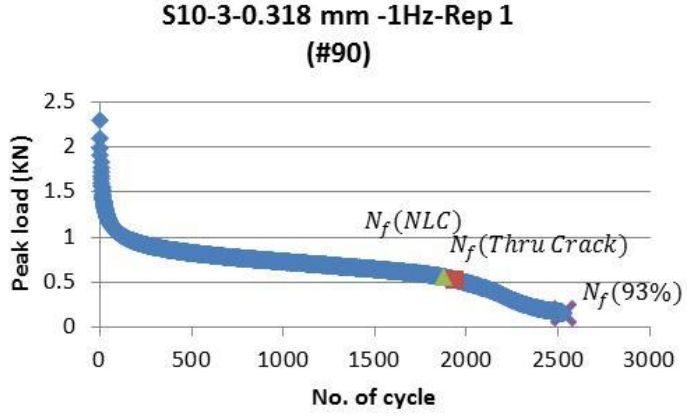

Figure B.35

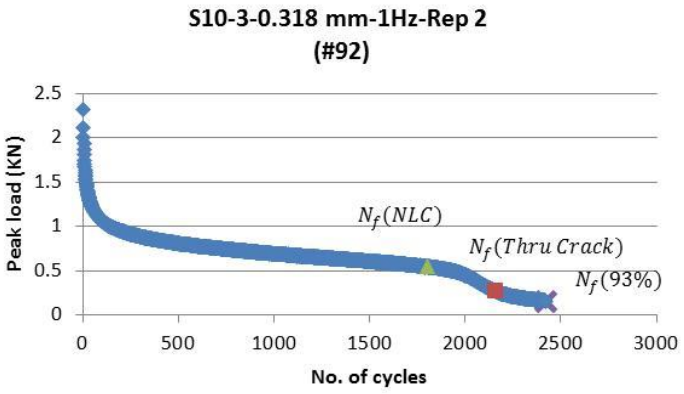

Figure B.36

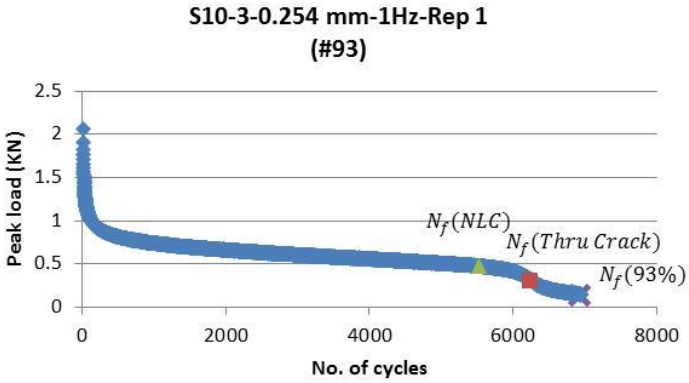

Figure B.37

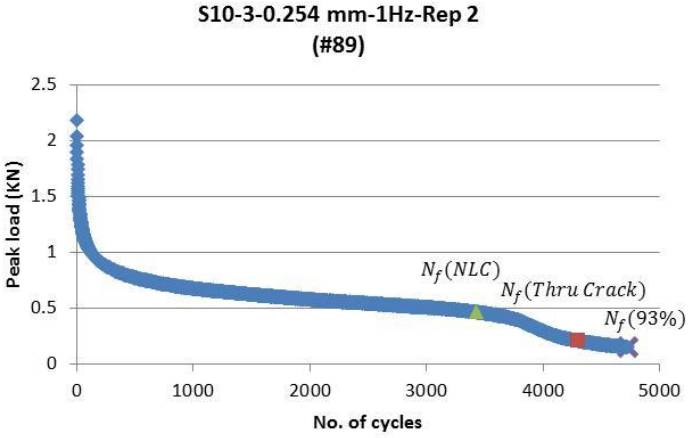

Figure B.38

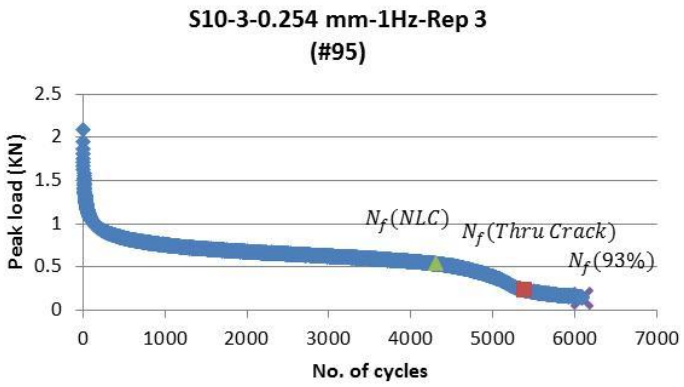

Figure B.39

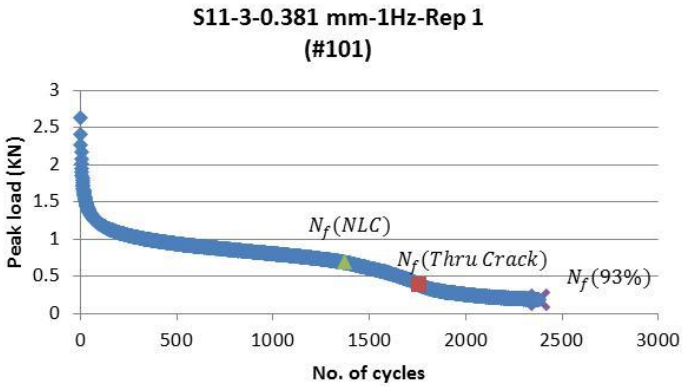

Figure B.40

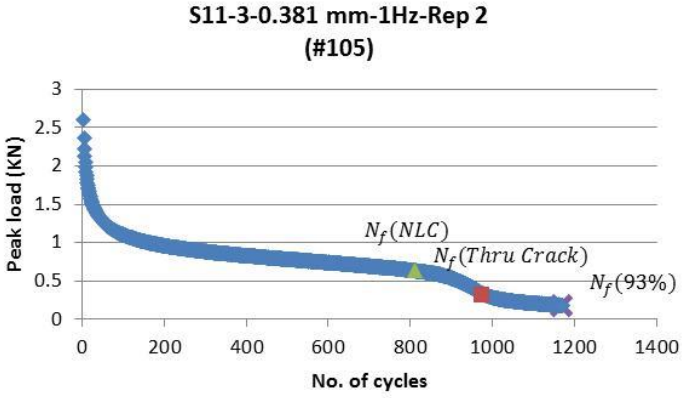

Figure B.41

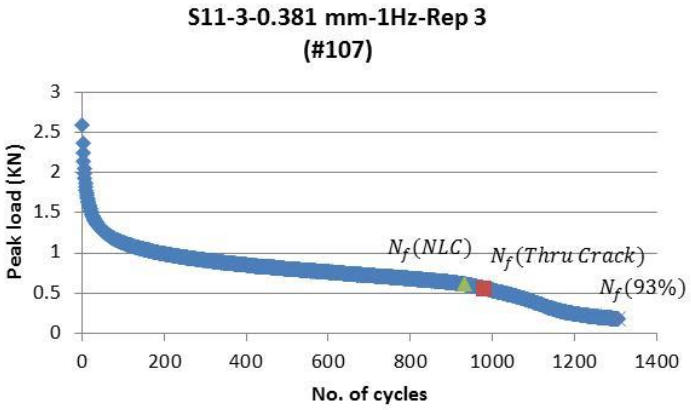

Figure B.42

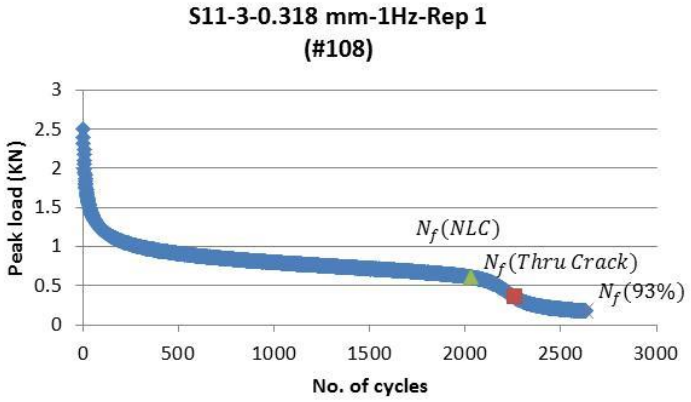

Figure B.43

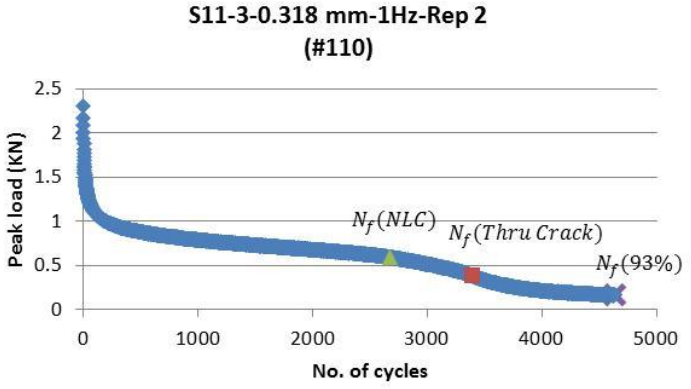

Figure B.44

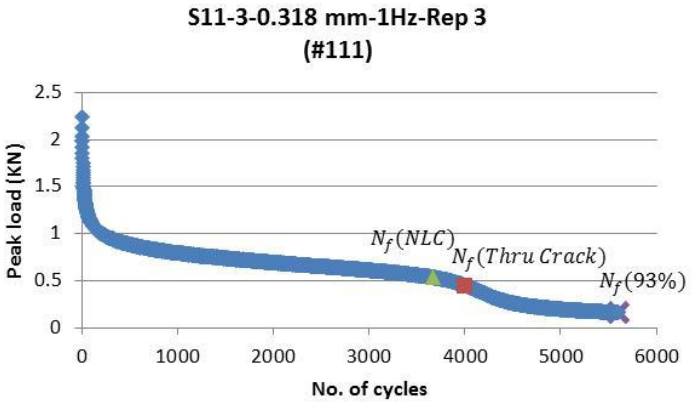

Figure B.45

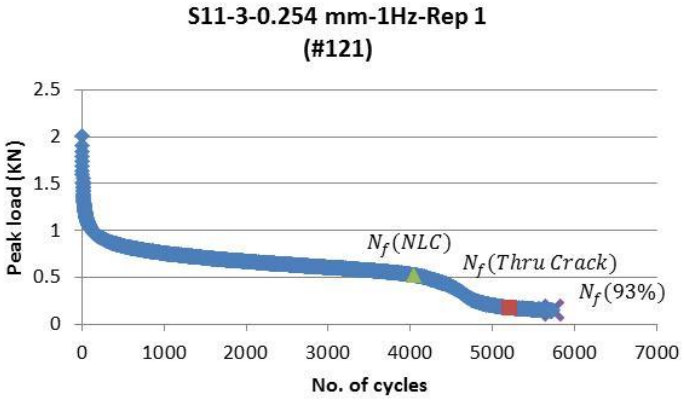

Figure B.46

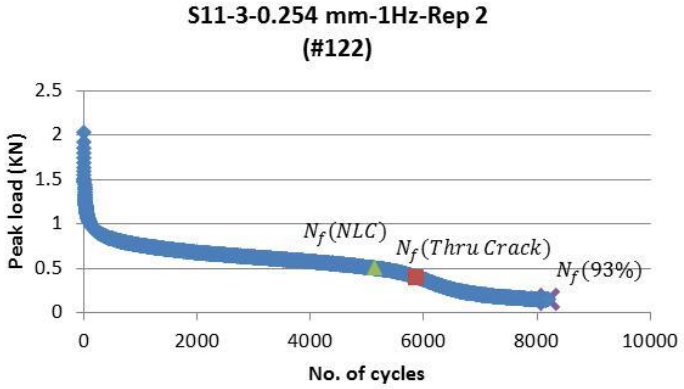

Figure B.47

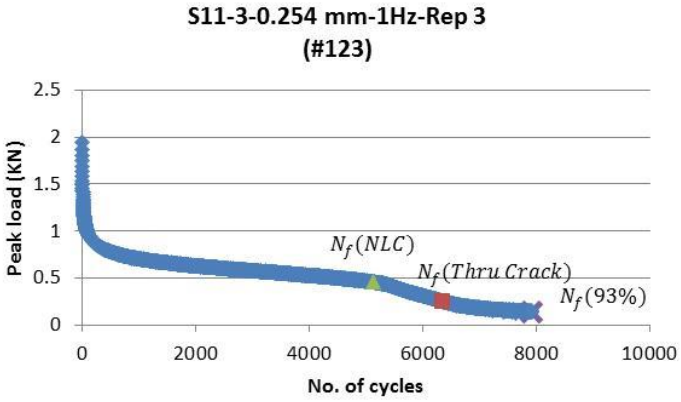
S11-3-0.254 mm-1Hz-Rep 3
(#123)
Peak load (KN)
2.5
2
1.5
1
0.5
0
0
2000
4000
6000
8000
10000
No. of cycles
$N_f(NLC)$
$N_f(Thru\ Crack)$
$N_f(93\%)$

Figure B.48

Appendix C

Minitab Outputs (Two-factor ANOVA with Tukey's Test, N11-3 Mix)

C.1 Analysis result using N_f(NLC) failure points

General Linear Model: Nf1 versus frequency, MOD

```
Factor     Type   Levels  Values
frequency  fixed       2  0.1, 1.0
MOD        fixed       3  0.254, 0.318, 0.381


Analysis of Variance for Nf1, using Adjusted SS for Tests

Source         DF   Seq SS   Adj SS   Adj MS      F      P
frequency       1  0.02857  0.02857  0.02857   1.32  0.273
MOD             2  4.07261  4.07261  2.03630  94.26  0.000
frequency*MOD   2  0.57048  0.57048  0.28524  13.20  0.001
Error          12  0.25923  0.25923  0.02160
Total          17  4.93090


S = 0.146979   R-Sq = 94.74%   R-Sq(adj) = 92.55%


Unusual Observations for Nf1

Obs      Nf1      Fit   SE Fit  Residual  St Resid
  7  3.35793  3.59935  0.08486  -0.24141     -2.01 R

R denotes an observation with a large standardized residual.


Grouping Information Using Tukey Method and 95.0% Confidence

frequency  MOD    N  Mean  Grouping
1.0        0.254  3   3.6  A
0.1        0.254  3   3.6  A
0.1        0.318  3   3.1    B
1.0        0.318  3   2.8    B C
1.0        0.381  3   2.7      C
0.1        0.381  3   2.2        D

Means that do not share a letter are significantly different.


Tukey 95.0% Simultaneous Confidence Intervals
Response Variable Nf1
All Pairwise Comparisons among Levels of frequency*MOD
frequency = 0.1
MOD = 0.254  subtracted from:

frequency  MOD     Lower  Center   Upper  --------+---------+---------+--------
0.1        0.318  -0.859  -0.456  -0.053           (---*---)
```

```
0.1        0.381  -1.831  -1.428  -1.025  (---*---)
1.0        0.254  -0.387   0.016   0.419               (---*---)
1.0        0.318  -1.180  -0.777  -0.374        (---*---)
1.0        0.381  -1.287  -0.884  -0.481       (---*---)
                                          --------+---------+---------+--------
                                               -1.0       0.0       1.0
```

```
frequency = 0.1
MOD = 0.318  subtracted from:

frequency  MOD     Lower   Center    Upper
0.1        0.381  -1.375  -0.9721  -0.5691
1.0        0.254   0.069   0.4721   0.8752
1.0        0.318  -0.724  -0.3212   0.0819
1.0        0.381  -0.831  -0.4282  -0.0251

frequency  MOD    --------+---------+---------+--------
0.1        0.381      (---*---)
1.0        0.254                    (---*---)
1.0        0.318            (---*---)
1.0        0.381           (---*---)
                  --------+---------+---------+--------
                       -1.0       0.0       1.0
```

```
frequency = 0.1
MOD = 0.381  subtracted from:

frequency  MOD     Lower  Center   Upper  --------+---------+---------+--------
1.0        0.254  1.0412  1.4442  1.8473                             (---*---)
1.0        0.318  0.2478  0.6509  1.0540                    (----*---)
1.0        0.381  0.1409  0.5440  0.9471                   (---*---)
                                          --------+---------+---------+--------
                                               -1.0       0.0       1.0
```

```
frequency = 1.0
MOD = 0.254  subtracted from:

frequency  MOD     Lower   Center    Upper
1.0        0.318  -1.196  -0.7933  -0.3902
1.0        0.381  -1.303  -0.9002  -0.4972

frequency  MOD    --------+---------+---------+--------
1.0        0.318       (---*---)
1.0        0.381      (---*---)
                  --------+---------+---------+--------
                       -1.0       0.0       1.0
```

```
frequency = 1.0
MOD = 0.318  subtracted from:

frequency  MOD      Lower   Center   Upper
1.0        0.381  -0.5100  -0.1069  0.2961

frequency  MOD    --------+---------+---------+--------
1.0        0.381              (---*---)
                  --------+---------+---------+--------
                       -1.0       0.0       1.0
```

C.2 Analysis result using $N_f(93\%)$ failure points

General Linear Model: N1(93%) versus Frequency, MOD

```
Factor     Type   Levels  Values
Frequency  fixed       2  0.1, 1.0
MOD        fixed       3  0.254, 0.318, 0.381


Analysis of Variance for N1(93%), using Adjusted SS for Tests

Source          DF   Seq SS   Adj SS   Adj MS      F      P
Frequency        1  0.20118  0.07877  0.07877   3.88  0.074
MOD              2  3.43494  3.49224  1.74612  86.08  0.000
Frequency*MOD    2  0.31766  0.31766  0.15883   7.83  0.008
Error           11  0.22313  0.22313  0.02028
Total           16  4.17691


S = 0.142424   R-Sq = 94.66%   R-Sq(adj) = 92.23%


Grouping Information Using Tukey Method and 95.0% Confidence

Frequency  MOD    N  Mean  Grouping
0.1        0.254  2   3.9  A
1.0        0.254  3   3.9  A
0.1        0.318  3   3.4    B
1.0        0.318  3   3.4    B
1.0        0.381  3   3.1    B
0.1        0.381  3   2.5      C

Means that do not share a letter are significantly different.


Tukey 95.0% Simultaneous Confidence Intervals
Response Variable N1(93%)
All Pairwise Comparisons among Levels of Frequency*MOD
Frequency = 0.1
MOD = 0.254  subtracted from:

Frequency  MOD     Lower  Center    Upper
0.1        0.318  -0.954  -0.511  -0.0680
0.1        0.381  -1.858  -1.415  -0.9714
1.0        0.254  -0.478  -0.035   0.4079
1.0        0.318  -1.024  -0.581  -0.1382
1.0        0.381  -1.339  -0.896  -0.4528

Frequency  MOD    ---------+---------+---------+-------
0.1        0.318           (----*---)
0.1        0.381  (----*---)
1.0        0.254               (----*---)
1.0        0.318           (---*----)
1.0        0.381        (---*---)
                  ---------+---------+---------+-------
                       -1.0       0.0       1.0


Frequency = 0.1
```

```
MOD = 0.318  subtracted from:

Frequency  MOD     Lower   Center    Upper
0.1        0.381  -1.300  -0.9034  -0.5070
1.0        0.254   0.080   0.4759   0.8722
1.0        0.318  -0.467  -0.0702   0.3262
1.0        0.381  -0.781  -0.3848   0.0115

Frequency  MOD    ---------+---------+---------+-------
0.1        0.381        (---*---)
1.0        0.254                  (---*---)
1.0        0.318               (---*---)
1.0        0.381            (---*---)
                  ---------+---------+---------+-------
                       -1.0       0.0       1.0


Frequency = 0.1
MOD = 0.381  subtracted from:

Frequency  MOD     Lower  Center   Upper
1.0        0.254  0.9829  1.3792  1.7756
1.0        0.318  0.4369  0.8332  1.2296
1.0        0.381  0.1222  0.5186  0.9149

Frequency  MOD    ---------+---------+---------+-------
1.0        0.254                             (---*---)
1.0        0.318                        (---*---)
1.0        0.381                     (---*---)
                  ---------+---------+---------+-------
                       -1.0       0.0       1.0


Frequency = 1.0
MOD = 0.254  subtracted from:

Frequency  MOD     Lower   Center    Upper
1.0        0.318  -0.942  -0.5460  -0.1497
1.0        0.381  -1.257  -0.8607  -0.4643

Frequency  MOD    ---------+---------+---------+-------
1.0        0.318          (---*---)
1.0        0.381        (---*---)
                  ---------+---------+---------+-------
                       -1.0       0.0       1.0


Frequency = 1.0
MOD = 0.318  subtracted from:

Frequency  MOD      Lower   Center    Upper
1.0        0.381  -0.7110  -0.3147  0.08169

Frequency  MOD    ---------+---------+---------+-------
1.0        0.381           (---*---)
                  ---------+---------+---------+-------
                       -1.0       0.0       1.0
```

Appendix D

EXCEL Outputs (F-test for Comparing Variances at Two Frequencies, N11-3 Mix)

D.1 For N_f(NLC) failure points

Regardless of MOD

	Variable 1	*Variable 2*
Mean	1960.778	1818.333
Variance	4129641	3741189
Observations	9	9
df	8	8
F	1.103831	
P(F<=f) one-tail	0.446151	
F Critical one-tail	3.438101	

MOD = 0.381 mm

	Variable 1	*Variable 2*
Mean	156	519.6667
Variance	4009	644.3333
Observations	3	3
df	2	2
F	6.221935	
P(F<=f) one-tail	0.138467	
F Critical one-tail	19	

MOD = 0.318 mm

	Variable 1	*Variable 2*
Mean	1462.333	674
Variance	270434.3	19152
Observations	3	3
df	2	2
F	14.12042	
P(F<=f) one-tail	0.066136	
F Critical one-tail	19	

D.2 For N_f(93%) failure points

Regardless of MOD

	Variable 1	*Variable 2*
Mean	3402.75	4096
Variance	12804751	16116281
Observations	8	9
df	7	8
F	0.794523	
P(F<=f) one-tail	0.387303	
F Critical one-tail	0.268404	

MOD = 0.381 mm

	Variable 1	*Variable 2*
Mean	354.3333	1142.667
Variance	14964.33	66412.33
Observations	3	3
df	2	2
F	0.225325	
P(F<=f) one-tail	0.18389	
F Critical one-tail	0.052632	

MOD = 0.318 mm

	Variable 1	*Variable 2*
Mean	2821	2389.333
Variance	699375	492465.3
Observations	3	3
df	2	2
F	1.420151	
P(F<=f) one-tail	0.413197	
F Critical one-tail	19	

(Continued)

D.1 For N_f(NLC) failure points

MOD = 0.254 mm

	Variable 1	*Variable 2*
Mean	4264	4261.333
Variance	3028368	1498533
Observations	3	3
df	2	2
F	2.020888	
P(F<=f) one-tail	0.331028	
F Critical one-tail	19	

D.2 For N_f(93%) failure points

MOD = 0.254 mm

	Variable 1	*Variable 2*
Mean	8848	8756
Variance	9248	13880512
Observations	2	3
df	1	2
F	0.000666	
P(F<=f) one-tail	0.018249	
F Critical one-tail	0.005013	

Appendix E

Minitab Output (T-test for Comparing the Means of Coefficients, "α_2" and "β_2")

Test and CI for Two Variances: α2 (BBF), β2 (OT)

```
Method

Null hypothesis         Sigma(α2 (BBF)) / Sigma(β2 (OT)) = 1
Alternative hypothesis  Sigma(α2 (BBF)) / Sigma(β2 (OT)) not = 1
Significance level      Alpha = 0.05


Statistics

Variable  N  StDev  Variance
α2 (BBF)  5  1.035     1.072
β2 (OT)   5  1.088     1.184

Ratio of standard deviations = 0.951
Ratio of variances = 0.905


95% Confidence Intervals

                                  CI for
Distribution   CI for StDev       Variance
of Data            Ratio           Ratio
Normal        (0.307, 2.948)  (0.094,  8.694)
Continuous    (    *, 4.666)  (    *, 21.770)


Tests

                                          Test
Method                          DF1  DF2  Statistic  P-Value
F Test (normal)                   4    4       0.91    0.925
Levene's Test (any continuous)    1    8       0.02    0.893
```

Two-Sample T-Test and CI: α2 (BBF), β2 (OT)

```
Two-sample T for α2 (BBF) vs β2 (OT)

          N  Mean  StDev  SE Mean
α2 (BBF)  5  5.21   1.04     0.46
β2 (OT)   5  4.96   1.09     0.49


Difference = mu (α2 (BBF)) - mu (β2 (OT))
Estimate for difference:  0.246
95% CI for difference:  (-1.303, 1.795)
T-Test of difference = 0 (vs not =): T-Value = 0.37  P-Value = 0.724  DF = 8
Both use Pooled StDev = 1.0620
```